SUITE an Innovative Bioreactor Platform for *in vitro* Experiments

PhD Thesis

PhD course on Automatic, Robotics and Bioengineering

XXII (2007-2009)

SSD: ING-IND/34, ING-INF/06

Student: Daniele Mazzei

Supervisor: Prof. Arti Ahluwalia

University of Pisa

Interdepartmental Research Center "E.Piaggio"

Pisa February 28, 2010

Abstract

In-vitro cell cultures are a fundamental step in preclinical drug testing and are of great interest to the pharmaceutical industry. The most common method for culturing cells is in cell culture incubators. These are large and cumbersome and all mechanical stimuli are absent. They are nevertheless used ubiquitously and their results quoted as "standards" of in-vitro protocols. Several alternative culture methods have been proposed, and many systems are currently available commercially. Indeed, systems and devices for maintaining cells and tissues in controlled physical conditions, or bioreactors, have become an important tool in many areas of research. This is not only due to the growing interest in tissue engineering but also because it is now being increasingly recognised that cells respond not only to their biochemical, but also to their physical environment, and both cues are necessary to create a biomimetic habitat. However most bioreactors for cell culture and tissue engineering are cumbersome and only provide a few cues such as flow or strain, allowing limited control and flexibility.

Since drug testing involves a large number of tests on identical cell cultures, a single well culture is inadequate and costly both in

time and money. The "High Throughput Screening" (HTS), is a methodology for scientific experimentation widely used in drug discovery, based on a brute-force approach to collect a large amount of experimental data in less time and using less animals. The parallel nature of HTS makes it possible to collect a large amount of data from a small number of experiments and in a very short time. HTS, however, suffers from a significant problem that may affect the relevance of tests: the environment discrepancy problem. Another problem related with the actual drug testing and tissue engineering experiments is the enormous number of animals that have to be scarified every year.

The aim of this study was to develop a generic platform or SUITE (Supervising Unit for In-vitro TEsting) for cell, tissue and organ culture composed of two main components: a universal control unit and an array of bioreactor chambers. The platform provides a biomimetic habitat to cells and tissues since the environment in the chambers is controlled and regulated to provide biomechanical and biophysical stimuli similar to those found in-vivo. In this work I describe how a new concept of cell culture bioreactor was developed by integrating different technologies and research fields. The data extracted using this new cell culture approach is more predictive of the in vivo response with respect to the multi-well approach, particularly for drug related studies.

The starting point was a thorough analysis of currently used in-vitro methods; their pros and cons were assessed to exploit their advantages and overcome or circumvent their disadvantages. As far as the culture chamber is concerned, the approach was to use the methods and materials commonly employed in microfluidic fabrication,

but at scales compatible with classical culture systems such as petri-dishes and multiwells. This renders the bioreactors more amenable to use by biologists and enables the use of cell densities comparable with classic systems as well as the use of conventional assaying techniques. In most cases, the cell culture chambers are thus made out of PDMS (Polydimethylsiloxane), using soft-moulding with micro- or mini-machined masters, or what we call "Soft Milli-molding". A "system on a plate" Multi Compartmental Modular Bioreactor (MCmB) was developed using this technology. The MCmB is a modular chamber for high throughput multi compartmental bioreactor experiments. It is designed to be used in a wide range of applications and with various cell types. A precise stimulus application is also very important to better understand the correlation between physical variables and pathologies allowing a more accurate study of the tissue physiology and pathologies. For this reason in these thesis three additional stimulation chambers for vascular and articular cartilage stimulation respectively were also designed and tested. The control system was developed to be user-friendly, flexible and expandable to include new stimuli and was based on modular components, including motors and sensors. Importantly a single software interface was designed to allow data acquisition and monitoring of several chambers in series or in parallel.

Using SUITE, high throughput experiments can be performed in an *in vivo*-like simulated environment for a long time to simulate different physiological or pathological scenarios or for toxicity testing of cells, tissues or in-vitro organ models.

Acknowledgment

A PhD is a three years long adventure and it is very difficult to remember all the people that have helped you to won this "race". The first person that I have to thank is the Prof. Arti Ahluwalia, my fortunately "not bossy" boss. She has been not a supervisor but a real tutor and her help has been pivotal not only for this thesis but also for my own growing process. Arti is the head of the fantastic team that I have had the luck to join. My team has not a real name but in the last few months we called it MCB Team, without knowing the real means of this acronym. All the members of this team help me so much during the past three years, but some of them has been very important for me. Giovanni usually disagrees with me on almost everything, but this is one of the most stimulating part of our friendship and it pushed me to investigate the rightness of my ideas. Carmelo is our "models man"; he requires a FEM model for everything (also for approaching women), and he approaches problems in a totally opposite way of me, that's why I learned from Carmelo a lot of things and I have to thanks him for his helpfulness. During this year I have met and joined also another team: the CVS lab team from the Pisa computer science department headed by Anto-

nio Cisternino. Antonio has been for me a tutor and a real friend: in one word "The master". This nickname comes obviously from Star Wars, but to think about Antonio as the wise is not exactly what I mean: he is the one who always knows the solution... But you have to be able to find it in the meta explanation that he gives you!

At the computer science department i have also met Vincenzo Gervasi.before knowing him, i used to think that the human mind had limits! He knows everything!!! He is the one who made me write this thesis in Latex, assuring me that in case of any problems i could call him (I called him so many times). Another person who helped me during this process was Gualtiero Fantoni. I met Gualtiero by chance in a café and that's where we and another great guy started to build the Lening Lab. Gualtiero showed me how to "build" something that would have last more than one hour and how to convert an idea into a product. All that helped me to build this thesis into a real commercial product.

Since now I have spoken of collaborators who have turned into friends, but during this adventure I have found all the commitment i needed also from lots of friends, all very important to me. One in particular: the "Omo Nero". He is who define the word "friend". We live thousands of kilometers far away but once a month my Skype window blinks and I can read on it something like: "Mi svuvvia il capo" or "isvuvvi pijaije aneba" ... This is enough to change my mood, giving me the strenght to go ahead.

This PhD made me travel around Europe and I spent almost six months in UK where I have worked at the Sheffield Dental School. Here I have found a fantastic team, always ready to help this funny Italian guy who didn't know how to speak english. When I went in

UK the first time I was able to speak only “by my hands” and they helped me with everything!

In UK I have also met other two special persons: Malcolm and Linda Wilkinson. Malcolm and Linda are the managers of Kirkstall, the UK company that commercializes the products developed during my PhD. Between us there is not just a commercial or professional relationship: they “adopted me”, allowing me to spend months with them learning not only English but also British traditions and heritage. They definitely made me change my mind about the “cold” Britons.

Finally this work HAS to be dedicated to the one who made all this possible, pushing me to become what I am now... George Lucas!! I am joking... I wish to dedicate it to my parents and everyone who loves me.

Daniele

Cover picture by Vera Papp

Contents

List of Figures

List of Tables

Introduction

Cell culture is an essential tool in biological science, clinical science, and biomedical studies. This approach is a fundamental step in preclinical drug testing and for this reason it is of great interest to the pharmaceutical industry to employ cheaper and more ethical systems which can supply accurate and predictive information on the effects of chemicals on the human body.

Since drug testing involves a large number of tests on identical cell cultures, a single well culture is inadequate and costly both in time and money. The "High Throughput Screening" (HTS), is a methodology for scientific experimentation widely used in drug discovery, based on a brute-force approach to collect a large amount of experimental data in less time and using less animals. HTS is achieved nowadays using multi-well equipment, to contain the cell cultures subject to treatment [1]. An automatic machine collects data, usually with an optical system, during the treatment. Collected data can vary widely in nature, for instance, concentrations of physiological metabolites or proteins. The parallel nature of HTS makes it possible to collect a large amount of data from a small number of experiments and in a very short time. The multi-well system, however, suffers from a significant problem that may affect the relevance of tests: the environment discrepancy problem [2].

The environment discrepancy problem lies in the fact that the tis-

sue grown in wells is only a brutal approximation of biological reality. There are several relevant factors that are missing in this environment; for instance the cells in the well are not subject to convective flow of nutrients present in the physiological environment. Another meaningful example is the lack of the typical pressure peaks, and the presence of constant solute concentrations, unlike in biological systems where gradients of concentration are the basis of most important processes. In [3] it is discussed how the multi-well approach does not scale fully as expected by an HTS system because the collected data are not directly usable in drug testing. This seems to be a paradox since the multi-well has been the core element of the HTS methodology. In the mean time, systems and devices tools for maintaining cells and tissue in controlled physical conditions or bioreactors have become important tools in drug testing or tissue engineering in general. This particularly due to the growing interest in tissue engineering and in-vitro testing. Moreover, it is now being increasingly recognized that cells respond not only to their biochemical [4, 5, 6], but also to their physical environment [7, 8, 9, 10], and both are necessary to create a biomimetic environment. Noticeably none of these innovative and more physiological cell culture systems is designed for high throughput screening.

Another problem related with the actual drug testing and tissue engineering experiments is the enormous number of animals that have to be scarified every year. Animal Testing occurs regularly throughout the European Union (EU) and it still plays a large role in research and drug development around Europe. In Europe, biomedical testing still remains the most widely used type of research for drug development. Toxicity testing for drugs, foodstuffs, household chemicals and various other substances is performed in laboratories throughout Europe. Rats and mice are the most commonly used animals while reptiles are the least com-

monly used animals. Recent years have seen a surge in the use of zebrafish and non-human primates. While ethical concerns regarding zebrafish are low, those involving non-human primates are high. The aim within Europe has been to reduce the number of monkeys and similar animals used for testing purposes. Although their likeness to humans has great value in animal testing, this same likeness raises extreme ethical concerns regarding their ability to feel pain and to experience suffering and psychological distress[11, 12].

European statistics showed that France used 2.3 million animals in 2005 while Germany used 1.8 million animals in that same year for testing purposes. Statistics for 2005 showed that Finland and Ireland both decreased their use of animals. In contrast, Sweden, Spain and Greece all increased their use of animals, either doubling or near-doubling their use. Across all of Europe, there are approximately 12.1 million animal testing experiments performed each year. While there is some debate regarding the statistics of which country is the highest tester of animals, Britain is thought to be the top user of animals with its use of nearly three million animal experiments each year. France is a very close second and generates a large amount of debate given that one of the major global cosmetics company is based in France and still tests on animals.

Europe's overall laboratory use of animals has actually increased very recently by 3.2 percent. This contrasts with the fall in animal testing over the last few decades. It's also important to note that one of the biggest animal testers from a global perspective is Huntingdon Life Sciences (HLS), which is based in Europe. HLS kills approximately 75,000 animals each year.

A shown in Table 1 most of the animal experiments are done for cosmetics and toxicology purpose. While the UK officially banned animal testing on cosmetics in the late 1990s, Europe has been somewhat slower

to implement a ban. A near total ban is, however, planned for 2009. While most of the EU supports the ban, countries such as France have voiced strong opposition to the ban, citing their belief that cosmetics testing on animals are necessary for sufficient health and safety testing of products.

Table 1: *Use of animal tests for the year 2001 in UK.*

Research	*Research for human medicine and cosmetics*	*Research for veterinary*	*Toxicity tests*	*Disease studies*	*Didattic*	*Other*
30%	57%	1.40%	7%	2.70%	0.30%	0.60%

Reducing animal suffering as a whole requires the use of alternative approaches to animal testing. While the scientific community generally supports the use of animals to further our knowledge of health and medicine, they still acknowledge the need for alternatives to reduce animal suffering. This is accomplished through the use of several different categories of alternatives, which are often described as the three "Rs" of biomedical research. They are:

- **Reduction** in the number of animals needed in a test
- **Replacement** of an animal test by a non-animal test
- **Refinement** of an animal test to reduce or eliminate stress or suffering

Reduction is probably one of the most promising areas in the sense that a great deal of progress has been made over the last decade. To reduce animal testing, researchers use techniques that allow them to obtain a level of information that is sufficient but requires fewer animals.

Conversely, researchers may be able to employ a method that allows them to obtain more information from the same number of animals. The end result is that animal use is maximized and more efficient, leading to fewer animals being used and therefore, fewer animals suffering from any pain or distress that occurs from the experiment. There are numerous ways that researchers can reduce the number of animals used or obtain more information from the same number of animals that an experiment would typically require for success. There are currently modified test methods that are essentially traditional models that have been advanced to provide comparable results with fewer animals. For example, newer versions of the Draize test can reduce the use of animals and additionally, can reduce the potential distress as well[1]. Many companies now perform more than one test on the same animal, which allows them to use fewer animals overall. Some companies are also using human volunteers instead of animals to test for skin irritation, which further reduces the number of animals used in testing.

Testing certain substances on cellular models first can rule out the use of animals if results are not favorable. In addition, the use of computer models, databases and similar sources of information can provide the history of a substance and its use as well as offering preliminary information on the safety of a formula.

Tissue cultures are also an extremely useful method for reducing the number of animals used in laboratory experimentation. By utilizing active cell cultures, companies can dramatically reduce the number of animals used while still obtaining comparable levels of information from the method.

In Europe, alternative testing methods are scientifically validated by

[1]The Draize test is used to assess toxicity of various chemicals and products through application of the product to the animal's skin or eyes.

the European Center for the Validation of Alternative Methods (ECVAM), an official body appointed for this purpose by the European Union. Validation by ECVAM means that these methods can be used across the different industries that test chemicals for safety purposes (chemicals, food, pharmaceuticals, etc). Validation is the process by which scientists and regulators establish whether a method is reliable and relevant for a specific purpose.

To work out how to mimic a complex biological response outside a living organism is a tremendous scientific challenge, and requires a revolution in current in-vitro culture methods. Validating an alternative method and proving it is safe also takes time To improve in vitro culture conditions, the conventional models used in flasks or microwell plates need to be re-evaluated and modified and transferred to a more realistic representation of the physiological environment through the use of bioreactors.

The design of a cell culture bioreactor requires a basic understanding of both chemical reactor design and cell biology. First, engineers must understand the effects of reaction rates and stoichiometry, mass transfer, heat transfer, and turbulence and mixing on product distribution, reactor productivity and size, and operational characteristics. These phenomena need to be expressed in accurate but tractable models that can be used for design and optimization calculations. Most bioreactors are cumbersome and only provide a few cues such as flow or strain, allowing limited control and flexibility. The aim of this work is to design and realize a single system which can be used to provide a physiological environment to cells on a 3D tissue engineered construct, on a cover slips or directly on tissue pieces and to enable in-vivo physio-pathological phenomena to be simulated in vitro, thus avoiding the use of animal experiments.

Thus, in this thesis, firstly the currently used methods were analysed

and their pros and cons were assessed to exploit their advantages and surpass their disadvantages. The most common method for culturing cells is in cell culture incubators. These are large and cumbersome and all mechanical stimuli are absent. They are nevertheless used ubiquitously and their results quoted as "standards" of in-vitro protocols. Owing to this dynamic culture methods have been proposed, and several systems are currently available commercially. Amongst these are low shear perfusion system [13, 14], stirred tank bioreactors [15], airlift bioreactors [16], hollow fiber perfused systems [17, 18], rotary cell culture systems [19].

The main advantages of these systems with respect to an incubator are the introduction of fluid-dynamics; the cells are subject to shear stresses, which in several cases are known to stimulate growth, and positively influence cell function. Most of them do however require the support of an incubator for pH and temperature control. A second generation of bioreactors has most recently been realized, these are systems for tissue engineering which provide a high degree of oxygenation through fibers or membranes, allowing adequate oxygen partial pressure with 3D constructs. Finally, the third generation comprises micro-fluidic systems in which small Reynolds number laminar flows are easily established. These also include microfabricated systems such as the perfused microarray bioreactor [20] and the micro cell culture chamber assay [21].

Third generation systems have one main drawback as far as tissue engineering applications are concerned; they are small. This implies that they cannot be used for culturing large numbers of volumes of cells or tissue, and in a closed loop system, fluid sampling and analysis can be difficult. Furthermore, in microfabricated systems, surface and edge effects are amplified whereas physiological cell-cell interactions are underrepresented

The key elements of a bioreactor are the cell culture chamber and the

environmental control system, and together they form an experimental platform on which a variety of experiments can be carried out. To offer a vaild substitute for classical *in-vitro* experiments, an bioreactor platform should should have the following characteristics:

- A **culture cell chamber** whose design permits a reconstruction of the fluid-dynamic conditions during operation
- A **control system** able to adjust all the environmental variables in order to simulate the phisyological reality
- A set of various **culture chamber** each one with a dedicated design in order to easily mimic the different compartments of an organism
- A **storing and viewing system** where the user can easily interact with the bioreactor system and where all the experimental data are collected and stored

To obtain the flexibility and use of new materials and fabrication methods of third generation bioreactors, combined with the control of essential operating parameters such as shear stress, flow rates, pressure, pH, temperature, O_2 concentration as well as the liberty of being stand-alone, we designed and realized a new concept in cell culture which offers platform of bespoke physical and topological environments has been designed and realized.

One of the main features the platform is the culture chambers; their ease of fabrication renders them highly flexible and simple to modify or remodel, and the low cost of manufacturing renders them disposable and compatible with high throughput systems. A further characteristic which is unique with respect to other systems reported in the literature is the principle on which the environmental control system is based and the simple software interface. In this thesis the bioreactor system is described

starting from its design philosophy, its construction and its control. A report on preliminary results of validation tests obtained with different cell types and tissues is also presented.

A generic platform or SUITE (Supervising Unit for In-vitro TEsting) for cell, tissue and organ culture composed of two main components: a universal control unit and an array of bioreactor chambers is presented, through which high throughput experiments can be performed in an *in vivo*-like simulated environment for a long time (more than a week). In this work it is describe how a new concept of cell culture bioreactor was developed by integrating different technologies and research fields. The data extracted using this new cell culture approach is more predictive of the in vivo response with respect to the multi-well approach, particularly for drug related studies.

This new system is a complete cell culture suite composed of:

- A custom made **electronic control block** that acquires signals from sensors, such as a pH-meter, thermocouple, flow sensor, pressure sensor and sends these signals to a PC through an I/O card
- A **mixing chamber** to allows the addition of oxygen or carbon oxide to the culture media so as to have the desired value of pH and oxygen concentration; it is also the location of the pH sensor
- A **peristaltic pump** to recreate the flow conditions of the tissue under examination
- A **heater** to heat the media culture to 37 C
- One or more **cell culture chambers**
- A freestanding **pressure generator** to be used in classic CO_2 incubator experiments

In this work Bioreactors are proposed as alternative in-vitro HTS system to overcomes the limits due to the environment discrepancy problem. More relevant and more predictive data from experiments can be obtained as a result of the capability of this innovative system to better simulate a physiological environment than the classic static cell culture protocols. The system is an innovative platform able to perform High throughput experiment in a more physiological like environments. With this platform it is possible to perform experiments using cell culture or tissues with a consequent reduction of required animals, the experiments done with the SUITE are organized as a High Throughput experiment, and the data collected by a main supervision system which can also impose control variables on multiple bioreactors running in parallel. With this parallel and distributed approach a pathology can be simulated in one bioreactor and the other used as a control reference. The system is modular and a various chambers can be plugged together in order to mimic the physiological district organization. With the SUITE is possible to do multi compartmental experiments for drug testing or stimulation experiments where the influence of the environmental variables on tissue physiology is investigated. These two apparently opposite approaches can be merged together using this platform in a more realistic experiments where the multi-compartmental approach can be fused together with the cell stimulation. With this new testing approach it is possible for example to investigate how drug efficiency is influenced by physiological environmental variables such us blood pH, vascular pressure, tissue oxygen concentration etc.

This system can be defined as a virtual mouses set, where all the animals are clones (tissues or cells coming from the same animal or donor can be used in different bioreactor) and where by changing the drug concentration or the control variables a pathologies can simulate and data

collected in parallel and autonomously.

This work was organized in two main parts, the first part was oriented to designing and realizing the control and stimulation systems (Environmental control and P.GIO) with the dedicated software and firmware. The second part of the work was oriented to the design and realization of innovative bioreactor chambers to be used as districts or organs simulators to be plugged together in different configurations. Merging together these two parts an innovative platform able to perform high throughput experiments in a condition less afflicted by the environmental discrepancy problem was realized.with this system is possible to do experiments requiring a lower number of animals, with the possibility of using not only cell cultures but also human or animal tissue, and with the option of applying physical stimuli to the samples.

Chapter 1

Environmental Control

In order to realize an innovative High throughput machine able to perform experiments in a more physiological way than the classic multi well approach, the first step was to define and develop the environmental control unit of the SUITE system.

The environmental control unit is the core of the system and is where all the environmental variables are collected by various sensors placed along the system connections and units. In this section it is discussed not only the electronic part of the system but the entire control unit and also the software and algorithm organization.

The aim of this system is to adjust the temperature, pH, pressure, gas flow and dissolved oxygen percentage of the culture medium. The control apparatus is consequently composed not only of the electronic and electro-valves unit, but also of the mixing chamber, the peristaltic pump, the heater unit and the control software.

In order to realize a real High throughput system, the entire design process was driven by the necessity of a system able to perform experiments in parallel, with an autonomous control and with a user friendly interface that easily allows the researcher to change the controlled variables in order to mimic different pathologies.

Another aim of this design process is the data storage approach. All

the data collected by the system using the XML data format [22] for storing and organizing application data, in order to allow an easily interoperability among different programs for further processing of generated data.

1.1 Materials and Methods

The SUITE platform is a complex system, in this section are described all the generic parts required to control the system and to create the required cellular environments. The dedicate bioreactor chambers used in the SUITE system are described in the following sections.

1.1.1 The Bioreactor Hardware

The SUITE platform consists of the following parts:

- Cell culture chamber
- Mixing chamber
- Heating system
- Peristaltic pump
- Electronic circuit and electro-valve box
- PC

The Mixing Chamber

The mixing chamber (Figure 1.1) is connected in series with the cell culture chambers and serves for pH and oxygen regulation as well as to remove air bubbles; essentially the medium is perfused with gas according

to the measured pH. The medium is inserted and removed in this chamber through a needle with the flow imposed by the peristaltic pump.

pH regulation is performed by inserting two different gases in the mixing chamber: Carbon dioxide and Air (not O2 because of flammability risks). The culture medium contains bicarbonate buffer and its pH can be closely regulated through diffusion of gases; in particular the diffusion of O_2 (Air) tends to raise the pH, while CO_2 tends to lower it [23].

The mixing chamber is made with a plastic autoclavable bottle with a screw cap. The cap is drilled and four silicone tubes are inserted and sealed with PDMS (polydimethlysiloxane, an elastomeric polymer also used for the fabrication of bioreactors). Two of these tubes are for the medium flow and the other two for insertion and removal of gases. The tubes present different lengths and just the gas inlet and the medium extraction tubes are long enough to reach the bottom of the mixing chamber. The other two tubes (medium insertion and gas removal) are just few millimeters long (over the internal part of the cap), this allows visual observation of the medium as the drops fall down the inlet tube. Drop formation is useful not only for a system check but also to increase the gas exchange processes. The gas outlet tube is shorter than the inlet in order to prevent medium foam being collected by the outlet tube and consequently removed from the mixing chamber and down to the cells.

Most pH probes are very sensitive to convective flow of the medium, therefore, the bottom of the mixing chamber is designed in order to minimize flow disturbance near the sensor. The bottom of the chamber where the pH probe tip is inserted is cone-shaped. Media mixing is located over the cone surface and in the probe tip zone the medium is mixed only by diffusion and the pH measurement is consequently very low in noise (Figure 1.1.b).

The gas inlet and outlet tubes of the mixing chamber are both con-

nected to syringe filters in order to keep the internal volume sterile and to prevent contamination coming from the gases. A syringe needle is connected to the outlet tube, and its high flow resistance ensures a constant pressure difference between the inlet and outlet. The outlet needle can be easily replaced and its diameter can be chosen in order to adjust the outlet flow resistance, so changing the correlation between the inlet flow and the internal pressure of the mixing chamber. The inlet tube is equipped with a one way valves in order to prevent the medium going into the control unit in case of system failure.

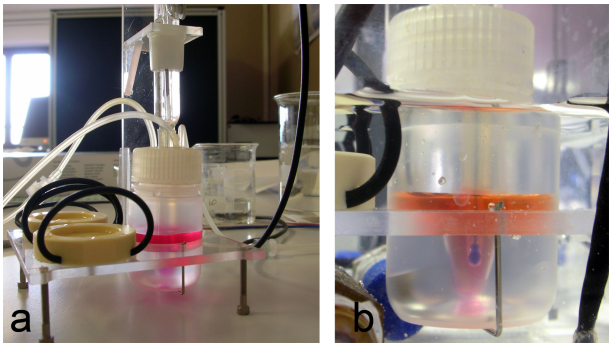

Figure 1.1: *a) The mixing chamber filled with medium and with the pH meter placed in. b) The pH meter tip (blue) in the mixing chamber's dedicated notch.*

The bioreactor mixing chamber allows also the insertion of Oxygen sensors that may be lodged through a dedicated cap with a different diameter hole. Alternatively a chamber equipped with oxygen sensor can be connected in series to the main mixing chamber.

It was decided not to realize a single mixing chamber equipped with both pH and Oxygen sensors because the O_2 probe is an optional sensor and it is preferable to have a small main mixing chamber to minimize media volumes.

The Electronic Circuit and Electro-Valves Unit

This part of the system is the heart of the bioreactor control unit. In this unit there are the electronic circuits for the sensors, for communication with the PC and for the actuation of the electro-valves, the pressure regulator and the electro-valves. The sensors plugged or inserted in this unit are (Figure 1.2):

- 2 temperature sensors (ntc thermistor [24])
- 1 gas flux sensor (AWM 3000[25]) (internal)
- 1 Pressure sensor (Phidgets 1115 - Pressure Sensor [26]) (internal)
- 1 pH sensor (Hamilton Biotrode pH probe [27])
- 1 Environmental Humidity and temperature sensor (1125 - Humidity/Temperature Sensor [28])

The main component of the electronic control box is an usb I/O board (1018 - PhidgetInterfaceKit 8/8/8 [29]) where all the analog sensors are connected. This I/O interface has 8 Digital in, 8 digital out and 8 analog in connections; this interface board is CMOS standard and the analog channels acquisition range is consequently 0-5V with 12 bit resolution. The digital channels are used to control the frontal status LEDs and to actuate, through a dedicated relay board, the gas electro-valves.

The pressure, environmental temperature and humidity sensors are directly plugged to the Phidget I/O board because they are directly compatible with it. For the flux sensor a simple signal adjusting circuit was required in order to convert the flux sensor signal to the Phidget 0-5V standard.

The two temperature sensors are read through a dedicated Phidgets component (1121 - Voltage Divider [30]) and connected to the Phidgets

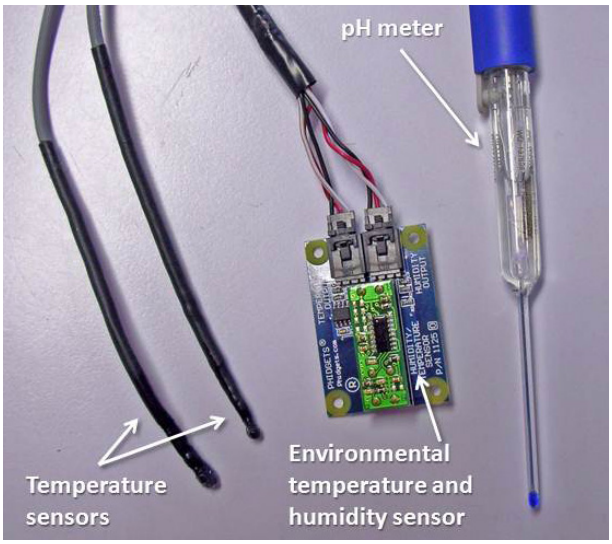

Figure 1.2: *The bioreactor external sensors: the two temperature sensors probe, the environmental temperature and humidity sensor and the pH meter.*

board through a resistive sensor. These conversion units act as a voltage divider where the base resistance can be adjusted through a trimmer in order to fit the connected sensors working resistance.

The pH and the Oxygen sensors are connected to two separated 4-20mA [31] reader units designed by Phidgets to read pH meter probes but usable in raw values mode to read all the sensors with the 4-20mA standard BNC current loop connection [32] (figure 1.4.b).

The electronic control box is connected to the CO_2 and O_2 lab connections through two dedicated pressure regulators equipped with a humidity removal filter. The connection with the electronic box is done with two quick plug connectors on the back side of the control box. Inside the bioreactor control unit the two gas lines are connected to the electro

valves through other two pressure regulators in order to prevent damage of the system in case of failure of the lab regulators. The two electro valve outputs are connected to the pressure regulator through a T connector.

In order to ensure CO_2 and O_2 mixing and also to reduce flow vibration introduced in the gas circuit by the pressure regulator and electro valve components an expansion chamber is inserted (gas mixer). The expansion chamber is where the pressure is measured and this chamber is connected in series to the pressure regulator. The outlet of the expansion chamber is connected to the flux sensor that is the last component before the gas outlet quick connector. 1.3.

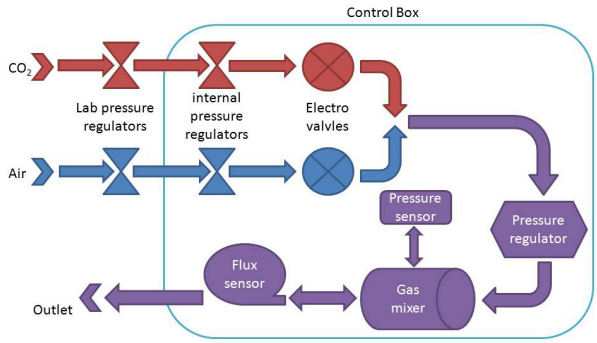

Figure 1.3: *Schematic connections of the pressure and gas regulation system.*

The electro-valves are used to select the gas that is injected in the mixing chambers and are connected to a pressure regulator SMC ITV0000 series [33] used to control the pressure inside the cell culture chamber. The electro-valves are powered at 24v AC and controlled by a Phidgets relays board [34].

The pressure regulator is powered at 24V DC and is controlled by a 0-10V DC analog signal made through a serial to PWM (Pulse Width

Modulation) generator chip (Pololu Micro dual serial motor controller [35]).

A commercial USB to serial adapter was used to generate the RS232 control signal. The PWM generator is mounted on a dedicated board designed for the purpose (Serial to PWM board). The serial to PWM board is a circuit able to control the Pololu chip and to generate two Analog signals in the range of 0-10V with a low ripple and with an on board feedback system that allows the system to have a real feedback of the analog generated signal. In the Serial to PWM board a reset circuit that can be activated by the control library 1.1.2 in case of serial communication problem (Figure 1.4) rising up one of the I/O digital channels is implemented.

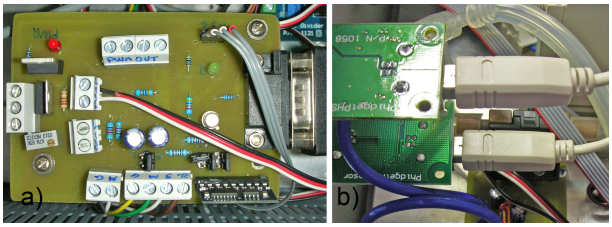

Figure 1.4: *a) The Serial to PWM board plugged to the USB RS232 converter and b) the Phidgets pH readers.*

The two pH readers, the I/O Phidgets board and the usb to serial converter are all connected to an USB hub placed on top of the control box and suitable also for USB data stick or other USB peripheral connection. The USB hub is powered by the control box power supply, this prevents over charge the USB computer ports and also to prevents electric failures of the system which may damage the connected computer. A dedicated 220V AC unit is also connected to the USB hub through an USB relays Phidgets board [36] allow the user to control four separated 220V sockets.

One of these 220V socket is used to power up the heater described in the next section 1.1.1. All the sockets are connected to ground and protected by a 3 Ampere fast fuse. The other sockets are usually used to connect the peristaltic pump and other equipments used during the bioreactor experiments.

This allows complete disconnection of all the bioreactor experiment components by the electrical network in case of failure. This safety routine is implemented through a classic "watch dog" routine in the control library.

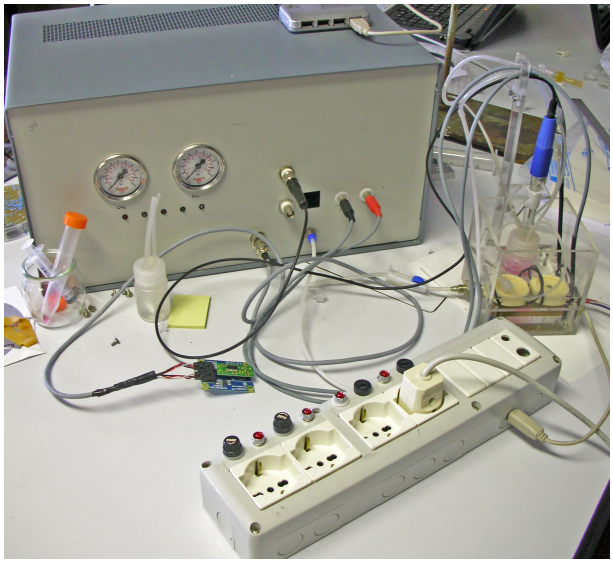

Figure 1.5: *The Bioreactor control unit, the heating box and the 220*V *sockets unit during an experiment.*

The Phidgets components were used to realize the control unit because these boards and sensors are very stable, resistant and with a well written driver and library package. The Phidgets libraries are compatible with

all the latest programming standards and languages such as C++, .NET, Matlab, Labview etc.

Heating Hox

The bioreactor heating system consists of a Plexiglas box where the mixing chambers and at most two modular culture chambers are inserted (Figure: 1.6.a). Distilled water heated by an electric 220V powered AC heater[37] is agitated using a bubble maker placed on the bottom of the heating box and connected to lab air line[1]. The bath and chambers temperatures are controlled by the two water proof temperature sensors placed directly near the mixing chamber.

The heating unit is not directly in contact with the water, but is placed inside a dedicated cooper support that prevents electric risk by a direct connection to the ground 1.6.b. The cooper unit is also designed in order to increase the heater exchange surface, the system takes at most 10 minutes to warm the entire water volume (≈400 mL) from 17 to 37°C[38, 39, 40]. The thermal coupling between cooper unit and heater is obtained through a silicone thermal gel, this gel is inserted in the internal part of the cooper unit and has no contact with the bath water. The used cartridge heater, a low power heater, was chosen in order to ensure a low thermal flow near the mixing in order to prevent over heating or non-uniform thermal distribution in the mixing chamber medium. The heater also has an internal temperature safety limit of 80°C that prevent any damage of the system in case of controller failure.

Culture chambers can be also heated independently using dedicated resistive heaters [41] placed directly under the MCmB trays. The resistive heaters are controlled by an electronic unit through a 24V PWM power regulator [42].

[1]The air line is split before the environmental control box inlet.

The heating box is equipped with a dedicated MCmB chambers tray which enables facile assembly of a bioreactor experiment under a laminar flow hood, without risk of contamination. The mounting tray is designed to fit perfectly the heating box only in one position in order to prevent risk of failure in the assembly phase. The tray system include also a pH Meter holder to prevent breakage of the very thin pH Meter tip during the bioreactor chamber procedures (sampling, cell insertion and removal etc).

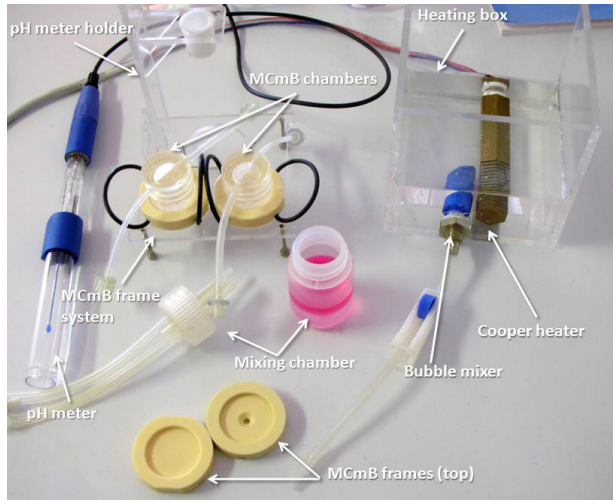

Figure 1.6: *The heating box and other bioreactor components during an experiment setup.*

Computer

The computer is plugged to the electronic control box through a USB cable and the signal is split by the previous mentioned USB hub. A netbook computer is used to control the whole system. Atom based boards for em-

bedded systems are widely available and will substitute the computer in the appliance.

Peristaltic Pump

To control the nutrient flow and the shear stress, it is necessary to regulate the speed of the peristaltic pump used to perfuse the nutrients inside the bioreactor, this control is operated by a dedicated connection between the pump and the electronic box, and is monitored in feedback mode through an appropriate control pin of the pump connected to the Digital I/O board. The peristaltic pump is 220V powered and is connected to the 220V sockets unit in order to allow an easily disconnection in case of failure.

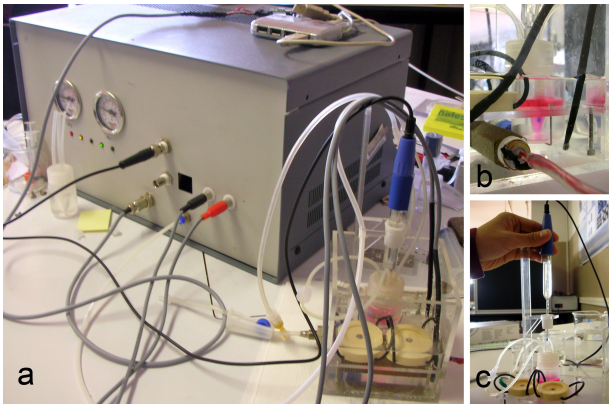

Figure 1.7: *A) The Control box with all the sensors plugged in and the heating box during an experiment. B) Detail of the mixing chamber in the heating box with the pH meter tip and the temperature sensors. C) The pH meter insertion phase.*

1.1.2 The Control System

A High Throughput bioreactor experiment employs many bioreactors with different cell culture chambers. A pathology can be simulated in one of the Bioreactors, and the others used for a control reference; the bioreactors environmental variables can be set in order to simulate one or more pathologies and observe the influence of this different environment on the physiology of the tissue function during an experiment. In order to deal with parallel management of multiple bioreactors a distributed programming framework for robotics has been used. The framework is called Robotics4.NET [43], and it has been developed to help programming the control system of a robot.

The framework architecture has been inspired by the human nervous system, and features the communication infrastructure required to connect the central system to the peripheral. Peripheral "organs" are called *roblets* and communicates with the central system, named *body map*, using XML messages. Communication is disconnected, and it is unreliable (it uses the UDP protocol), thus roblets have to continuously inform the body map about their state. The disconnected nature of the communication implies that a local crash does not imply a global crash. In fact each of these elements can be restarted without need for a global restart; this is an important aspect because if one unit of an experiment fails other units can continue functioning without need for aborting the whole experiment.

A program based on Robotics4.Net is composed of three ingredients.

- Brain: The core of the control system
- Bodymap: A sort of black board used to send and receive messages
- Roblets: The appendix of the system, like the parts of the nervous system. They read data from the environment and convert the

Brain signals into actions

In this case each of the bioreactor systems is composed of the electronic box connected to a netbook computer and it is perceived as a roblet (figure 1.8). Each Bioreactor (roblet) communicates through the network protocol with the supervision program installed on another remote computer hosting the Bodymap. Because the connections among the roblets and the bodymap are based on a datagram-oriented protocol the brain can be powered off and restarted afterwards without affecting the activity of roblets.

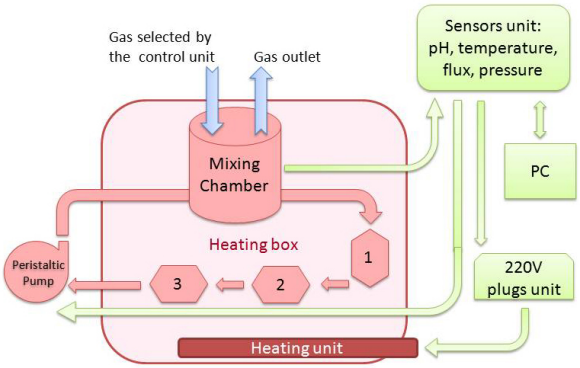

Figure 1.8: *Schematic flowchart of the entire Bioreactor system; in green are the electronic control units and connections, in red the culture chambers and the medium circuit, the gas connections and apparatus are represented in blue and the light red is the heating box unit that contains part of the system.*

This is a fundamental feature of this control architecture, each bioreactor is able to control it environment autonomously and it requires the connection with the supervision software (interface) just to receive the target values and to show the collected and stored data.

In a bioreactor system it is necessary to control many parameters: the amount of nutrients flowing in the cell culture chamber, the hydrostatic pressure inside the system, the flow generated shear stress on the cell culture, the flow of gas, the temperature flux generated by the heating system and the pH of the medium. These parameters are established using a graphical interface and sent to the roblets running on the bioreactors.

Since Ethernet is a communication bus, the graphical application used to control an experiment can receive UDP packets from several units running in parallel. This is very important in the context of HTS methodology [44]. The network also allows connections through the Internet, allowing remote monitoring of experiments, an important feature since experiments run for several days [43].

Each bioreactor roblet runs an instance of the bioreactor control library (BioreactorControl.dll)1.1.2 developed for the purpose using F# [45, 46], a functional programming language based on ML and developed by Don Syme et al at Microsoft Research^{TM}.

Data collected during the experiments is stored by the roblets on the hosting computers as XML files that can be directly opened with any spread sheet application supporting this format at the end of the experiment. This feature is implemented using the .NET XML serialization ability, allowing to directly write on a text file the state messages sent by the roblet to the bodymap.

Bioreactor control library

The Bioreactor Control library is developed in F# .NET and compiled as a dedicated library in order to maintain the control system independent of the roblet architecture. This hierarchical architecture is safer than a classic direct control approach, because the roblet and the control library

library are developed and maintained separately. With a control library independent of the roblet architecture it is possible to compile a direct control console interface that was used during the preliminary library debug phase and allow a direct check in case of hardware failure.

With a separated .NET library one can also choose to change the control architecture without completely re-design of the hardware control system. For example, it is possible to move to other control frameworks without need to re design the control algorithms and vice-versa.

The bioreactor control library defines the sensor reading units and the control strategies. Each sensor is designed not only as a reader, but as an active part of the system capable to influence the actuation strategy. The implemented sensor units are:

- pH sensor and gas selection unit
- pressure sensor and regulator unit
- temperature sensor and heater unit

Other sensors such as the environmental temperature and humidity probe are designed as reading unit and they do not implement an actuation behavior.

pH control strategy

As mentioned in [47], the pH is more complex to control than other parameters because of the delays between gas infusion and ionic dissociation, for this reason in order to control the pH in the medium a dedicated control adaptive algorithm, based on a step strategy was developed. This control algorithm is a high priority service running on the pH Sensor unit of the bioreactor control library.

The pH response to the diffusion of CO_2 and air is very difficult to predict, because it strongly depends on the environmental variables of the particular experiment such cell type, temperature, volume of medium, type of medium, hydrostatic pressure etc. Therefore rather than using a mathematical model [48] of the CO_2 and air diffusion in water, a function defined by an algorithm was used.

Before designing a complex and not linear algorithm a formal model of the algorithm using the Abstract State Machines (ASM) formalism [49] was defined. Using ASM any algorithm can be described in a formal mathematical system. It is a very effective approach for specifying the algorithm and study its properties.

The system continuously inserts air in the mixing chamber through an appropriate needle (blue zone in figure 1.9); when the pH goes over the safety threshold (selected by the user through the control interface) the control inserts a known CO_2 impulse (red zone in figure 1.9), in the mixing chamber, and waits a Delay Time. In this way a known amount of CO_2 is inserted in the mixing chamber and the control wait the CO_2 dissolution and reaction time before evaluate the effect of this operation. If the pH returns under the safety threshold the pH control routine is stopped, otherwise after the Delay Time has passed, the control inserts a new impulse of CO_2 and waits for the Delay Time.

The Delay Time is constant, the CO_2 spray amount (Spray Time) is adjusted at every step in a manner dependent on the value of pH and the derivative of pH with time [2].

The pH control strategy includes a safety logic test used to evaluate whether the pH is decreasing or not; in the case of a negative derivative, if the pH value is under the safety positive threshold (green zone in figure

[2]The derivate is calculated on a time span of 2 second because of the CO_2 dissolution time.

1.9, the control does not insert CO_2 because it is possible to assume that the last CO_2 spray was sufficient and the pH can return under the threshold in a short time; this test prevents an excessive fall in pH, because the CO_2 spray causes a large drop in pH but with a substantial delay.

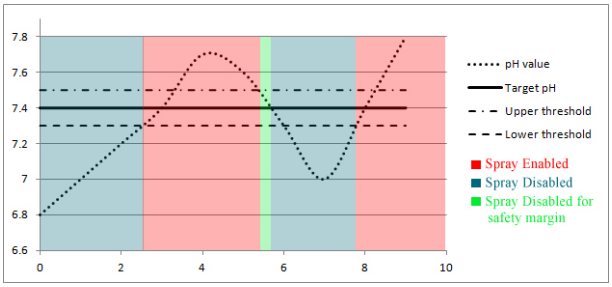

Figure 1.9: *pH control algorithm working zone.*

Equation 1.1 describes how the Spray Time is calculated by the bioreactor control library. The Spray Time to use is an increment of a default spray time (AverageSprayTime) calculated adding an amount proportional to the difference between the pH value and the selected target value (pH*) and also an amount proportional to the pH derivate [2].

$$SprayTime = AverageSprayTime + A(pH - pH*) + B(\frac{\Delta pH}{\Delta t}) \quad (1.1)$$

The multiplicative constants A and B are selected by the user through the user interface and depended on the medium and volume, the user can also choose the margin span through the pH margin variable of the interface.

With a formal model based on ASM [50] the constants for a water environment were predicted, but they are very sensitive to the physical conditions of the experiment (volume and type of medium, pressure, temperature). Consequently the ASM predicted constants were used as

default values that are suggested by the configuration interface. During the experiment, these constants can be adjusted in order to match the pH control parameter with the experimental set up. The code below is the pH control algorithm.

```
let controlloph = seq {

  while (true) do
    if (this.DeltapH < 0.) &&
      (this.PhValue < (this.targetValue + this.Range)) then
      yield 0.

    else
      while(this.PhValue > (this.targetValue-this.Range)) &&
        (this.controlState = InterfaceState.Auto) && ((this.DeltapH >= 0.)||
        (this.PhValue >(this.targetValue + 2.*this.Range))) do
          this.SetGas <- GasType.CO2
          this.spraytime <- this.averagespray +
            (float(this.avalue)*(this.PhValue-this.targetValue)) +
            (float(this.bvalue)*(this.DeltapH))
          yield this.spraytime

     this.SetGas <- GasType.Air
     this.waitingtime <- this.averagewait
     yield this.waitingtime

     yield 0.
   }
```

As shown in the pH control algorithm F# code 1.1.2 the *seq* construct was exploited to let the compiler generate a finite state automa that performs the computation defined in the body and pausing and saving the state of the computation whenever the *yield* expression is reached. In the control library the pH control sequence is triggered by the pH sensor event handler and it is active only if the control state is set to Auto, otherwise the routine will return 0 that is considered as a timer stop. The pH sensors require a temperature compensation that in the

control library is obtained through the two temperature sensors inserted in the heater box, the temperature sensor used as pH compensator can be selected throught the user interface.

Pressure and gas flow control

The pressure in the mixing chamber is obtained through a needle placed on the outlet tube in order to have a high flow resistance on the outlet tube.

The pressure is controlled through the serial to PWM board that generates the analog 0-10V control signal for the pressure regulator. Note that the system does not use a calibration function that converts the digital value sent to the serial port to the pressure regulator obtained pressure.

Typically the pressure regulators are designed to be used in a closed system and the imposed pressure is guaranteed for a static environment. In the case of an open system with flow the pressure read-out is not linear and there may be large errors between the real pressure and the read-out 1.10. In this case the mixing chamber has an outlet connection and the system is always subject to flow, it is consequently impossible to use the data sheet pressure regulator correlation factors.

For this reason use a ramp approach has been followed; the control library use the pressure sensor to read the mixing chamber pressure and increases or decreases the PWM signal in order to reach the target pressure. In this case the pressure regulator under flow dis-alignment issue can be adjusted, and the system can be actuated in a flow control strategy in which the the flux sensor instead of the pressure is used as feedback.

The pressure in the mixing chamber is obtained with a flow resistance imposed by a needle, with this ramp approach the outlet needle diameter can be changed in order to change the flow rate/pressure ratio without

needing to re calibrate the system.

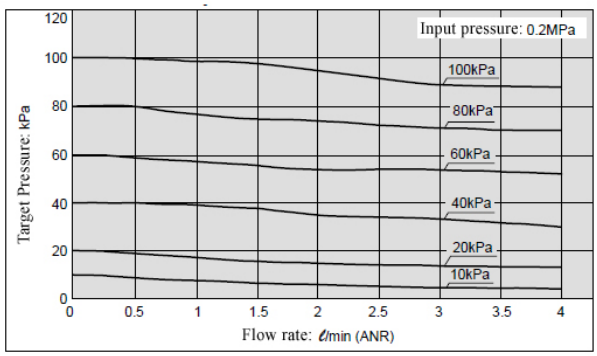

Figure 1.10: *Pressure regulator characteristic at different flow rates.*

The iteration approach is incremental it is not necessary to send more than one step per time, the ramp speed can be chosen through the user interface in order to change the pressure adjustment and reactivity speed. The user can also choose the pressure threshold that is used to calculate the margin around the target pressure where the pressure control is stopped and the pressure attained is considered acceptable.

All the control variables and the flux or pressure control strategy can also be selected through the user interface during an already started experiment.

The control routine also implements a safety control test that rises up an exception in case the pressure regulator is unable to reach the target pressure, this can occur for example if the outlet needle diameter is too large and the flux imposed by the pressure regulator is unable to pressurize the mixing chamber at the requested value1.1.2. The routine below reports the code for the safety control test.

```
let DoControl (value:float) (target:float) (range:float)  =
  if (value < target-range) && (this.State = InterfaceState.Auto) then
```

```
    if not(this.pwm = 127uy) then
      this.pwm <- this.pwm + 1uy
      pwmset this.pwm

    else
      this.timer.Stop()
      this.pwm <- 0uy
      this.Pressuretrigger(new StatusEventArgs(EventType.targetpressure_fluxtohigh))

  else if (value > target+range)&& (this.State = InterfaceState.Auto) then
    if not(this.pwm = 0uy) then
      this.pwm <- this.pwm - 1uy
      pwmset this.pwm

    else
      this.timer.Stop()
      this.pwm <- 0uy
      this.Pressuretrigger(new StatusEventArgs(EventType.targetpressure_fluxtolow))

  else
    this.timer.Stop()
```

The GUI Software

The Graphical User Interface is developed in C# and is based on a multi-tab structure;the GUI is used to read data from the bioreactors and to setup the experimental variables of each module. The user interface also serves as a tool for sensor calibration, in order to perform the sensor calibration with the same software used for bioreactor control. The user has control over the experiments, including a manual overdrive, though the autonomous control software running on the roblet avoids commands that could damage the system or the experiment. When the User Interface is open, it seeks for connected bioreactors; when one is found, the GUI switches in the view mode figure 1.11(a). In this section the data pertaining to each bioreactor can be viewed by selecting its menu and experimental settings can be changed through the configuration tab.

The Bioreactor control GUI has a set of default variables stored in the system registry during the installation, all the changes to this variable such as calibration or control parameter are stored on the Windows registry and are saved as new working values. The installation default values can be easily restored with a dedicated button1.11(b).

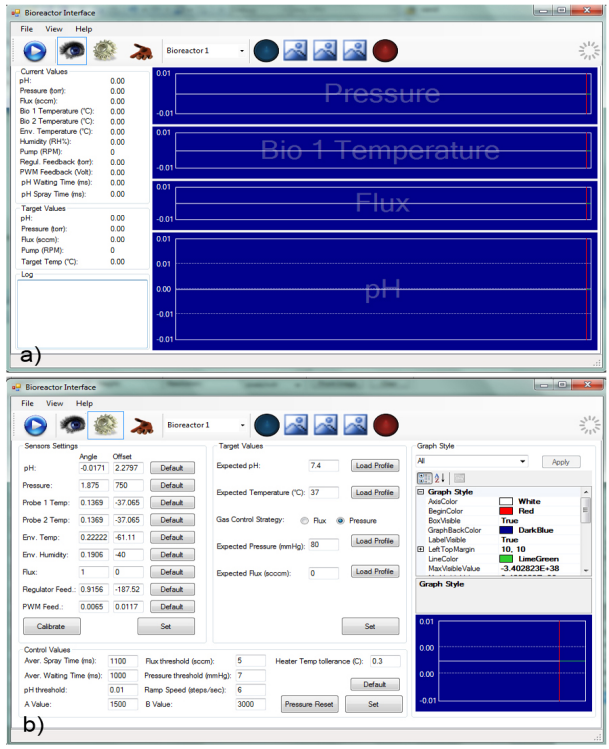

Figure 1.11: *The bioreactor control user interface in the view mode (a) and in the config mode (b).*

1.2 Environmental Control Test

The Environmental control system was tested in order to ensure its time stability and also to calculate and verify the accuracy and resolution of the sensors and electronic acquisition units. In order to verify the system stability, a 48h experiment was performed. A mixing chamber filled with 5 ml of fresh medium was placed in the heating box, plugged to the peristaltic pump and the experiment started. The target values for this experiment where: pH 7.4, Temp 37°C and pressure 30 mmHg. No cells where used in these preliminary experiments because cell cultures do not significantly influence the maintenance of the environmental variables. With this experiment the capability of the system to maintain the target environmental variables without problem for long periods was demonstrated. When the experiment starts, the control chooses the gas to insert in order to keep the pH near the target value, with a tolerance chosen by the user (in this case 0.04 pH units), the first 10 minutes of experiment show an excursion of 0.2 pH units around the target pH values because the controller has to adjust the CO_2 *Insertion Time* and the *Waiting Time*1.1.2 in order to fit the experimental setup[3]. After the starting phase, the pH excursion is reduced to a range of ±0.1 pH unit around the target value that is impossible to remove due to the non linear and large delay time of the pH regulation process. This experiment enables calculation of the experimental resolution of the pH control system ; the pH reading resolution is of 0.01 pH unit and the target value can be chosen with a resolution of 0.1 pH unit, with a control tolerance down to 0.1 pH unit.

Unlike the pH controller, the pressure control system does not show any adjusting phase during startup. When the experiment starts the

[3]Medium type and volume, chosen pressure, target pH and other experimental variables which influence the pH control routine.

system is able to rapidly reach the imposed target pressure. The pressure reading resolution is of 0.1 mmHg and the target pressure can be chosen with steps of 1 mmHg with a tolerance (used as controller activation threshold) down to 1 mmHg. Due to the complicated gas circuit and to the problem related with the inability of the pressure regulator to work with high accuracy in case of continuous flow, the target pressure is maintained with an oscillation around the target value of ± 1 mmHg that is enough to ensure a stable cell culture stimulation. The silicone tube connections and the presence of an air volume in the mixing chamber[4] help to smooth these pressure oscillation acting as a low pass filter. As described in the pressure controller code section 1.1.2 the pressure regulator use a ramp approach to be controlled, the ramp speed can be chosen in the range 1-10 samples per second, higher ramp speeds imply a faster pressure controller reaction but they could introduce oscillations in the system. The default ramp speed is set to 3 steps per second and can be be adjusted by the user depending on the experimental setup (needle dimension, mixing chamber volume, etc).

The target temperature is reached after 15 min since the experiment starts due to the low power of the cartridge heater and to the safety cartridge temperature limit imposed at 80°C. After the warming phase the temperature is kept around the target value with an oscillation that is dependent only on the temperature tolerance imposed by the user. The temperature reading resolution is of 0.05°C and the target value can be chosen with step of 0.05°C and with a tolerance down to 0.1°C. The temperature control tolerance could be lower but the minimum level was fixed to 0.1°C in order to prevent fast switching of the cartridge heater

[4]The mixing chamber has an internal volume of 12mL but is filled with 5 ml of medium, the 7 mL of air helps to smooth the pressure oscillations working as a capacitor.

that could damage it.

After 48h of experiment, before the control routine was halted, some failure simulations where made. In order to investigate the stability of the system in case of failure of the lab gas lines the main air and CO_2 valves where alternatively closed. When the CO_2 is missing, the system is unable to keep the pH under the target values and the pH values slowly rise up as consequence of the air insertion. The system pressure is maintained but with higher oscillations around the target value due to the pressure falling down when the CO_2 gas is selected. In case of air line failure the system presents the same pressure instability problem but the pH fall down very fast due to the higher diffusion of CO_2 in water than O_2. In both cases the system do not stop its control of the other variables such us temperature, pump speed etc and data collection is still guaranteed. If the broken gas line is repaired the system works to reach the selected target values again.

A network failure was also simulated. As previously described in section 1.1.2 the control software is split between a netbook or embedded board that acts on the system through various peripherals and a supervisor that is used to setup the experimental targets and to show the collected data. In case of network disconnection, the system does not present any changes because the entire control system is not network dependent, and the BioreactorControlLibrary is hosted by the roblet running on the netbook. Without network connection is not possible to change the target values or observe the bioreactor data from a remote station in real time. In this case, using a netbook, the bioreactor control is still guaranteed through the netbook monitor, in case of a system equipped with an embedded board a computer with a bioreactor GUI installed on it can be connected to the environmental control box in order to interact with it.

The bioreactor system is designed not only to control the environ-

mental variables but also to impose stimulations to the cell cultures, in order to verify the environment stability during a pressure stimulation experiment the system was tested using a pressure profile as target value. The first experiment was to test the pressure regulation response speed, and it was a profile where three different pressures where imposed (30, 90 and 120 mmHg). As shown in figure 1.12 the system instantly reaches the imposed pressure and the gas flux changes to maintain the required pressure. The flux also depends on the needle used as gas outlet resistance[5] (described in section 1.1.1), the pH is controlled independently of the selected pressure, but the oscillations around the target value are influenced by the changes of the gas flow rate.

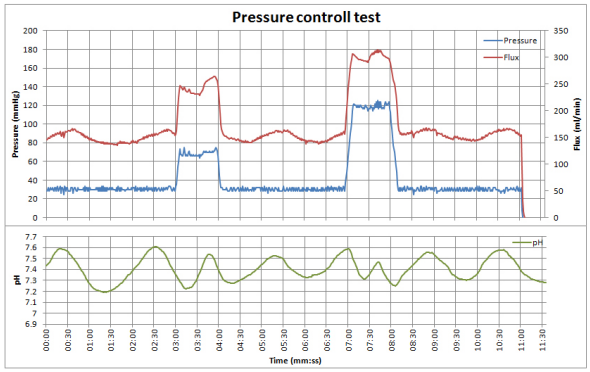

Figure 1.12: *Pressure maintaining test, a profile of three pressure is imposed (30, 90 and 120 mmHg).*

As shown in figure 1.12 the error on the pressure value is independent of the pressure level and is a consequence of the electronic noise and of the pressure regulator inaccuracy. The lowest pressure that the system is

[5]For these experiments a syringe needle with a diameter of 21 Gauge was used (internal diameter of 0.495mm).

able to maintain depends on the mixing chamber outlet needle diameter and also on the limits of the pressure regulator hardware. The tests demonstrate that a target pressure lower than 15 mmHg results in an unstable pressure control due to the inability of the pressure regulator to maintain very low pressures[6]. In these experimental conditions, the gas flow rate is very low and the inserted CO_2 amount is not enough to keep the pH at the desired value, this results in a very high pH oscillation.

To obtain very low pressure levels, the system has to be controlled in flux mode and the mixing chamber outlet opened (without a needle), in this configuration the pressure in the mixing chamber can be regulated in the range 0 - 30 mmHg and the flux is enough to ensure stability of the pH control . In case of flux control the system works switching on and off the pressure regulators, and the gas mixer and mixing chamber air volume are used as capacitors to smooth the switching oscillations. In this case the pressure is not a target variable and its stability is not guaranteed, the system works only in order to keep the flux and pH stable.

Another pressure control test was conducted in order to demonstrate the system capability to generate a pressure profile used for cell stimulation. As described in [51], in order to investigate the retinal glaucoma disease, rat retinas are placed in bioreactor chambers and stimulated with cyclic pressure profiles. In this case a stimulation path with a base level of 30 mmHg and seven steps of 120 mmHg was defined.

As shown in figure 1.13 the system is able to generate pressure profiles and to keep the pH in acceptable ranges also in case of continuous flux or pressure changes.

The pH control algorithm was tested for a pH perturbation due to ex-

[6]The pressure regulator data sheet indicates a pressure regulation range of 7.5 - 750 mmHg in zero flow conditions. In flow conditions the pressure range is reduced.

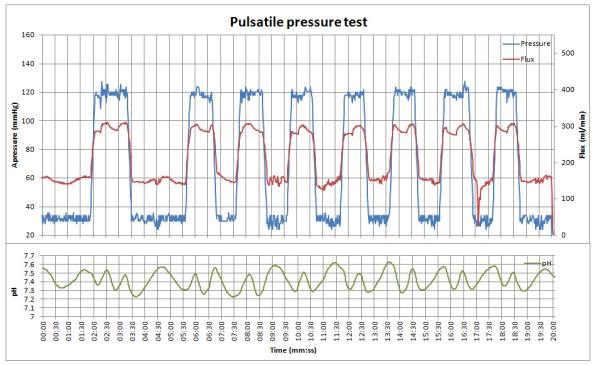

Figure 1.13: *Pressure control test for pressure profile generation. The requested path was made of seven pressure steps at 120 mmHg with a base line of 30 mmHg.*

ternal stimuli. The mixing chamber was filled with 5mL of fresh medium and after the pH stabilization phase (3 minutes after the beginning of the experiment), 0.5mL of acid solution with pH 4 was injected through one of the mixing chamber medium tubes and the system reaction observed. When the pH reached the new stable point, a new external stimulus was imposed by injecting 0.5mL of basic solution with pH 10. In both cases the controller is able to adjust the pH value inserting Air or CO_2 with impulse times dependent on the pH error. As shown in figure 1.14 the pH adjustment time in case of acid injection requires longer times than in case of base injection, this is due to the lower oxygen diffusion time than CO_2. The controller is consequently faster in decreasing than increasing the pH.

As demonstrated by these tests, the Environmental control box is able to maintain the bioreactor cultures in the environmental conditions chosen by the user also in case of external perturbation or variable target values. The system is also able to impose variable stimulation and it can

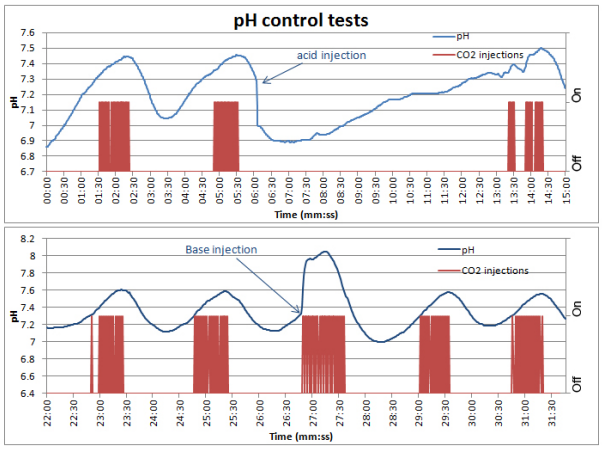

Figure 1.14: *pH control tests, an acid and base insertion is done in order to test the pH controller capability to react to external stimuli.*

be used as a long term cell culture stimulator.

Chapter 2

P.GIO Pressure Generator of In-vivO environments

The environmental control is a complex array of *sensors, transducers and actuators* able to control different variables of the bioreactor environment. During this work a "light" version of the environment control system was also developed. With this "lighter" system the environmental variables (5% CO_2 atmosphere, humidity, tempertaure and sterility) are maintained using a classic CO_2 incubator. The P.GIO (Pressure Generator of In-vivO environments) system is an innovative free standing unit able to control stepper or DC motor in order to generate controlled pressures or micro movements. As described in figure 2.1 P.GIO is a component of the SUITE platform and can be used as autonomous motor control, as environmental control box "slave" actuator or in connection with a PC for a direct user interaction. The P.GIO DC motor control capability can be used to impose *hydrostatic* pressure stimuli on cell cultures through dedicated stimulation chambers described in the next sections 5, as viscous material extrusor in micro-fabrication processes or as drug dispenser in connection with the Environmental control box. The stepper motor control capabilities can be used for the generation of *squeeze* pressures for cell stiumlation as described in 5.1 or as micro positioning system.

The P.GIO system was designed in order to be easy to use, stable

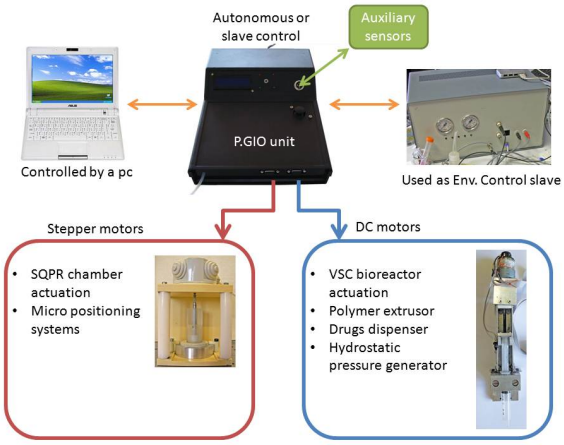

Figure 2.1: *P.GIO features and connections schema.*

and autonomous. With this system is possible to design a wide range of experiments where pressure stimulations, micro movements, polymers extrusion or drug tests are studied on cell cultures with or without the environmental control "supervision".

2.1 Material and Methods

2.1.1 The P.GIO Hardware

P.GIO is an all inclusive and standalone unit able to control DC or stepper motors, it is equipped with an LCD display [52] (16 characters per 2 lines) and the user interaction is provided by a 2 axis joystick with one button. The motors are plugged in the front side of the unit through two DB9 connectors and only one motor can be controlled at any one time. The motor type selection is done through a switch placed on the top of the unit where the status LEDs are also located. The unit is

powered at 220V AC and is equipped with an internal stabilized power supply board described in section 2.1.1. The P.GIO unit is controlled through a micro controller board based on an Atmel micro controller and programmed in a programming language close to C (described in section 2.1.1). In case of connection with the environmental control unit, the system can be controlled through the USB connection located on the back of the unit and the experimental variables chosen through the bioreactor supervising GUI. The USB connection is used also for firmware upgrades of the micro controller programming GUI. The system box is completely made of plastic to allow easy cleaning of the system and the power unit is connected to ground and protected through a fast fuse.

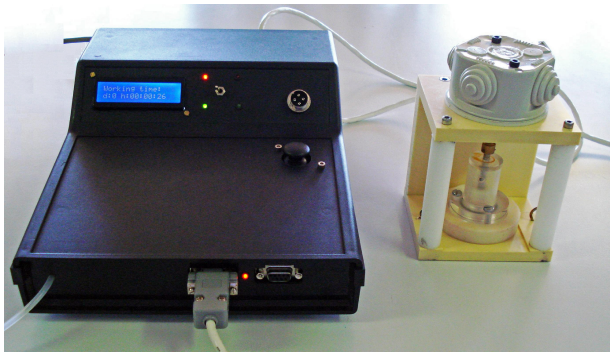

Figure 2.2: *The P.GIO unit with the SQPR chamber plugged in.*

The two motors unit are based on two dedicated motor drivers: the L298 H-Bridge for the DC motor and the Easy Driver controller for the stepper motor both described in section 2.1.1.

The core of the system is the interface board which is designed to connect all parts of the P.GIO system and to adjust and filter the signals coming from the sensors and going to the motor drivers or to the display. In addition the pressure sensor, the joystick, the status leds, the

motor switch selector and the auxiliary connector are all plugged into the interface board.

The pressure sensor is the same used in the environmental control hardware [26] and is used here in the hydro static pressure working mode as pressure feedback. The pressure sensor is powered with a 5V stabilized line from the power supply unit 2.1.1.

Arduino ontrol board

The control board used for the P.GIO system is "Arduino" [53]. Arduino is an open-source electronics prototyping platform based on flexible and easy-to-use hardware and software. It is intended for artists, designers, hobbyists, and anyone interested in creating interactive objects or environments.

Arduino is based on the ATmega168 [54] micro-controller. It has 14 digital input/output pins (of which 6 can be used as PWM outputs), 6 analog inputs, a 16 MHz crystal oscillator, a USB connection, a power jack, an ICSP header, and a reset button. It contains everything needed to support the micro-controller2.3.

We decided to use Arduino for this project because this platform since it is cheap, ready to use and backed by a large developers community that continuously releases bug fixes and code snippets.

The complexity of the P.GIO system required all the the digital input/output pins of the Arduino board to be controlled (7 are required just to control the display). In order to enlarge the number of available digital pins we changed the default Arduino configuration converting two analog pins into digital ones. This configuration change is allowed by the Arduino firmware, it requires an explicit declaration in the configuration part of the firmware and it can not be changed during the run time.

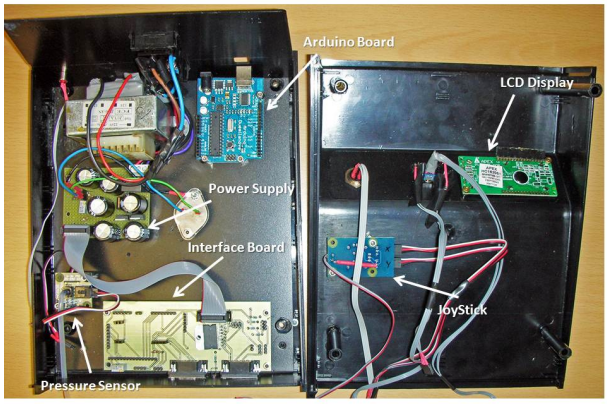

Figure 2.3: *The P.GIO box with all his components.*

The power supply board

The P.GIO system requires different power supply voltages, a stabilized 5V supply is required for the Arduino board, the Phidgets pressure sensors and the display, the DC and stepper motors required 12V supply with high current capabilities and a stabilized ±12V supply is required for the auxiliary port where a signal processing electronic unit could be plugged 2.3. The motor supply voltage is usually 12V but could also be changed in case of use of a different motor or actuation unit.

In order to realize an all in one solution that completely supplies the P.GIO hardware a dedicated power supply board has been designed. The P.GIO power supply board is based on a double secondary transformer plugged to a diode bridge with a current capability of 6A. The various voltages are obtained through 4 dedicated voltage regulators. The +12V is obtained using a 7812[55] voltage regulator and the -12V using a 7912[56] voltage regulator. The +5V stabilized power supply is obtained

limiting the already stabilized +12V line with a 7805[57] voltage regulator. All the different voltages are stabilized with a set of electrolytic capacitors of 100µF and 100pF, in the case of the 5V line, a ceramic capacitor of 10ρF is also used to ensure a very low ripple signal to avoid electronic noise into the Arduino board or in the pressure sensor. The +12V with high current capabilities line, is obtained through a LM338[58] a voltage regulator able to drain until 5A. The LM338 is mounted using a dedicated adjustable feedback resistor in order to allow a voltage adjustment in case of motor changes. The high current 12V supply is stabilized using a bigger electrolytic capacitor of 450µF.

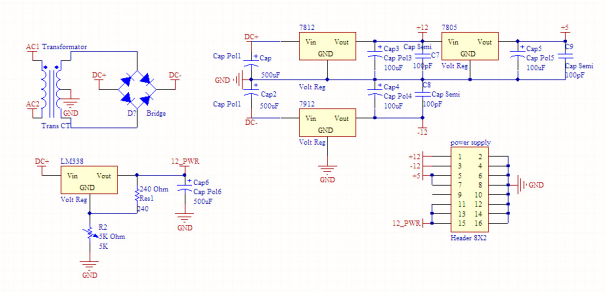

Figure 2.4: *Power supply board schematic.*

The P.GIO interface board

The P.GIO interface board is the routing unit of the system; it is equipped with a large number of connectors and with the two motor drivers 2.5. The interface board is a PCB designed during this work and industrially printed in order to ensure a high quality and stable product. This interface is designed in order to prevent assembly error and only one way connectors are used. In the interface board, the signals coming form the Arduino board are routed to the various system components. One of

the various interface connections that requires a detailed description is the motor selector switch connection. This selector switches the signals coming from the pins Analog 0 and 1[1] of the Arduino board between the two motor drivers, consequently only one motor driver per time can be controlled by the system. When a motor driver is selected, the other one is disconnected by the system and its control pins are floating. The LCD display is connected to the Arduino control pins through a dedicated 16 pin connector of the Interface Board. This connector routes the seven display control pins to Arduino digital pins 4 to 10 and to the back light power supply and contrast adjustment unit located on the interface board.

The Joystick is connected to the interface board through a 4 pin connector and the button and position signals coming from the joystick are routed to the digital pin 13 and analog pin 5 of the Arduino board.

A reset button placed on the rear panel of the P.GIO system is also connected through the Interface Board, and is used in case of failure or after the firmware upgrades.

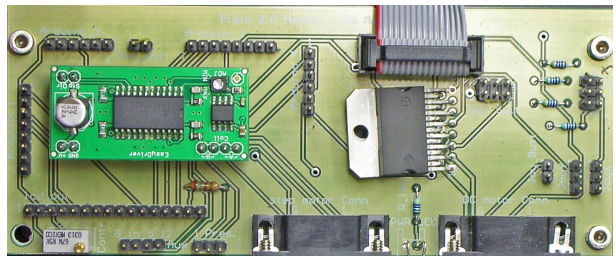

Figure 2.5: *The P.GIO interface board equipped with the motor drivers during the assembly phase.*

[1]Used in this case as digital pins.

Motor drivers

As previously described, the P.GIO system is able to control stepper or DC motors. Only one type of motor per time can be plugged to the system and the motor selection is done through a dedicated switch. The stepper and DC motors requires two different control strategies and power managements and these two different control approaches are managed by two separate motor drivers. Both these drivers are powered by the High current power line and the supply voltage is usually regulated to 12V.

Stepper motor driver Easydriver v3.0

The EasyDriver is a stepper motor driver able to drive up to about 750mA per phase of a bi-polar stepper motor. It is a chopper micro-stepping driver based on the Allegro A3967 driver chip[59]. It is permanently set to use 8 step microstepping mode which allows a control resolution 8 times *higher than that of a single step mode.*[2] The EasyDriver is equipped with a trimmer that allows the current per phase to be adjusted from about 150mA to 750mA. It can take a maximum motor drive voltage of around 30V, and includes on-board 5V regulation for the internal logic, so only one supply is necessary.

Due to the easy driver current capabilities, two low power stepper motors could also be connected to the P.GIO system in a parallel control strategy in order to run two stimulation experiments in parallel. For the two motor parallel connection a 1 to 2 DB9 adapter is required.

DC motor driver L298

The L298 is an integrated monolithic circuit in a 15-lead Multiwatt and

[2]In the microstepping control mode, the motor phases are powered at different voltages and not using a ON/OFF strategy, in this way is possible to divide each motor step in 8 sub steps positions, increasing the motor resolutionby 8.

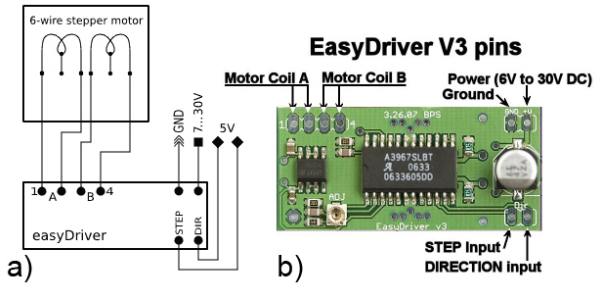

Figure 2.6: *a) The easy driver connection scheme and b) the EasyDriver V3 board.*

PowerSO20 packages. It is a high voltage, high current dual full-bridge driver designed to accept standard TTL logic levels and drive inductive loads such as relays, solenoids, DC and stepping motors. Two enable inputs are provided to enable or disable the device independently of the input signals. An additional supply input is provided so that the logic works at a lower voltage. In the P.GIO system, the L298 driver is used to control the DC motor through two dedicated signals coming from the motor selector switch. The l298 driver is able to control contemporary two DC motor, but here is used to control only one motor. The driver input pin 1 and 2 are connected through the motor switch to two Arduino digital pins and are used to select the state of the motor (forward, backward or brake). The motor speed is chosen through a PWM signal generated by the Arduino board on pin 11 and directly connected to the L298 enable 1 pin through the Interface Board. The DC motor control system requires three pins and when the stepper motor routine is chosen (only two Arduino pins are required for stepper routine) the Arduino digital pin 11 is set to low level in order to disable the L298 power circuit (no PWM signal on pin 11 is generated in stepper control mode). The

L298 power pin is connected to the high current line and the logic power pin is connected to the 5 Volt stabilized line both provided by the power supply board2.1.1.

2.1.2 The P.GIO Control Software

The P.GIO firmware was developed in order to allow high usability of this stimulation system, the software is written in the Arduino language (very similar to C), and is based on two separate control and programming parts: The DC motor and the stepper motor control routine. When the system is turned on, the user is invited to select the experiment type. The user interface does not ask if the user is interested in a stepper or DC experiment, the different type of pluggable chambers are shown in the menu and the software knows which motor is required for each chamber. When the experiment is chose, the user is invited to insert the control variables and the experiment targets typical of the selected experiment. After the programming phase the experiment starts and can be stopped using the joystick button. The experiments can be stopped and the target variables changed, but is not possible to change the experiment type without resetting the P.GIO.

Stepper motor control routine

To control the stepper motor, the software has to generate a set of pulses on the easy driver speed pin (analog 0) and choose the direction using the direction pin (analog 1)[3]. The pulse frequency is proportional to the obtained motor speed and the stepper motor direction depends by the direction pin status. The Stepper motor routine is a cycle where the step

[3]The speed and direction pins are Arduino's analog pins used in digital mode as previously described.

pin is raised with a frequency proportional to the requested motor speed and where each step is counted incrementing a variable used to trace the stepper motor position. The stepper stimulations are usually cyclic and they are implemented comparing the motor position counter with the cycle length variable. When the motor reaches the start or the end of the cycle position (position is egual to 0 or to cycle length), the motor direction is inverted and the speed changed. In the case of the SQPR Chamber stimulation 5.1 the stepper motor pushes a piston in a chamber where a cell culture is inserted. The piston's speed of approach speed has to be very fast in order to generate a pressure on the cell culture, likewise the piston has to be lifted up very slowly in order to avoid generating negative pressure in the chamber. In this case the cycle length is chosen during the programming phase and stored as a variable. During the "push and lift" phases two different speeds, calculated using the variables stored during the programing phase, are used. The stepper motor routine is implemented using a *while* cycle that can be interrupted pushing the joystick button. In case of experiment interruption, the software activates a special routine that brings the piston/stepper motor to the "Home" position in order to allow a re-start of the experiment without requiring a new system calibration. The home position is chosen during the calibration routine of the programming phase and is based on a routine that uses the stepper motor to measure the piston/motor range of motion. The home position is not coincident with the upper or lower limit of the stimulation cycle but it is chosen in order to allow chamber assembly.

The stepper motor routine can also be controlled through the serial USB connection of the P.GIO system. In this case the experimental variables can be selected and programmed through the bioreactor GUI and after the experiment starts the P.GIO system controls the motor actuation procedure autonomously. The USB connection can be used also

to stop and start the experiment and allow changing of the frequency and the range of the stimulation over the time. With this system plugged into the Environmental Control unit the SUITE system becomes a complete platform for long term complex cell stimulation.

DC motor control routine

The DC motor routine is based on the generation of a PWM signal used to control the motor speed and the direction pins. In the DC routine the pins required for the direction management are two, one more than in the stepper motor because of the possibility to move the motor forward, backward or brake it. Forward and backward movements are chosen alternating which pin is set to high and which is set to low, the brake mode is obtained raising up both the direction pins which acts like an electromagnetic brake. The brake routine is very useful to actuate a fine control of the motor position and is used in the VSC (Vascular Stimulation Chamber)2.2.1 experiments. The DC motor routine is based on a while cycle where the pressure sensor is continuously read in order to know the pressure generated by the system and the motor moved in order to keep the chamber pressure constant. As described in the next section, the P.GIO DC motor mode is used to compress or decompress a syringe pump that generates a hydrostatic pressure in a bioreactor chamber. The routine is not a simple motor on off approach, the system changes the motor speed during the approaching phase in order to allow a fine positioning of the piston. During the pushing phase the pressure is constantly read and compared with the target pressure, the compressing motor speed is constant *(approaching speed)* it was chosen during the firmware testing phase and it is dependent on the mechanical properties of the system (gear ratio, motor maximum torque etc). When the chamber pressure is 20 mmHg lower than the target one, the speed is increased to 30%

(proximity speed) for 300ms after that the motor is braked. This strategy was experimentaly developed considering the mechanical property of the syringe actuator and it is designed in order to allow a position reaching using the system's inertia. With this approach the inertia provided by the increase of the speed near the target point allows the system to reach the target during the braking phase. If the system were be actuated by just stopping the movement and braking the motor in a pressure threshold around the target, the system would oscillate around the target due to the starting and stopping phase. The increase of the speed before the target allows the breaking phase to be used as a fine positioning strategy. Owing to the complex circuit and the presence of biological samples during experiments, pressure drops are quite likely. For this reason the system continuously controls the chamber pressure even in the braking phase and if the pressure falls 5 mmHg below the target pressure the system applies a 300ms pulse at the *proximity speed* and brakes the motor again. This strategy has demonstrated to be the best solution to perform micro movements of the piston which help to keep the pressure chamber stable during the time. In case of tube disconnection, a failure routine is implemented through the continuous check of a micro switch placed at the end of the syringe actuator. If the safety switch is pushed the system retracts the piston for 1s at the approaching speed and goes into failure mode. If the system is in failure mode a user interaction is required and the system can be re activated pushing the joystick button and positioning the piston on a new starting point. The failure mode is implemented in order to prevent of motor or mechanical parts in case of tube disconnection.

The DC motor part of the firmware also includes a serial control mode in which the motor movements are controlled through the USB serial communication. This routine is used in case of connection of the P.GIO

system with the Environmental control box. We decided to design the P.GIO system as a slave of the Environmental Control system, in order to use it as an actuator and to do all the calculations and the feedback in the control roblet. The value read by the P.GIO pressure and auxiliary sensors is continuously sent to the master through the serial connection and the system has a while cycle that reads the serial incoming data (motor speed, direction and duration of the action) and actuates the system moving the motor. This connection allows the system to be used as an external pressure generator of the SUITE system that can be used for example secondary pressure generator or as a drug dispenser or as a extrusor for polymers and viscous materials such as alginate or agarose [60].

2.2 P.GIO Controller Tests and Results

The P.GIO system was tested for both the control strategies and routine, in order to check both the hardware connections and motor control drivers.

2.2.1 DC motor tests and results

The P.GIO system was tested for the DC motor control part using the syringe pressure generator system. In this configuration it is possible to generate hydrostatic pressure in a closed chamber and it is used to pressurize bioreactor chambers or as an extrusion or dispensing system.

The system consists of a commercial syringe inserted in a linear actuator that compresses the syringe in order to pressurize a chamber connected to the syringe outlet. The linear actuator is moved through a DC motor with an embedded encoder (not used in this experiment). The pressure feedback is obtained using a T connector to split the syringe

outlet to the chamber and to the P.GIO pressure sensor as described in figure 2.7. For the system tests we used a bioreactor mixing chamber previously described 1.1.1 filled with 5 ml of medium. The system was programmed to maintain different pressures inside the chamber (20, 80, 130, 500, 1000 and 1300 mmHg) for 24h, at the end of the experiments the system was switched off and the chamber pressure tested using the Environmental Control System1.1.1 as reference[4]. The tests demonstrated that the P.GIO hydrostatic pressure generator system is able to maintain pressures up to 1300 mmHg for 24h without external intervention. This system therefore be used as hydrostatic pressure generator for bioreactor chambers and can be used as lighter version of the Environmental Control system. With this system a pressurized cell culture environment can be run in a laboratory without a piped gas supply as a stand-alone application or as pressure generator apparatus of the SUITE system.

The pressure generator system can also be used as a drug dispenser to be connected to the Environmental Control unit, and controlled through the Bioreactor interface. The system can be controlled in order to insert precise amounts of drug in the bioreactor circuit during the experiment to automate drug testing protocols.

In addition this system can be used as a pressure generator system for polymer extrusion and can be plugged to a CAD/CAM system for scaffold fabrication.

2.2.2 Stepper motor tests and results

The stepper motor P.GIO control capabilities were tested using the SQPR bioreactor chamber described in section 5.1. This chamber actuates a piston through a linear stepper motor with a resolution of 16.7 μm per

[4]The environmental control pressure sensor tube was plugged in parallel to the P.GIO sensor.

Figure 2.7: *The P.GIO system connected to the hydrostatic pressure generator.*

step[61]. The stimulation given by this innovative bioreactor chamber is a cycle of compression and decompression where the compression and decompression phases have two different speeds and where the period of the stimulation cycle has to be very accurate.

The system was tested for this control routine at three different stimulation speeds (1, 2, 5 sec. of cycle duration) in order to check the stability and accuracy of the system during the time. The SQPR chamber equipped with the linear stepper motor was placed in a 37°C, 5% CO_2 incubator in order to test the system in the real working conditions, and plugged to the P.GIO control unit through the dedicated cable. In order to verify the stability of the system, the piston action range was set to 2mm[5] and the action range was measured using the SQPR chamber base

[5]The SQPR piston goes through a cycle where the distance between the

as reference. After 24h the SQPR was stopped and the piston action range checked in order to identify misalignments. A misalignment of the action range could mean that the stepper motor skips some steps during the run with a consequent shift of the action range particularly in long time experiments.

The stepper motor tests do not shown any action range misalignment demonstrating that the system does not skip any steps during the experiments and that the control routines are stable over time. This system can be used as innovative cell stimulation system, independently or in connection with the Environmental Control system, creating a complete high throughput stimulation bioreactor SUITE.

lowest and the upper points can be changed.

Chapter 3

MCmB (Multi Compartmental modular Bioreactor) chamber design

The microwell (MW) plate has become a standard in cell culture. The plates are available in a variety of formats (6-1536 wells), although for most general cell culture and tissue engineering applications, 12, 24, 48 and 96 well formats appear to be most common [62]. However, the complexity of the physiological environment is not replicated in petri dishes or microplates. All cells are exquisitely sensitive to their micro environment which is rich with cues from other cells, and from mechanical stimuli due to flow, perfusion and movement. Microwells do not offer any form of dynamic chemical or physical stimulus to cells, such as concentration gradients, flow, pressure or mechanical stress. This is a major limitation in experiments investigating cellular responses in vitro since the complex interplay of mechanical and biochemical factors is absent [63]. Most researchers and industry now accept that classical in vitro experiments offer poor predictive value or mechanistic understanding, and there is a shift to new technologies, generally in the form of bioreactors. A large number of bioreactor systems for cell culture have been designed and described. They range from commercial bioreactors which apply laminar flow [64],

membrane systems [65], rotating vessel systems [66] to purpose designed devices for specific tissues such as blood vessels [67], heart valves [68] and livers [69]. In most cases, the bioreactors described are custom designed for specific requirements and necessitate the use of particular seeding methods or scaffolds with narrow dimensional and design specifications. Size-wise they can be large scale bioartificial livers with several billions of cells and several milliliters of fluid [70] down to microfluidic systems with a few hundred microliters of medium [71]. In fact microfluidic microfabricated bioreactors which enable the culture of different cell types in a shear stress controlled environments [72], are highly popular, but remain very much a niche research tool. In a micro-bioreactor, the cell culture surface is generally around 0.5-0.8 m^2m [71] and this tiny surface is seeded with a few thousand cells. Such a small number of cells, organized on a tiny surface can be only a rough approximation of an organ and cannot meaningfully predict in-vivo physiology or pathophysiology [3]. Another problem encountered in micro-bioreactors is the so-called "edge effect". In a micro-scaled surface, the percentage of area close to the edge of the system is higher than in a millimeter-sized surface. A large fraction of the cell population will therefore be found in a peripheral zone of the system. Cell cultures in the edge zone are usually organized differently and have higher cytoskeletal tensions [73], and they may also have different viability or activity [74]. The edge effect is consequently a problem that can directly affect the results obtained in micro cell culture systems as demonstrated Lundholt in [75].

Furthermore, most microfluidic bioreactors are fabricated using PDMS (polydimethylsiloxane) or other elastomeric polymers, which are known to adsorb small hydrophobic molecules [76]. In a microfluidic circuit, the surface to volume ratio is high and PDMS adsorption can lead to nutrient or ligand depletion so giving rise to experimental artifacts such as

increased metabolic consumption rates. Finally, microsystems and microbioreactors are difficult to use and assemble and the seeding and filling processes are quite complicated. This could lead to increased experimental failure and decreased reliability, and limits their usefulness and scope and also puts them out of reach of many cell culture experiments which could benefit from added dynamic stimuli. In fact, for alternative tools to become acceptable as cell culture standards, the transition from wells has to be as smooth as possible. Only then will biologists and technicians adopt and adapt to new culture methods. For this reason, a "system on a plate" Multi Compartmental Modular Bioreactor (MCmB) was developed with dimensions of the order of a few millimeters, which enables microwell protocols to be transferred directly to the bioreactor modules. The main design criteria for bioreactors are based on maximizing mass transport between the cells and the culture medium and on the application of mechanical, electrical, chemical or other stimuli.

Given that hepatocytes present a major challenge in cell culture [77, 78], and are probably the 'limiting' cell in an in-vitro system, the MCmB was designed using hepatocytes as a reference cell type. Hepatocytes are known to rapidly loose phenotypic expression in-vitro due to the absence of an adequately equipped micro-environment, and they are a particular focus of attention in bioreactor development [79]. As the main orchestrators of endogenous and exogenous metabolism in mammals, hepatocytes are extremely sensitive to oxygen concentration, with high metabolic demands [80, 81]. One of the main engineering issues in bioreactors for in vitro liver models is therefore the balance between high mass transfer and low wall shear stress to cells. Several reports describe the effects of flow and shear stress on hepatocyte cultures; [82, 20, 83, 72]. Moreover, many investigators have shown that the viability of hepatocyte cultures under high shear is usually lower than that of static controls, indicating

that the cells are under conditions of stress [84]. Hepatocytes are therefore very sensitive to shear, and according to [85] hepatocyte function is compromised at wall shear stresses greater than 0.03 Pa. To realize a generic bioreactor system, a modular chamber with shape and dimensions similar to the 24 MW was designed. The new bioreactor unit is called the Multi Compartmental modular Bioreactor (MCmB) and it consists of a cell culture chamber made of PDMS (polydi-methylsiloxane), a biocompatible silicone polymer. By plugging together different chambers in different configurations (series or parallel) it is possible to mimic different metabolic pathways in order to investigate and test multi-compartmental biological models in vitro without having to design dedicated equipment or culture chambers, but just by connecting together a set of prefabricated chambers. The MCmB stems from a previous Multi Compartmental Bioreactor (MCB), in which the metabolic circuit has a fixed topology [86, 87]. To mimic salient features of the glucose consumption pathway, the MCB system was designed with four chambers representing the pancreas, the liver and 2 target organs respectively. The chambers were connected by channels, and the circuit dimensions were calculated using allometric laws [88]. The MCmB is a further evolution of the MCB system, and allows any tissue or organ model to be simulated simply by connecting the modular chambers in a desired configuration. The bioreactor design process started with the analysis of the oxygen concentration and with the assessment of the minimum concentration allowed near the cell surface, using hepatocytes as a reference. Subsequently a fluid dynamic model of the MCmB chamber was developed in order to investigate the shear stress and to estimate the optimal chamber size to obtain both adequate oxygen diffusion and low shear stress near the cell surface.

3.1 Material and methods

3.1.1 Mass transport and flow modeling

The first model of the MCmB (MCmB 1.0) was based on the dimensions of the classic 24 MW so as to directly compare static and dynamic cell cultures in equal sized chambers. The MCmB 1.0 was designed to allow the use of 12 mm glass or plastic cover slips, commonly used for cell culture, or different types of scaffolds. It is also possible to place a slice of tissue, pre-grown cell construct or pellets directly on the cell culture zone. A FEM (Finite Element Modeling) model of the cell culture chambers was developed in order to study the oxygen concentration and the shear stress at the cell surface. Cosmos Floworks, a Solidworks[1TM]extension that allows fluid-dynamic FEM analysis and Comsol Multiphysics[2] were used for this purpose. In both the fluid dynamic and mass transport models the following system constants were used: viscosity=10^{-3}Pa s, fluid density =1000 kg/m^3, medium flow rate in the range between 60 and 1000 μL/min, pressure= 1 atmosphere or 760 mmHg, temperature= 37°C and no slip boundary conditions. Water was chosen as a reference fluid, so that the actual values of shear stress on the walls will depend linearly on the density and viscosity of the culture medium used. Initial considerations were focused on a flow rate of 180 μL/min for the sake of comparison with a previous test in the MCB system [86, 87]

In order to study the fluid dynamics of the modular bioreactor a parametric model was developed in which the effect of changes in height on flow parameters (flow speed, shear stress and stream lines) could be observed. As shown in figure 3.1, the first model had a base height H which varied between 3 and 9 mm, and a 13 mm diameter base with a

[1]Dassault Systmes SolidWorks Corp. Concord, MA, USA.
[2]COMSOL AB, Stockholm, Sweden.

modelled 160 µm thick 13 mm in diameter cover slip placed on the bottom of the bioreactor. The distance between the roof and the 1 mm diameter inlet and outlet tubes was fixed at 3 mm, and the FEM model was solved for different heights (H) between the tubes and the cell culture surface: 3, 4, 6, and 9 mm

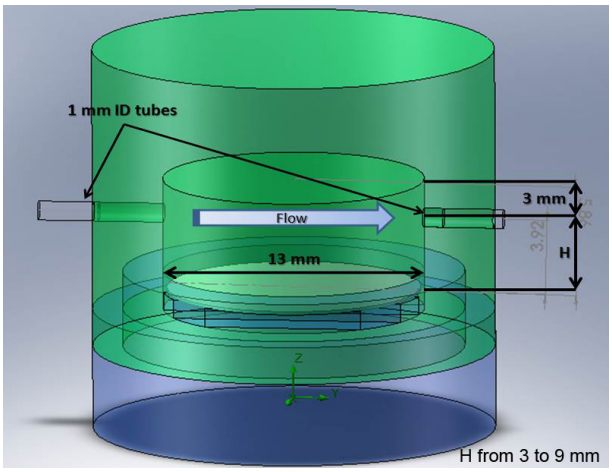

Figure 3.1: *The FEM model geometry for the first modular bioreactor chamber. H is the variable height in the range 3-9* mm.

Oxygen concentration analysis

A steady state model of oxygen diffusion in the McmB chamber was developed, in order to investigate if the cells were adequately supplied with oxygen during the experiments. Michaelis-Menten (MM) kinetics were used to model oxygen consumption and Ficks laws to model oxygen diffusion in water. In the bioreactor circuit, which is described in a previous section 1, air rather than O_2 is used for safety purposes. The O_2 concentration $C[O_2]$ in the medium just below the gas-liquid interface is directly

dependent on the O_2 partial pressure in air, typically 20% or 159 mmHg, through Henry's law C[O_2] can be calculated using tabulated values of the Henry constant:

$$P[O_2] = K[O_2] \cdot C[O_2] \tag{3.1}$$

With K[O_2] = 932.4 Atm/mol/L and P[O_2] = 0.2 Atm (20%), below the gas-liquid interface C[O_2] = 214 µmol = 0.214 mol/m^3. In the presence of oxygen consuming cells, the O_2 concentration will decrease as a function of distance from the interface and the metabolic requirements of the cells. The steady state flux of O_2 in the bioreactor chamber is due to cellular oxygen consumption at the base. The oxygen consumption rate, per unit volume is given by the MM equation:

$$\frac{\delta C}{\delta t} = \frac{Vm \cdot C}{Km + C} \tag{3.2}$$

C is the oxygen concentration in mol/m^3, Vm is the maximum volumetric consumption rate in mol/m^3, and Km is the MM constant in mol/m^3.

The flux at the base of the chamber where the cells lie is:

$$J_C = -D\frac{\delta C}{\delta x} \cdot \frac{Vm \cdot C}{Km + C} \cdot \frac{1}{cells\ number} \tag{3.3}$$

Where J_C is the O_2 mass flow at the cell surface, $\frac{\delta C}{\delta x}$ is the O_2 concentration gradient at the cell surface calculated along the axis perpendicular to the cell culture layer, D is the O_2 diffusion coefficient (in water) $D = 3 \cdot 10^{-9} m^2/s$ @ 37°C, and Vmax is the maximum consumption rate in m^2/s.

The kinetic model was calculated for a medium flow rate of 180 µL, for a comparison with the MCB result, and a cell monolayer of 1.13 cm^2[3]

[3] 12 mm cover slip area.

surface area with 5 x 10^5 cells, which represents typical cell numbers observed 48h after seeding HepG2 cells on a 3D scaffold [89].

In order to choose the height of the bioreactor, a minimum oxygen concentration of the medium at the cell surface was fixed; C_min= 0.04 mol/m^3. Below this concentration it is assumed that cell function is compromised. In fact typical oxygen concentrations in the liver are of the order of 0.04 - 0.15 mol/m^3 (4-15%), while 0.021 mol/m^3 (2%) is known to inhibit mitosis in hepatocytes [90]. Using the data in [91], Vmax = 0.048 nmol/s for 1 million cells, giving a value of 0.024 nmol/s for 5 x 10^5 cells (Vmax(5 x 10^5)), and Km = 0.5 mmHg.

Figure 3.2 illustrates that the O_2 concentration in the MCmB is always higher than the minimal threshold, and falls rapidly at the edge of the chamber near the outlet. Increasing bioreactor height from 3 to 9 mm, the oxygen concentration decreases rapidly but cell survival is always guaranteed in the central region of the chamber. Above H=9 mm however, at the bottom of the chamber the oxygen concentration is constantly below the Cmin threshold of 0.04 mol/m^3. The maximum oxygen s at the base are 0.17, 0.12, 0.10 and 0.007 mol/m^3 for H= 3,4,6, and 9 mm respectively.

Fluid dynamic model

To investigate the fluid-dynamics of the modular bioreactor, a parametric model similar to the mass-transfer model was developed. The height H was varied to determine its influence on the shear stress generated at the cell surface, assuming again that the cells are seeded on a 12 mm, 160 µm thick cover slip placed in the bioreactor. Table 3.1 summarizes the results, showing how the shear stress at the cells surface decreases rapidly with increasing H. However the laminarity of the flow is compromised by increasing the height of the bioreactors. This is a consequence of the

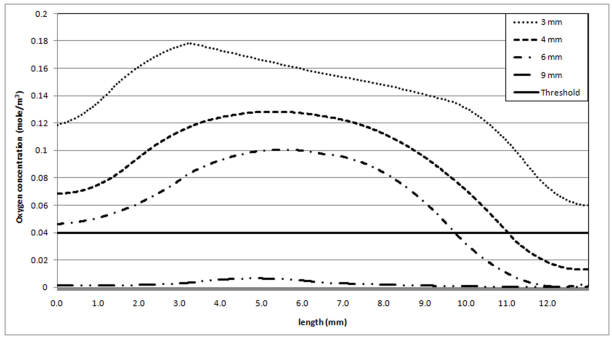

Figure 3.2: *Theoretical oxygen concentration profile across the bioreactor chamber for different heights H, calculated using Michaelis Menten kinetics and a flow rate of 180* µL/min*. The minimal concentration threshold of 0.04* mol/m^3 *is indicated by the solid line.*

separation of flow stream lines caused by the difference in height between the inlet tube and the base.

After evaluating the results from the fluid dynamic and mass transport modeling, a Modular Bioreactor chamber with tubes placed 6 mm over the cell surface (H) was realized. A distance of at least 1 mm between the wall of the tube and the top of the chamber is necessary to ensure mechanical stability of the tube/chamber junction. Since standard silicone tubing with an inner diameter of 1 mm has an outer diameter of 3 mm, the total height of the chamber is 10 mm. This is the best compromise between shear stress, flow, oxygen diffusion and mechanical feasibility.

Figure 3.3 shows the three dimensional FEM model of the H = 6 mm MCmB with an internal diameter of 13 mm, sufficient to place a slice or a scaffold of 12 mm in diameter. This bioreactor has a peak shear stress value of 6.85 X 10^{-6} Paand a velocity peak of 10^{-6}m/s near the center of the base.

Height (H)	*Shear Stress Peak (Pa) @180* µL/min	*Shear stress profile (log Pa)*	*Velocity Peak (m/s) @180* µL/min	*Velocity vector*	*Stream Line*
*3*mm	3.21710^{-5}		4.42910^{-6}	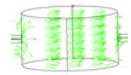 Parallel to the cell surface	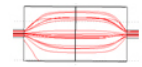 Parallel to the cell culture
*4*mm	1.19510^{-5}		1.66510^{-6}	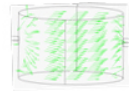 Parallel to the cell surface	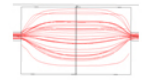 Parallel to the cell culture
*6*mm	6.85610^{-6}	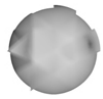	9.88710^{-7}	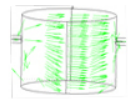 Slightly sloped	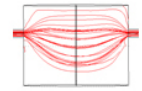 Nearly parallel to the cell culture
*9*mm	8.74710^{-7}	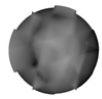	1.38910^{-7}	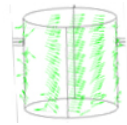 Sloped	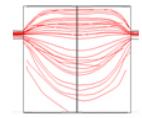 High impact angle on the cell culture surface

Table 3.1: *Fluid Dynamic FEM model results for a fixed flow rate of 180* µL/min *for the first MCmB model as a function of height H.*

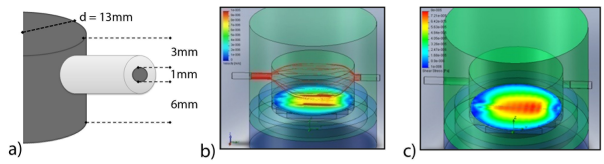

Figure 3.3: *FEM model of the H=6* mm *MCmB 1.0. a)Velocity and b)shear stress. The analysis takes into account a 160* µm *thick glass cover slip placed on the base of the chamber.*

3.1.2 Chamber Fabrication

A first prototype of the bioreactor chamber (MCmB 1.0) was fabricated using "milli-molding" in order to investigate the performance of the system. Milli-molding is similar to micromolding [92], in that PDMS is used as a mold, but the master is machined using a mill or rapid prototyping rather than lithographic methods, and the features of the mold are of the order of tenths of millimeters, rather than microns. The chamber is composed of two separate parts which are plugged together through a friction fit system. In the friction fit system two complementary geometries form a seal when brought together thus avoiding the use of o-rings or additional parts [93]. PDMS [4] is used to fabricate the chambers. Along with the friction fit system, the use of PDMS , which is self adhesive and deformable, ensures that the seal is watertight. The two parts of the chamber (figure 3.4)are made by casting and curing PDMS according to the manufacturer's instructions on aluminum masters purposely machined. Each master is made of two separate pieces which allow easy removal of the chambers after polymerization.

[4]Sylgard 184, Dow Corning, Silverstar, Italy.

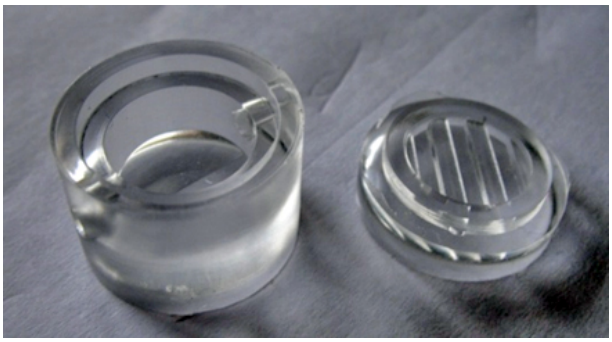

Figure 3.4: *The two parts of the MCmB 1.0 chamber. The top part (left) has two holes for the 3* mm *silicone tubes insertion, on the bottom part (right) is possible to see the fit system.*

Turbulence Tests

The first prototype of the MCmB 1.0 cell culture chamber had severe problems with the build-up of air bubbles during the initial phases in which the bioreactor is filled with medium. This resulted in the formation of a bubble of air at the top of the chamber (Figure 3.5.a) which disturbed the flow profile, causing turbulence and more importantly unpredictable values of shear stress. In order to evaluate the effects of the bubble induced turbulence, a small drop or blob of alginate was introduced in the chamber as a turbulence sensor. An alginate blob is easily disaggregated under turbulent or high impact flow, and for this reason is a good indicator of the presence of altered flow profiles. Moreover, cross-linked alginate at the concentrations used here has approximately the same elastic modulus as the liver (≈10kPa), [94, 95].

The alginate blobs are made placing 166 μL of 2% sodium alginate[5] dissolved in MEM[5] on top of a glass cover slip in the chamber and cross

[5]Sigma, Milan, Italy.

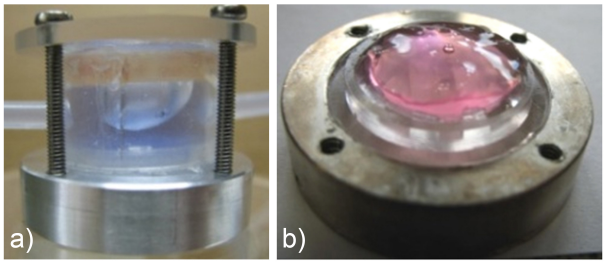

Figure 3.5: *a) Bubble formed at the top of the first MCmB 1.0 chamber , and B) alginate drop used for turbulence tests placed on the bottom half of the chamber.*

linking in-situ with 104 µL of 0.1 M $CaCl_2$ (Figure 3.5.b). The volume of the blob was chosen in order to form a thin uniform coating of the glass cover slip, without interfering with the inlet tube. A peristaltic pump [6] was attached to the inlet, and keeping the flow rate constant at 180 µL/min, the consistency of the alginate blob after 24 hours in the MCmB 1.0 @ 37°Cwas analyzed. The alginate drop was completely disaggregated, showing that the bubble induced a turbulent environment. 180 µL/min was chosed in order to test the MCmB prototype in the experiemtnal conditions described in the MCB works [86, 87].

3.1.3 Design Improvements: MCmB 2.0

In order to eliminate bubble entrapment and turbulence in the bioreactor chamber, a second prototype (MCmB 2.0) of the modular bioreactor was designed. The new bioreactor is slightly larger in diameter (15 mm) to enable 13 or 14 mm slides to be easily inserted and its top surface is sloped along and perpendicular to the axis of flow, so that bubbles are

[6] Ismatec, Glattbrugg, Switzerland.

collected and conveyed to the outlet tube (Figure 3.6.a). Furthermore, the diameter of the outlet tube was increased to 2 mm to facilitate the removal of bubbles. This also reduces the impact angle on the cell culture surface and the recirculation near the outlet wall as shown in table 3.2. The final height of the MCmB 2.0 is 11 mm at the inlet side and 13 mm at the outlet side, with the tubes positioned respectively at H=9 and H=10 mm from the cell surface (Figure 3.6.b).

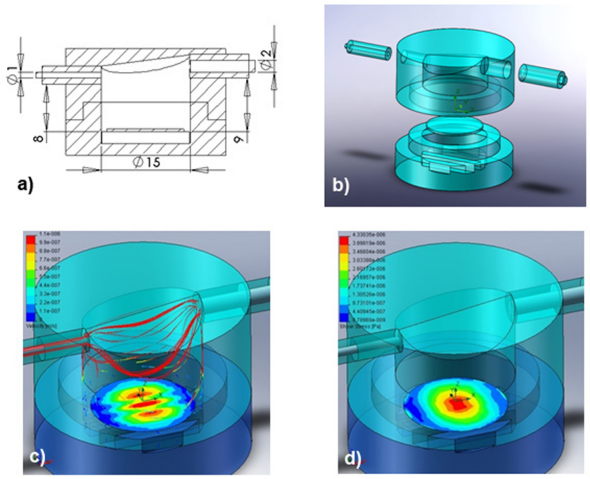

Figure 3.6: *a) dimensions of the new chamber, b) three dimensional representation of the sloped roof and ridged base, c) MCmB 2.0 Velocity profile, showing stream lines and d) Shear Stress at the base.*

Through FEM modeling a tenfold decrease in fluid velocity and shear stress on the cell surface with respect to MCmB 1.0 was observed with the introduction of the sloping roof and the increased outlet tube diameter. The MCmB 2.0 is 3 mm higher than MCmB 1.0, the increase in the height of the new chamber design was chosen because this allows a further

reduction in shear stress in comparison with MCmB 1.0 (6 mm in height) while maintaining the oxygen concentration over the 4% threshold.

Flow rate (µL/min)	*180*	*300*
Shear Stress Peak (Pa)	$4.295 \cdot 10^{-6}$	$6.456 \cdot 10^{-6}$
Shear stress profile (*log* Pa)	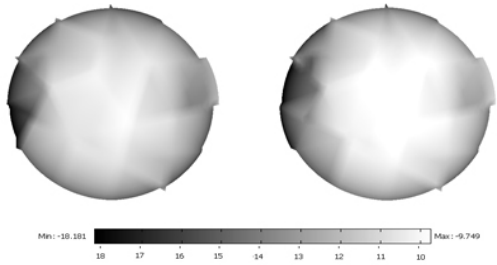	
Velocity Peak ($\frac{m}{s}$)	$5.939?10^{-7}$	9.04810^{-7}
Velocity vector	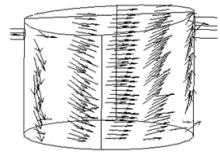 Parallel to the cell surface	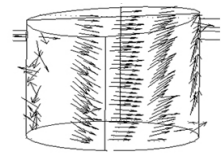 Parallel to the cell surface
Stream Line	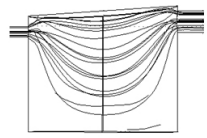 Parallel to the cell culture	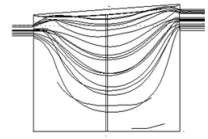 Parallel to the cell culture

Table 3.2: *Fluid Dynamic FEM model results for the MCmB 2.0 at two different flow rates, the average height (H) of the MCmB 2.0 is 9.5* mm.

The base of the bioreactor chamber was also modified to ensure easy removal and support of coverslips, since the slides and thin substrates tend to stick to the flat silicone base. The three small rectangular oxygenation ridges, shown in figure 3.6.b, provide support and also allow medium to flow under the support, supplying nutrients to the lower surface of tissue slices or scaffolds. Without the oxygenation ridges the removal of

cover slips by the bioreactor bottom could be very complicated due to the adhesion the thin cover slips to the silicone bottom of the chamber. Two different types of bases, with or without oxygenation ridges, were realized. The bottom with ridges is useful for coverslips or scaffold experiment but is not suitable in case of use with little pieces of tissue or gel seeded with cells because the tissue pieces can fall down the ridges or the gel may stick between the ridges.

3.1.4 Modular Mould Design

The first prototypes of the MCmB bioreactors were made using two aluminum moulds one for the top and one for the bottom part of the chamber. Both the MCmB moulds where composed of two parts, an internal shape that is the core of the chamber design and an external frame that is the mould wall. The external dimension of the two chamber parts are exactly the same in order to provide a perfect fit and consequently a good sealing effect. The aluminum moulds where not suitable for a long term bioreactor production, because the aluminum is easily damaged during the mould cleaning process and oxidize very fast in presence of oxygen and high temperatures. PDMS polymerization is very sensitive to metal oxides that can block the polymer cross-linking process. Moreover, removal of the PDMS parts was difficult and required the use of sharp instruments. Therefore a new mould was realised that can be used for long term, for the production of a high number of bioreactors and that do not present any problem of oxidation or wear during the cleaning process. The new mould is a modular mould made of a frame system and a set of three different inserts, all the parts that are in contact with the silicone are made of stainless steel AISI 316L in order to prevent polymer cross linking problems due to metal oxidation processes. With the modular mould is possible to fabricate six bioreactor parts in parallel, and it is

consequently possible to produce 2 complete chambers (2 tops, 2 bottoms with or without oxygenation ridges) or other combinations. The modular mould frame is made of two specular parts (except for the tube hole positions and dimensions) that assembled together form the external wall of the six bioreactor parts, these parts require a high dimensional tolerance especially in the coupling surfaces. The high tolerance is required in order to allow a perfect coupling of the two parts to prevent any leakage of the liquid silicone polymer during the casting phase and also to prevent the formation of ridges in proximity of the coupling surface in the bioreactors obtained. The internal part of the chambers is made using the three inserts that are fixed on a dedicated mounting base made of aluminum (it is not in contact with the silicone) and allows a perfect insert alignment. All these parts are described in detail in figure 3.7 where the dimensions are also indicated .

In particular it is important to highlight the sloped roof of the top part modular insert. The top part of the insert presents two different inclinations of the roof, the top is sloped 7° degree along the inlet outlet axis because in this direction a high slope is not required to move the bubble due to the force imposed by the flow of medium. Perpendicular to the direction of flow a higher slope is required (14° degree) in order to ensure bubbles are collected on the upper part of the roof. The top and bottom inserts have two complementary geometries at the base, these geometries embody the snap/friction fit system of the bioreactor chambers previously described 3.1.2. The snap fit system consists of a male female geometry step shaped with dimensions of 3 X 3 X 3 mm (shown in figure 3.7.a.1), the total contact/sealing surface is consequently 9 mm even if the bioreactor wall width is only 6 mm. This large contact surface due to the self adhesive properties of PDMS ensures a perfect sealing effect that prevents any leakage of the system and works also as a self alignment

system [93]. The bioreactor internal cavities do not present any sharp angle and all the edges are rounded so as to avoid any discontinuities which may damage the chambers during extraction.

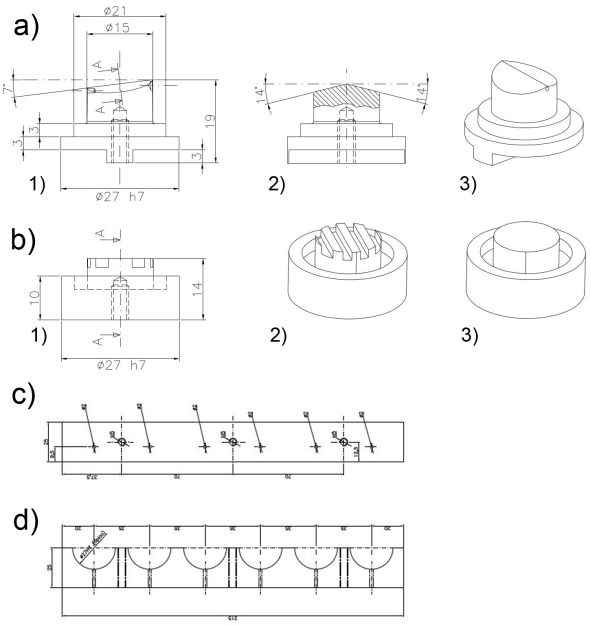

Figure 3.7: *Design of the modular mould. a) Bioreactor top part design , b) bioreactor bottom part design (the bottom is shown with (2) or without (3) oxygenation ridges), c) Lateral and d) top views of a modular mould frame.*

As shown in figure 3.7 all the bioreactor mould parts are polished in order to facilitate the PDMS extraction phase and also to ensure complete transparency of the chambers. Transparency is a very important factor because due to the optical properties of the PDMS is possible to observe cell cultures under microscope without requiring bioreactor disassembly. This aspect is very important because one of the main reasons

why biologists hesitate to migrate from multiwell technology is that most bioreactors do not allow optical observation of cell cultures under a microscope during the experiments. Another advantage of the modular mould is in the tube insertion procedure. With the first prototype mould, the tubes where manually integrated after the curing phase using some drops of silicone polymer as glue. In these conditions the coupling between the chamber top parts and the tubes was very fiddly and tube alignment was not perfect. This approach also required another curing process with an increase in bioreactor production time. With the modular mould the tubes are inserted directly in the two frame parts and are integrated into the top part of the chamber due to the high tolerance of the holes which prevents any misalignments. Before the polymer casting stainless steel wires of 1 and 2 mm (the inlet and outlet tube of MCmB 2.0 have different diameters) are inserted in the tubes in order to prevent the cavities being occluded with polymer and also to perfectly align the tubes with the higher and lower parts of the top roof. The tube alignment is obtained through two holes (1 and 2 mm in diameter) made on the higher and lower part of the top roof as shown in figure 3.7.a.3.

3.2 MCmB 2.0 design validation

3.2.1 Oxygen Consumption and Shear stress in the MCmB 2.0

Figure 3.9 shows the oxygen concentration in the two bioreactor designs; for a given flow rate, the mean value is slightly lower in the new MCmB 2.0 design. As far as oxygen consumption is concerned, the difference between the two chambers is the value of H (6 mm in MCmB 1.0 and 9 mm in MCmB 2.0) and their respective volumes 1.32 and 1.94 mL. The

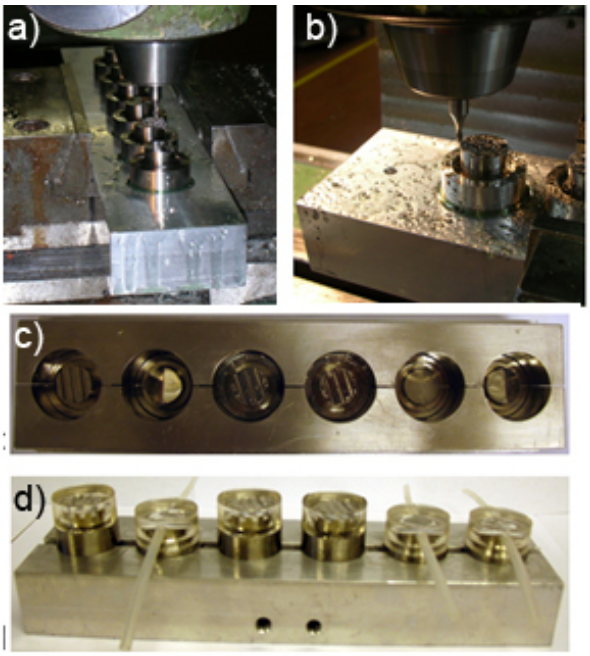

Figure 3.8: *Modular mould fabrication and testing. In a) and b) the bottom ridges obtained from the milling process are shown, in c) the mould ready for the silicone casting in d) bioreactor extraction after the curing and cooling phase.*

MCmB 2.0 chamber has a larger volume (47% more) so the total amount of oxygen available is greater. Therefore, despite the greater distance between the tubes and the cell surface in the new chamber the minimal oxygen concentration is still guaranteed except at the outer edge of the base closest to the outlet. It should be noted that the number of cells used in the model was more than twice that used in the experiments (decribed in the MCmB validation section 4), and that the oxygen concentration is highly dependent on the flow rate and metabolic requirements of the

cells.

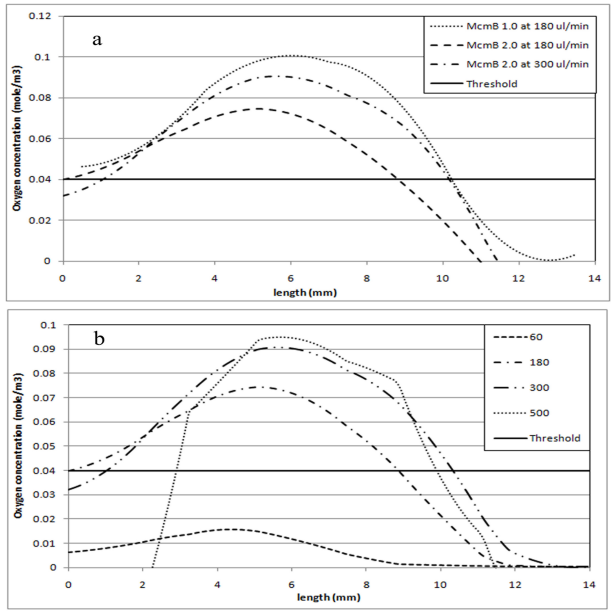

Figure 3.9: *a) Oxygen concentration in the MCmB 1.0 for a flow rate of 180 l/min and MCmB 2.0 for a flow rate of 180 and 300* µL/min *and b) Oxygen concentration in the MCmB 2.0 for different flow rates between 60 and 500* µL/min.

The Graetz number which is a dimensionless number indicating the ratio between the characteristic diffusion time and the convection time respectively perpendicular and parallel to the direction of flow was also characterized.

$$Gr = \frac{D}{L} Re \cdot Sc \tag{3.4}$$

In the Graetz number equation, D is the internal diameter in round tubes or hydraulic diameter in arbitrary cross-section ducts, L is the

length of the conduct that in the MCmB case is 15 mm (internal diameter of the chamber). Re and Sc are respectively the Reynolds[7] and the Schmidt number[8]. In the MCmB 2.0 The Graetz number calculated near the outlet hole through the chamber FEM model is greater than 100 even for low flow rates (60 μL/min) showing that the fraction of oxygen consumed per reactor is insignificant and so downstream chambers do not suffer from any input oxygen depletion. This is a very important aspect of the MCmB 2.0 chambers because its demonstrate the capability of this bioreactor to be used as modular system.

Using the FEM model empirical equations were established allowing to calculate the wall shear stress and peak fluid velocity at the cell surface as a function of flow rate.

$$Shear(Pa) = Flow\ (\mu L/\min) \cdot 1.8 \cdot 10^{-8} + 1.1 \cdot 10^{-6} \tag{3.5}$$

$$FlowSpeed\ (\frac{m}{s}) = Flow\ (\mu L/\min) \cdot 2.6 \cdot 10^{-9} + 1.3 \cdot 10^{-7} \tag{3.6}$$

Therefore the wall shear stress at 180 and 300 μL/min is respectively 4.3410^{-6} and 6.510^{-6} Paand the peak flow velocity is 5.9810^{-7} and 9.110^{-7}m/s.

3.2.2 Bubble and Turbulence Testing

As shown in Tables 3.2, the MCmB 2.0 has lower values of shear stress, and the stream lines are parallel to the base of the chamber, even though

[7]the Reynolds number Re is a dimensionless number that gives a measure of the ratio between inertial forces and viscous forces.

[8]Schmidt number is a dimensionless number defined as the ratio of momentum diffusivity (viscosity) and mass diffusivity.

its height (H) is 3 mm greater than MCmB 1.0. The MCmB 2.0 was bubble free, as the sloped roof and the position and respective diameters of the inlet and outlet tubes forced bubbles to be conveyed out of the chambers. In the turbulence tests carried out with the alginate blob, the gel showed no signs of wear even after 48 hours under a flow of 500 μL/min. At a flow rate of 1000 μL/min the alginate gel showed signs of disaggregation after 24 hours, due to the direct high impact of fluid on the base of the chamber as well as the high wall shear. The alginate blob turbulence test is not only a simple method for investigating turbulent, high impact, or disturbed flow in the system, but can also be used to create a cell culture environment more similar to the in-vivo liver environment. As shown in [86, 87], coating the cells in an alginate or collagen gel increases hepatocyte viability and phenotypic stability during the culture.

Chapter 4

MCmB 2.0 Cell Testing

The MCmB 2.0 is a modular chamber for high throughput multi compartmental bioreactor experiments. It is designed to be used in a wide range of applications and with various cell types. For this reason this innovative chamber was tested with different cell types and experimental procedures in order to validate the MCmB 2.0 for generic cell culture testing. The first test performed on the MCmB 2.0 was aimed at demonstrating the capability of the chamber to maintain the vitality and function of one of the most important yet most delicate cells in the human body: hepatocytes.

With the hepatocyte tests the mass transport and fluid dynamic FEM models previously described3.1.1 were validated. In fact, through these experiments we verified that the oxygen concentration in the MCmB chamber allows hepatocyte survival and showed that their vitality is shear stress dependent. The second set of tests was focused on establishing an *in-vitro liver* model in the McmB 2.0, in which different chambers are plugged in series and parallel in order to simulate a human liver. The third test served to demonstrate that the MCmB 2.0 can be used to study other cell types in a flow system. The MCmB 2.0 was used to investigate the behavior of condrocyte cultures, in monolayers and in scaffolds, under different levels of shear stress.

4.1 Validation of Shear Stress and Oxygen Concentration Models

Hepatocytes present a major challenge in cell culture [77, 78], and are probably the "limiting" cell in an in-vitro system, the MCmB 2.0 was designed using hepatocytes as a reference cell type. Hepatocytes are known to rapidly loose phenotypic expression in-vitro due to the absence of an adequately equipped micro-environment. Hepatocytes are extremely sensitive to oxygen concentration, with high metabolic demands. For this reason a series of experiments were conducted on hepatocytes to evaluate the effective oxygen diffusion and the effects of shear stress in the MCmB 2.0 .

4.1.1 Material and Methods

Primary rat hepatocytes were used to test the performance of the MCmB 2.0 bioreactor at various flow rates. Hepatocyes were isolated from adult male Wistar rats weighing between 250 and 300 g as described in [96, 97]. Isolated cells were assessed for vitality by trypan blue[1] exclusion[2], and then seeded on glass cover slips ($2x10^5$ cells per sample) pre-treated with 0.1 mL collagen extracted from rat tails according to standard procedures [98], placed in 24-MW plates and left at 37°Cand 5% CO_2.

About 5 hours after seeding, the medium was removed and replaced with FBS-free William's E complete medium. The following day, the hepatocyte seeded coverslips were placed into the MCmB 2.0 chambers and coated with 250 µL collagen gel prepared by mixing ice-cold collagen solution and acetic acid 0.2 N (to a final collagen concentration of

[1] All cell culture reagents were purchased from Sigma, unless otherwise specified.

[2] Vitality routinely greater than 90%.

about 1.1 mg/mL). The collagen coating used in these experiments has a Young's modulus similar to the alginate blob used to evaluate the turbulence in the chamber [99]. It also provides an adhesive roof to the cells, and shields the cells from the effects of direct flow.

MCmB Assembly

Prior to assembly the bioreactors with hepatocyte seeded and collagen coated slides were left in the incubator for 40 minutes to allow the collagen to set. The MCmB system was then assembled by connecting 2 chambers in series to a peristaltic pump and the mixing chamber. Finally, the system was filled with 10 mL FBS-free complete William's E, and run for up to 24 hours. The first experiment was run at a flow rate of 180 μL/min. At 2, 4, 6 and 24 hours a 100 μL sample of medium was withdrawn for analysis of rat albumin. A second set of experiments was carried out at various flow rates (60-100-180-250-300-500-1000 μL/min) to determine cell viability as a function of flow rate. The bioreactors were run for 24 hours after which the cover slips were removed and assessed for cell viability. Control experiments with cells from the same rat liver were run using glass slides seeded with the same number of cells, coated with collagen and placed in 10 mL petri dish plate multiwell[3].

Viability and Albumin Testing

Albumin, which is an important marker of hepatic function, was measured using a commercial ELISA kit[4], according to the manufacturer's instructions. Rat albumin production is expressed as total quantities of albumin per seeded cells. Each experiment was repeated at least three

[3]BD Biosciences, Milan, Italy.

[4]Bethyl Laboratories, Montgomery , TX, USA.

times, and comparisons were only made between cells extracted from the same liver.

The viability kit used was CellTiter-BlueTM Cell Viability Assay[5], a resazurin-based fluorescent compound metabolized by mitochondrial cytosolic and microsomial enzymes to resorufin which can be detected with a fluorimeter[6] at 573 ηm. Viability was assessed both in control static cultures and in the MCmB 2.0, and the results are expressed as ratio between hepatocyte viability in dynamic and static conditions after 24 hours. The static control was a hepatocyte seeded and alginate coated cover slip placed in a bioreactor base filled with medium and left open in order to allow oxygen exchange without medium flow. Each experiment was repeated at least three times, and comparisons were only made between cells extracted from the same liver.

4.1.2 Cell viability and albumin production results

Figure 4.1.a illustrates the viability ratio between the MCmB dynamic culture at different flow rates and a static control. The figure shows that below 180 µL/min the viability is compromised, this could be due to the lower oxygen concentration at the bottom of the bioreactor chamber for these low flow rates (shown in figure 3.9.b). For flow rates in the range between 180 to 500 µL/min the viability is very close to the control and the viability peaks at 300 µL/min, this could be due to the high oxygen concentration as demonstrated in figure 3.9.b. A further increase in flow rates above about 500 µL/min causes a significant reduction in viability. At higher flow rates, despite the increased availability of oxygen, the cells

[5]Promega Madison WI USA.

[6]FLUOstar Omega, BMG Labtech, Offemburg, Germany.

suffer, and this is due to the high shear and impact angle of flow on the collagen coating and cells. Figure 4.1.b shows the albumin production after 24 hours in the MCmB for different flow rates in the range 100 - 1000 μL/min, and the static control. Albumin in the bioreactor chamber, is slightly up regulated except for the 1000 μL/min flow rate, where the cells are damaged by the shear stress as previously discussed. These results are confirmed by several reports describing dynamic hepatocyte cultures [70, 20, 85] where the albumin production is maintained at control levels even in the presence of shear. We have suggested that this induction is due to two factors: the circulation of medium which provides a sustainable supply of nutrients, as well as efficient removal of metabolic products, and the mechanical stimulus due to the presence of a low velocity porous or percolative interstitial-like flow which is established through the collagen coating [89]. In fact, in the human liver, hepatocytes are never subject to direct or tangential flow; they receive nutrients through a rich capillary network and consequently only through interstitial flow driven by concentration and pressure gradients [100, 101]. Not surprisingly a large number of reports on liver bioreactors use co-cultures of hepatocytes with non-parenchymal cells, typically fibroblasts [85, 102, 84]. These supporting cells not only provide heterotypic signals, but they also secrete collagen which likely forms a protective coating over the cells shielding them from direct fluid flow.

4.2 In-vitro Liver Model in the MCmB Bioreactor

Hepatocytes, like all cells, are dramatically affected by the physical and chemical nature of their micro-environment. This is one of the reasons why in vitro cell culture experiments are so difficult to compare from lab-

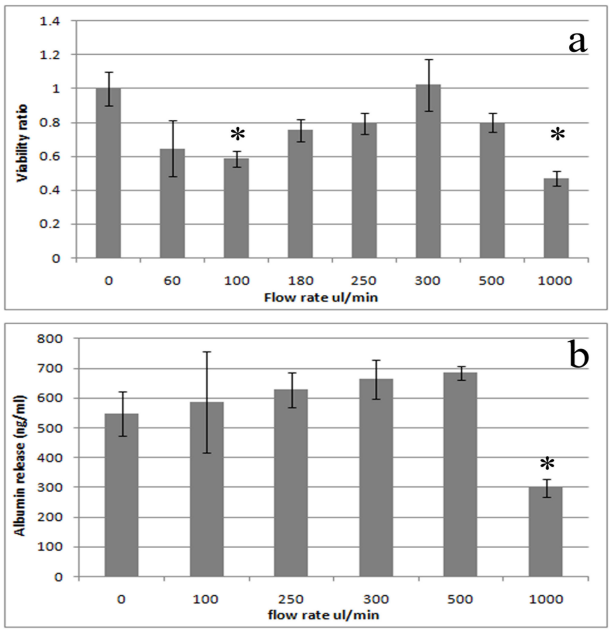

Figure 4.1: *a) Hepatocyte viability, expressed as the ratio between viability in the MCmB 2.0 and a bioreactor static cultures after 24 hours at different flow rates and b) Rat albumin production after 24 hours in the MCmB 2.0 and in the control.* $*p < 0.05$

oratory to laboratory. The hepatic cell habitat comprises 3 main features, or cues, which are known to influence cell behavior; the biochemistry, the architecture and the supply of nutrients to meet the metabolic demands of the cells. With this experiment we investigated 2 of the main cues which are known to influence hepatocyte function, a 3D topology and convective flow. Several investigators have shown that cell culture in 3D represents a more physiologically relevant environment. However the extent to which this influences hepatocyte function with respect to the provision of oxygen and other nutrients is unclear. Moreover, the relationship

between the topological features of a scaffold and hepatic function have not been studied in depth [89]. Hepatocyte function on three-dimensional micro-fabricated polymer scaffolds realized with the Pressure Activated Microsyringe (PAM) [103, 104, 105] was tested in static and dynamic conditions. Hepatocyte cell density, glucose consumption, and albumin secretion rate were measured daily over a week.

4.2.1 Material and methods

Since primary hepatocytes rapidly lose liver morphology and differentiated functions in vitro, in this study we used the HepG2 cell line as an alternative model cell. HepG2 cells maintain the main synthetic and endogenous functions of primary hepatocytes, as well some exogenous metabolic functions [106]. The cells were grown in Eagle minimal essential medium (EMEM, 1 $\frac{g}{L}$ glucose) supplemented with 5% foetal bovine serum, 1% non-essential amino acids, 1% EMEM vitamins, 2 mmol L-glutamine, 100 Unit/mL penicillin and 100 µg/mL streptomycin)[7] in a humidified incubator at 37°C, 5% CO_2[8]. The cells were all used at the same passage (no. 22 after receipt) and passaged using 0.05% trypsin with 0.02% EDTA in PBS. Cells were seeded (10^5 cells/c^2m) on the films or scaffolds using 2 mL of complete medium per well. After 24 hours, the structures were moved to a new microwell plate to eliminate interference from non-adherent cells. Both scaffolds and films were coated with an alginate film consisting of 250 μL 1% sodium alginate dissolved in serum-free medium, cross-linked with 50 µL 1% $CaCl_2$[9]. Excess alginate was removed with a pipette. The resulting film had a thickness of a few tens

[7]All reagents from Eurolone, Milan, Italy, unless otherwise specified.
[8]Heraeus SpA, Milan, Italy.
[9]Sigma-Aldrich, Milan,Italy.

of microns as measured by an optical profilometer[10], having a nominal resolution of 1 μm. The profilometer uses a small laser spot (0.7 mm X 0.5 mm) which is reflected off a surface. Displacements were calibrated using an uncoated glass slide as a reference. The coating was not uniform and flat as observed by an optical microscope, and this was also reflected in the scatter of the profilometer readings across the slide (40 - 100 μm). At the low alginate concentrations used, the diffusion coefficient of oxygen and of small solutes is similar to water [107, 108]. Finally, 2 mL fresh medium was added to each well to begin the experiment. Cells were maintained on the structures for a week and cell counting and medium collection was performed daily. The experiment was performed in triplicate using 21 structures (3 series of seven bioreactors ran in parallel through a multi way peristaltic pump) three samples were removed for counting per day, and the culture medium was changed every third day (figure 4.2). Medium was perfused through the chambers at a flow rate of 250 µL/min.

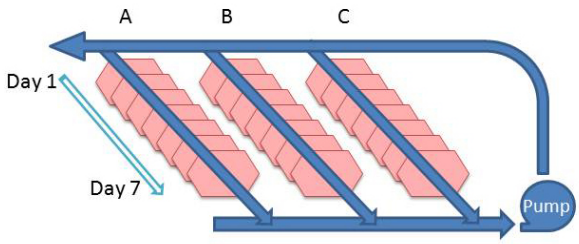

Figure 4.2: *In vitro liver experiments organization; every day a chamber from each series is unplugged and analyzed. The three series of seven bioreactors are connected as separated circuits to the peristaltic pump.*

In addition up to 200 µL of media (50 µL per assay) was withdrawn for

[10]Opto NCDT, model ILD1400-10, UK.

analysis at fixed intervals. All cell culture experiments were carried out in the same incubator. The cells adhered on the structures were trypsinised and counted using a Burker chamber. Cell viability was evaluated using tryptan blue exclusion, and this was always greater than 95%. Because the 3D scaffolds are composed of 3 layers of hexagons, the "true" area available for cell adhesion is difficult to estimate. Therefore we use the term "nominal area" to refer to the effective surface area which the scaffold or film occupies in the well or bioreactor. Cell densities are expressed as the total numbers of cells counted divided by the nominal 2D-surface area of the samples. The PAM scaffolds have a nominal surface area of 0.8 c^2mand a large percentage of this is free space of the pores, while the spin-coated films have an area of 1.33 c^2m.

Albumin production, was measured as previously described 4.1.1, glucose consumption was quantified using a commercial enzymatic kit [11]. In order to compare data from different experiments with different cell numbers and media volumes the glucose and albumin data are expressed as quantities consumed or produced per cell per day.

4.2.2 Results of In-vitro Liver Experiments

Before testing the different hepatocyte costructs in the MCmB a comparison between 2D films and 3D scaffolds in static culture was done. The cell density was higher on the scaffolds than on films particularly from day 4 onwards (ANCOVA[12], $p < 0.01$). The cells on the 2D films consumed a higher quantity of glucose than 3D scaffolds in the first two days. After this period, the glucose consumption per cell was constant and similar to that of the 3D scaffolds. Albumin is one of the functional

[11] Megazyme International Poncarale, Italy.

[12] Analysis of covariance (ANCOVA), Matlab Statistics Toolbox, The MathWorks Inc.

marker proteins of the liver. Human albumin was produced in similar quantities by 3D scaffolds and 2D films during the experiment.

In the bioreactors, the cell density increased smoothly over time and density values were similar to those in static conditions. Glucose consumption was higher in the MCmB with a constant consumption rate of 7.6±0.1 ηg/(cell/day) (p=0.0001 ANCOVA) with respect to the 3D scaffold in static conditions (5.2±0.2 ηg/(cell/day), p=0.001, ANCOVA) (figure 4.3.a). Therefore the cell energy requirements are greater in the bioreactor, and glucose is used as a substrate. This may be due to an upregulation of liverspecific synthetic function in the bioreactor.

As shown in figure 4.3.b a large increase in albumin production per cell was observed in dynamic culture, particularly in the first 2 days; albumin production was 10 times higher in the MCmB than in static conditions and then decreased progressively maintaining a value 4/5 times greater than in static culture. In fact, the average albumin production in the bioreactor over the 7 days was 3.12±0.43 ηg/(cell/day), compared with 0.65±0.16 ηg/(cell/day) (p=0.02, ANCOVA) in the static conditions scaffolds . To ensure that the increased albumin production was not due to the increased volume of medium in the bioreactor, a final experiment was performed using 3D scaffolds cultured in 50 mm Petri dishes in which the total medium volume was 10 mL. The albumin production rate was 0.50±0.14 ηg/(cell/day) over the 2 day period of analysis, indicating that the volume of medium does not influence the secretion rate of this protein in static conditions.

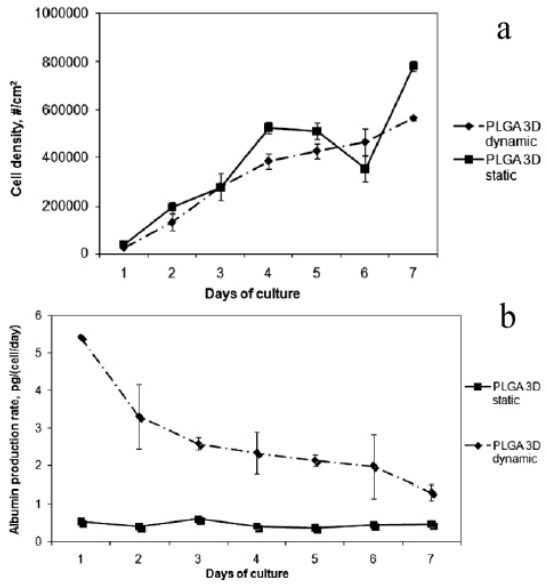

Figure 4.3: *(a) Cell density (defined as* $\frac{cellnumber}{nominalarea(\mathrm{c^2m})}$ *for PLGA scaffolds in the bioreactor and in static conditions and (b) Albumin production rate in static and dynamic conditions for PLGA 3-D scaffolds (in both case n=3 per data point).*

4.3 MCmB Bioreactor Tests with Skeletal and Epithelial Tissue Cells

Articular chondrocytes are well known to respond to mechanical forces in the native tissue by synthesizing matrix components (e.g. collagen II and proteoglycans). This ability is rapidly lost in monolayer culture due to cell de-differentiation resulting in a more 'fibroblastic' phenotype in which the cells do not synthesize the matrix components found in native cartilage [109]. For example, collagen I is synthesized by chondrocytes instead of

collagen II and little aggrecan, the main proteoglycan of native tissue, is produced. Therefore early passage cells (P1) maintain more chondrocyte features than later passaged cell (e.g. P4). In these experiments the effect of flow rate on passage number was determined in extended culture in monolayer to see if the cellular response to shear stress was changed with passage number.

4.3.1 Materials and methods

Cartilage cells (chondrocytes) were isolated from bovine metacarpophalangeal joints and cultured as described in [110]. Human oral fibroblasts were isolated from biopsies of oral tissues obtained with consent under appropriate ethical approval from patients undergoing oral surgery procedures [13]. Rat osteosarcoma cell lines ROS 17/2.8 were a commercial frozen cell line.

For experiments using monolayer cultures the Condrocyte, fibroblasts and ROS experimental protocol was the same. 500 x 10^3 cells were seeded onto Petri dishes with 5 collagen-coated glass 12 mm coverslips and left for 48-72 h for the cells to attach and become confluent. In the expansion phase DMEM medium added with 10% FCS and 10µL/mLof FGS was used. When at confluence the cell cultures were examined microscopically and photographed. Two coverslips were placed in individual bioreactor culture chambers to form the test groups and two more coverslips placed in open MCmB 2.0 chambers (only the bottom part of the chamber was used) to form the control group. The bioreactor was connected up to the mixing chamber and the peristaltic pump and placed in an incubator (37°C, 5% CO_2 atmosphere). The two bioreactor circuits were filled with 10 mL of DMEM medium added with 5% FCS and no FGS [111] in or-

[13] School of Clinical Dentistry, Sheffield, Uk.

der to promote the matrix prodution phase instead of the expansion one. The cells were either left without perfusion (static bioreactor culture control) or perfused with culture medium in the bioreactor chambers for 24h (perfused cultures). At the end of the incubation time the coverslips were removed from the MCmB and transferred into small culture dishes and covered in medium to check cell morphology and viability by microscopy and by quantitative measurement of reduction of the vital dye Alamar Blue[14] as described in[112].

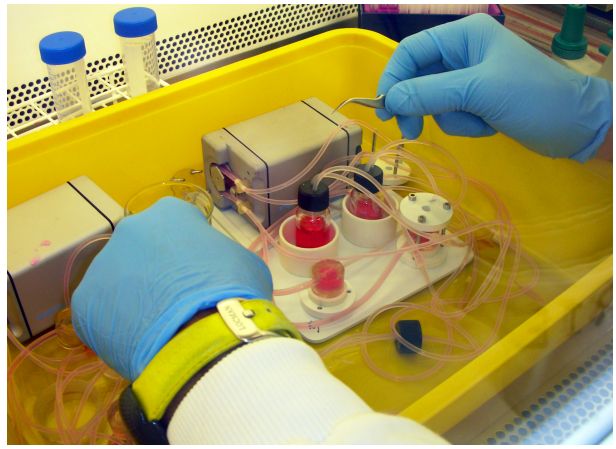

Figure 4.4: *Assembly of two flow experiments in MCmB 2.0 bioreactor. In this experiment two MCmB kits were used, in order to run in parallel two experiments with different flow rates.*

3D cartilage constructs of bovine articular chondrocytes were prepared by culturing the cells on scaffolds of polyglycolic acid (PGA) as described in [110]. Bovine articular chondrocytes at P2 were seeded onto PGA scaffolds (5x2 mm, $4 \cdot 10^6 \frac{cells}{scaffold}$). The resultant chondrocyte scaffold construct was incubated on an orbital shaker for a total of 14 or 21

[14]Invitrogen.

days to allow initiation of chondrocyte differentiation and extracellular matrix deposition. Constructs were either transferred to the bioreactor chambers (1 construct per chamber) or kept under static conditions in the same volume of medium used for the bioreactor circuit (10 mL). After incubation, the constructs were removed and the level of cell activity was measured. The constructs were then analyzed for matrix production by quantifying the levels of sulphated glycosaminoglycans (GAGs) in both constructs and culture media. GAG quantification is a measure of the amount of one of the main cartilage matrix components, proteoglycan.

3D constructs of human fibroblasts were formed by culturing the cells at passage 3 on the commercial collagen support Alloderm©[15]. Constructs were transferred to the bioreactor chambers (one per chamber) and perfused with appropriate medium (10 mL) for 24h or kept under static conditions in the same volume of medium used for the bioreactor. Proteoglycan production was determined by measurement of the glycosaminoglycan content of the tissue constructs and media using dimethylmethylene blue as described in [113]. The constructs in the bioreactor were perfused with medium at a flow rate of 110 µL/min. After incubation, the constructs were removed and the level of cell activity was measured using Alamar Blue dye, a resazurin-based fluorescent compound metabolized by mitochondrial cytosolic and microsomial enzymes to resorufin which can be detected with a fluorimeter at 573 nm.

[15] 2009 LifeCell Corporation.

4.3.2 Effect of bioreactor conditions on mono-layer cell cultures

Effect of flow rate on bovine chondrocytes at different passage number

Table 4.1 shows micrographs of condrocyte mono-layers at different passages before and after 24 hours in the MCmB 2.0 compared with their static counterparts. P1 cells do not show any signs of damage after 24h at 110 μL/min, the cells are morphologically similar to the static control but it is possible to observe a reduced deposition of ECM products on the coverslips (background of the picture has a higher contrast). This could be due to the effect of flow which continuously removes the ECM produced by the cells. Therefore in these conditions cells are stimulated to increase their matrix productivity because they do not reach steady state concentrations in the vicinity of the cells. At 290 μL/min P1 cells show signs of damage, the number of rounded dead cells is high and adhered cells are more elongated and spread.

For the P4 cells culture, signs of damage are evident even at 100 μL/min. Increasing the passage number, chondrocytes de-differentiate to a more fibroblastic phenotype. The condrocyte de-differentiation process can be also observed by a comparing the morphlogy of P1 and P4 controls. P4 cells show a more spread shape with a preferential direction of elongation. As is well known, fibroblast are not able to support shear stress and for this reason chondrocyte cultures with high passage numbers are damaged by flow as demonstrated by these experiments.

As shown in figure 4.5 a and b, for a flow rate of 110 μL/min the viability of P1 chondrocytes was around 20% higher than the controls. The wall shear stress on the cell surface at this flow rate is in the order of 3.510^{-6} Pawith a flow average residency time of 20 minutes. In the

Table 4.1: *Effect of flow rate at different passages in the MCmB 2.0 on the cellular morphology of monolayer cultures of bovine chondrocytes.*

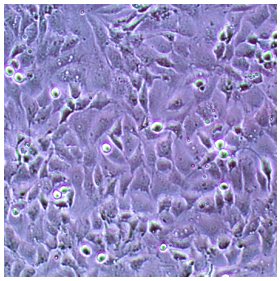

P1 static control

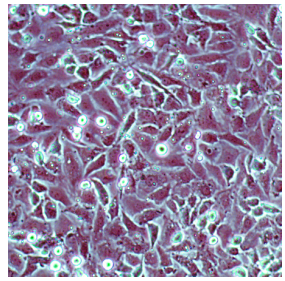

*P1 after 24h @ 110*µL/min

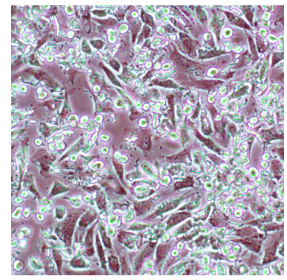

*P1 after 24h @ 290*µL/min

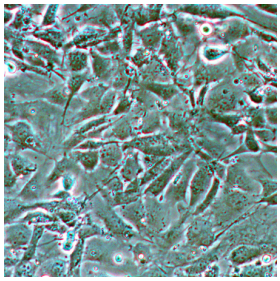

P4 static control

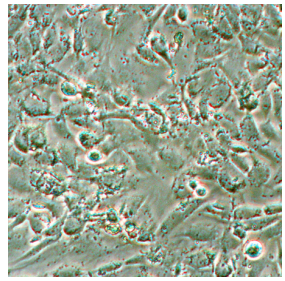

*P4 after 24h @ 110*µL/min

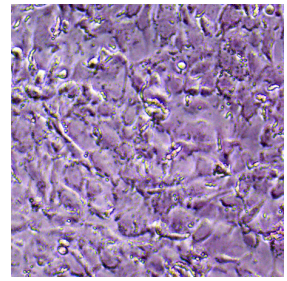

*P4 after 24h @ 290*µL/min

in-vivo environment articular cartilage is mechanically stimulated by the movement of synovial fluid over the surface of the tissue. This stimulus is critical for maintaining the unique mechanical properties of cartilage. In the MCmB 2.0 chambers this process is mimicked through flow mediated shear stress. The continuous removal of ECM products results in a higher metabolic demand because the cells are induced to upregulate ECM production with a consequent increase in mitocondrial activity.

For flow rates higher than 200 µL/min P1 cells also show signs of damage and detached dead cells could be observed. P4 chondrocytes at 295 µL/min clearly show a large degree of cell damage and in this case

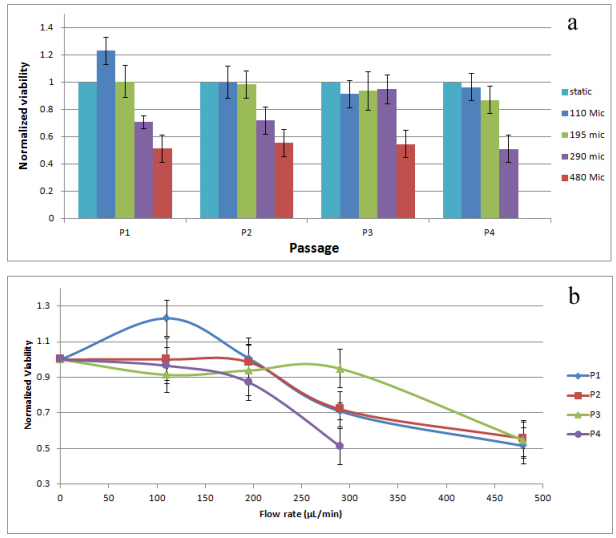

Figure 4.5: *Normalized viability of chondrocyte cultures after 24h in MCmB 2.0 at different flow rates. Graphs a and b show how the flow rate influences cell viability and how fibroblast cultures with high passage number are unable to support shear stress.*

the viability is less that than 50% of the controls.

Effect of increasing flow rate on human oral fibroblasts

Due to the low chamber volume, the MCmB 2.0 system does not require a high number of cells, and it is consequently possible to use human tissues extracted during surgery or biopsy. In this experiment oral mucosa tissue extracted during implantation procedures were used as a source of human fibroblasts. The MCmB 2.0 was used to test the effects of flow rate and shear stress on human oral fibroblasts in order to investigate the difference between of chondrocytes and fibroblasts when exposed to shear stress. Fibroblasts at the same passage number were used for these

experiments. Perfusion rates up to 195 µL/min had no apparent effect on fibroblast morphology (Table 4.2). Higher perfusion rates caused the fibroblasts to round up and detach from the glass coverslips. Changes in fibroblast morphology were reflected by greatly reduced changes in cell activity that were more marked than those observed in P1 chondrocytes cultures at the highest flow rate.

Table 4.2: *Effect of flow rate in the MCmB on the cellular morphology of monolayer cultures of human fibroblasts.*

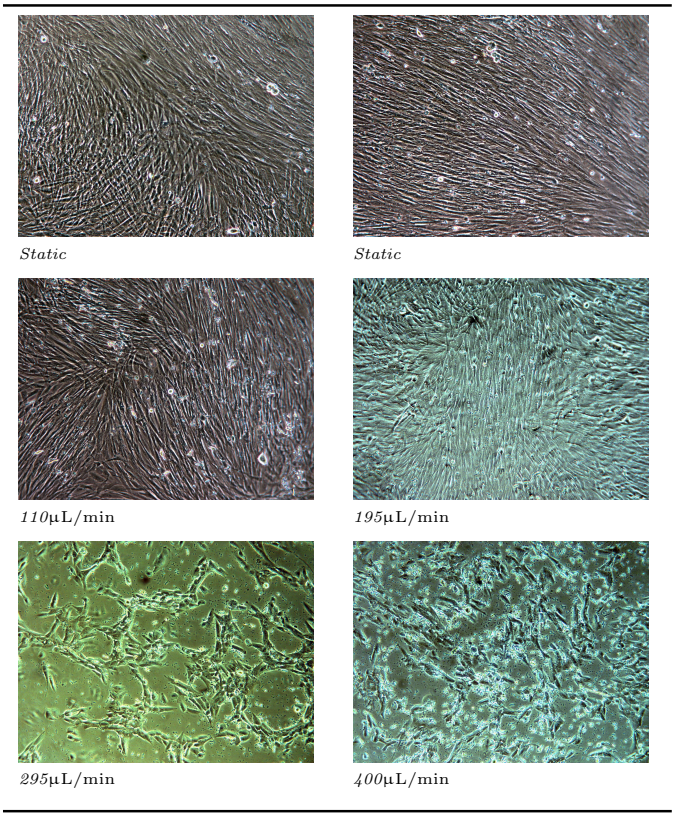

Figure 4.6 compares the viability at different flow rates for P1, P4

chondrocyte and fibroblast cultures. The P4 chondrocyte curve is more similar to the fibroblast curve than to the P1 because of the phenotype de-differentiation effect. P1 chondrocyte cultures are stimulated to increase viability and ECM turnover by the gentle laminar flow and shear stress at 110 µL/min. On the other hand P4 chondrocytes and fibroblasts do not support this level of stimulation.

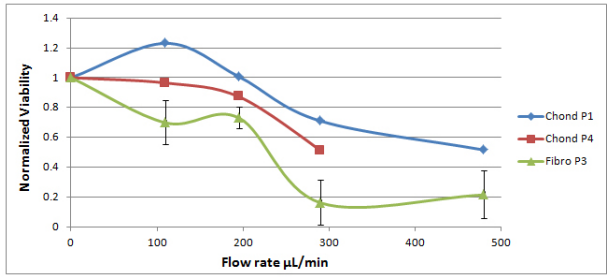

Figure 4.6: *Viability comparison at different flow rates for different cell types. The Chondrocyte culture with low passage number are able to support shear stress and have increased viability at 110* µL/min*, while high passage number chondrocytes and fibroblasts are not able to support shear stress induced stimulation.*

4.3.3 Effect of increasing flow rate on monolayer cultures of a ROS osteoblastic cell line

Preliminary observations indicate that incubating the ROS cells at low flow rates (110 µL/min and 195 µL/min) had a stimulatory effect. The microscopy analyses did not show any morphological changes due to the flow.

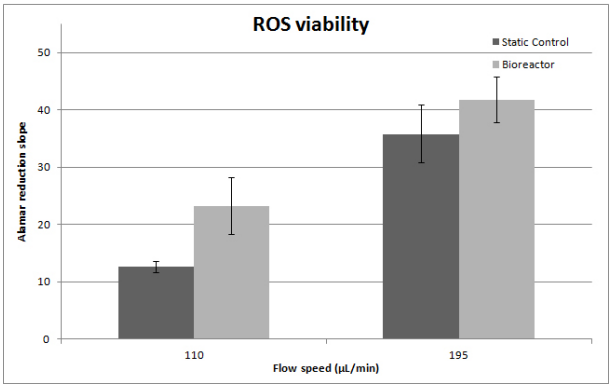

Figure 4.7: *Effect of flow rate on viability of monolayer cultures of ROS osteoblasts.*

4.3.4 Effect of bioreactor conditions on 3D cultures

A set of experiments with 3D constructs of different cell types was performed in order to investigate the differences between mono-layers and 3D cultures when exposed to shear stress stimulation in the MCmB 2.0. As shown in figure 4.8 the 14-day chondrocyte constructs incubated in the bioreactor had a higher cellular activity compared to the static controls. These stimulated constructs also demonstrate a 45-60% increase in the total amount of GAGs dissolved in the constructs with a similar increase in their proteoglycan content.

The stimulated construct was also shown to have increased levels of GAG in the medium (double that of controls), indicating an upregulation of the matrix synthesis rate (Table 4.3). These results indicate that the bioreactor significantly enhanced matrix synthesis over the static control. Mechanical stimulation is known to enhance matrix production, and as mentioned previously, the flow conditions in the bioreactor are capable of

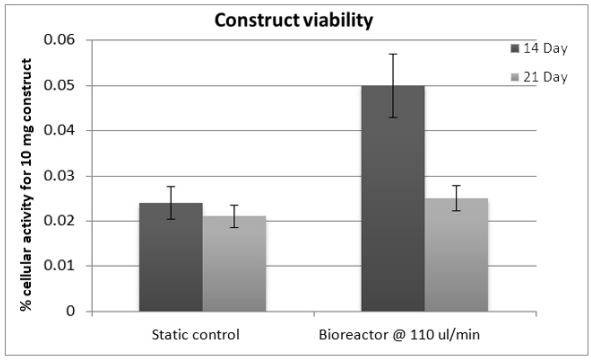

Figure 4.8: *Effect of a 72h culture period in the bioreactor on construct cellular activity normalised to construct wet weight at a perfusion rate of 110* μL/min.

reproducing this stimulus. In summary, chondrocytes are stimulated to matrix production by flow in the MCmB 2.0. The mechanical stimulation and continuous removal and dilution of cellular products helps to maintain the chondrocyte culture in the matrix production phase, as a result the cells have a higher viability and show a considerable increase in matrix production rate.

In contrast, after incubating the 21-day construct in the bioreactor there were no significant changes in cell activity (Figure 4.8) or an increased accumulation of GAGs into the construct matrix. However, a small increase in GAGs is detected in the medium compared to the static control (Table 4.3). This would suggest that there was some increase in GAG synthesis but not in incorporation into the extracellular matrix of the construct and this could be due to the "age" of the construct. These experiments show that the 14-day construct cells are in a more active phase and their metabolic activity can be driven to the matrix production, whereas the 21-day construct seems to be in a quiescent phase in

which the matrix levels are established and the cells are in a sort of steady state of ECM production. These experiments suggest that chondrocyte matrix production can be induced and stimulated by gentle flow and shear but only for "young" (14 day) constructs made with low passage cells (P1) that do not suffered from the the chondrocyte de-differentiation process.

Table 4.3: *Effect of 72h bioreactor culture at a perfusion rate of 110* μL/min *on proteoglycan accumulation in 14 and 21 day cartilage constructs.*

	GAGs in medium μg/mL	*GAGs (% of matrix dry weight)*	*Total GAGs in each construct* μg	*Construct wet weight* μg
Static control	1.95±0.25	15.75±2.12	219.05±42.22	18300±2923
14 Day construct	4.25±0.25	24.75±3.95	363.05±10.15	15100±2100
21 Day construct	4.9±0.6	16.55±0.15	214.65±1.85	16450±250

The construct experiments were also performed with fibroblast cultures in order to investigate if a 3D organization can enable fibroblast cultures to withstand shear stress. The experiment was conducted inserting a 14-day fibroblast construct in the bioreactor and stimulating it with a flow rate of 110 μL/min for 72h. The results showed that even in 3D culture, fibroblasts are unable to support shear stress and cell viability is reduced to 26±1.1% in comparison with static controls.

These experiments demonstrate that the MCmB 2.0 chamber is not only a modular bioreactor for the construction of in-vitro organ models for metabolic and toxicity studies, but can also be used as a cell culture stimulation unit, in which experiments can be designed with different types of stimuli applied to connected cultures, allowing investigation of tissue and organ physiopathology in an more in-vivo-like environment.

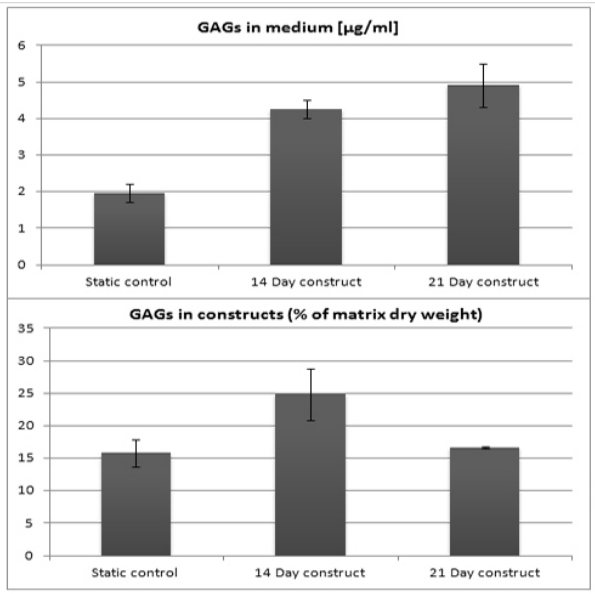

Figure 4.9: *Effect of 72h bioreactor culture at a perfusion rate of 110* µL/min *on proteoglycan medium and matrix accumulation in 14 and 21 day cartilage constructs.*

Chapter 5

Stimulus Specific Chambers Design and Realization

5.1 SQPR SQueeze PRessure stimulation Chamber

Articular cartilage serves as the load-bearing material of joints, with excellent friction, lubrication and wear resistance characteristics [114]. It is a white, dense, connective tissue, from 1 to 5 mm thick, that covers the bony articulating ends inside the joint. It consists of two phases, a solid organic matrix (50% mass by dry weight collagen fibrils and 20-30% mass by dry weight proteoglycan macromolecules)[115] [116] [117] and a mobile interstitial fluid phase (predominately water) [118]. In humans, chondrocytes contribute only about 1% of tissue volume [119] and maintain this matrix, synthesizing and secreting extracellular matrix, to balance extracellular degradation and matrix turnover. The biomechanical properties of articular cartilage are dependent on the integrity of the collagen network and on maintenance of a high proteoglycan content within the matrix. Expression of the genes for aggrecan and link protein, two major components of the aggregates of protepglycans, can be modulated by mechanical forces [120, 121, 122, 123, 124] as well as chemical stimuli

(growth factors and cytokines). Diseases of hyaline cartilage represent one of the major health problems especially in industrialized countries with high life expectancy [125]. Due to its avascular nature, cartilage exhibits a very limited capacity to regenerate and to repair. Moreover, it has been stated that the natural response of articular cartilage to injury is variable and, at best, unsatisfactory. The clinical need for improved treatment options for the numerous patients with cartilage injuries has motivated tissue engineering studies aimed at the in vitro generation of cartilage replacement tissues (or implants) using chondrocyte-seeded scaffolds [126, 127, 128, 129]. The normal loading environment of chondrocytes involves a combination of intermittent cyclical fluid pressurization. Under normal conditions, chondrocytes are able to balance their synthetic and catabolic activities to maintain the integrity of articular cartilage in vivo. In order to restore aspects of the articular physiologic environment in vitro an innovative stimulation chamber was developed.

5.1.1 Material and methods

In this section the simulation and design of an innovative cell culture stimulation chamber is described. The SPQR (SQueeze PRessure) bioreactor chamber is designed to impose a cyclic hydrodynamic pressure that replicates the physiological environment of the joint on different types of cell cultures or tissues slices. One of the most important features of the SPQR chamber is the ability to generate a squeeze pressure without requiring any contact with the samples. The SQPR chamber was designed through analytic and FEM models in order to simulate the fluid-dynamics of the chamber and to verify the squeeze pressure generation principle. After model validation the chamber was designed, realized and tested together with its control unit (P.GIO)2.

Analytical and FEM analysis

The fluid dynamics inside the bioreactor can be described using the fluid film lubrication theory. The introduction of a fluid film between two moving and rough surfaces provides a lubricating effect which substantially reduces the coefficient of friction between them [130]. Such films are usually sufficiently thin such that viscous forces are large in comparison with inertia forces, so that the latter may be neglected.

The fluid dynamics of the SQPR bioreator was simulated from an analytical and numerical point of view. The analytical model does not consider the presence of the external walls, for this reason a complete FEM model is required in order to evaluate how the chamber walls influence squeeze pressure generation.

The analytical model stems from Reynolds equation which describes fluid flow in a narrow gap with well defined dimensions and geometry. In its most general form, the Reynolds equation has the following form:

$$\frac{\partial}{\partial x}\left(\frac{\rho h^3}{\mu}\frac{\partial p}{\partial x}\right)+\frac{\partial}{\partial y}\left(\frac{\rho h^3}{\mu}\frac{\partial p}{\partial y}\right)= \tag{5.1}$$
$$6(U_1-U_2)\frac{\partial(\rho h)}{\partial x}+6\rho h\frac{\partial}{\partial x}(U_1+U_2)+12\frac{\partial(\rho h)}{\partial t}$$

where x, y are mutually perpendicular coordinates within the fluid, p is the local pressure within the film, ρ and μ are the density and absolute viscosity of the lubricant, and h is the film thickness, and U_1 and U_2 are the velocities of sliding of upper and lower surfaces respectively. The physical significance of this equation is that the generation of hydrodynamic pressure within the film is a function of three terms the wedge, stretch, and squeeze contributions to load support.

Pressure generation inside the bioreactor is based on the squeeze contribution, which is due to normal approach of the surfaces, whether or

not sliding motion occurs between them. The term squeeze films applies to the case of an approaching surface (usually planar) which attempts to displace a viscous liquid between them.

$$p(r) - p_a = \frac{3\mu V}{h^3} R^2 \left(1 - \frac{r^2}{R^2}\right) \tag{5.2}$$

$$v = \frac{3Vr}{h^3} z(z-h) \tag{5.3}$$

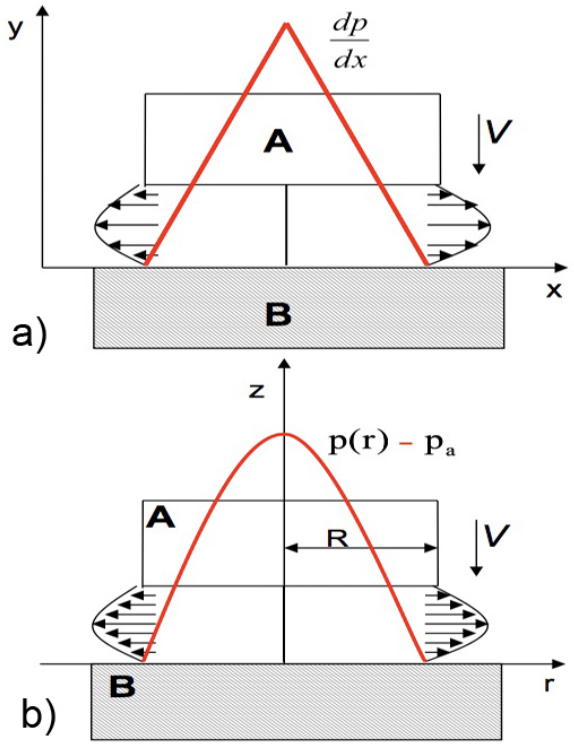

Figure 5.1: *a)Pressure and b) Velocity analytical profiles.*

Is possible to note that v is a function of three coordinates, r, h and z, of which only h is time-dependent. This equation shows clearly that

at any fixed h and radius r the velocity distribution is parabolic over the cross-section of flow and its mean value at a fixed height increase linearly with r. Shear stress at bottom (τ_w) site can be obtained from Newton's viscosity law from equation 5.3, fixing z=0

$$\tau_w = -\frac{3\mu V r}{h^2} \tag{5.4}$$

In order to simulate the hydrodynamics of the SQPR bioreactor the commercial software COMSOL Multiphysics[1] was used. The Axisymmetric Incompressible Navier-Stokes for Newtonian flow (constant viscosity) application mode was used to calculate the velocity field **u**, pressure distribution p and shear stress on the bottom wall.

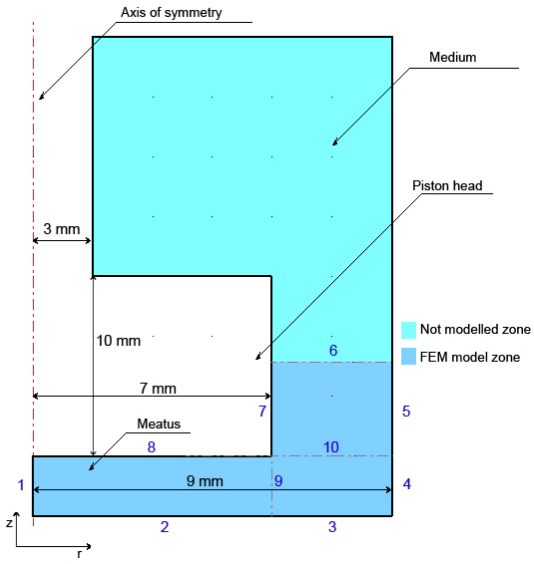

Figure 5.2: *SQPR FEM model scheme.*

[1]COMSOL Multiphysics is a registered trademarks of COMSOL AB.

The geometry, designed as in figure 5.2, represents the culture medium filled domain, and it is characterized by a density of 1000 kg/m^3 and a viscosity of 0.02 Pa s. Predefined elements type Lagrange - P_3 P_2 was chosen. Boundary conditions are set as follows (referred to the wall indexes of figure 5.2): (1) Symmetry boundary - Axial symmetry, (2-3-4-5) Wall - No slip, (6) Outlet - Pressure with no viscous stress - P_0=0 Pa, (7-8) Wall - Moving/leaking wall - U_w=0, V_w= *vel* and (9-10) Continuity.

In our model *vel* is the piston velocity and it is equal to -0.0116 m/s during the approaching phase and 0.002 m/s in the retraction phase. Mapped mesh (594 elements) was obtained fixing the number of edge elements on boundary 1-2-3-7 respectively to 9-42-12-4 linearly distributed elements. A 3D model was also obtained by rotating the 2D geometry around the z-axis and by extrusion of coupling variables p, u, v, and K_r_ns. Models were implemented in COMSOL Multiphysics 3.4 and solved with the UMFPACK direct solver (in a parametric mode with parameter *vel*)[2].

SQPR chamber design and realization

The main purpose of this design was to realize a bioreactor chamber able to impose hydrodynamic pressure stimulation on cell cultures without requiring complicated machines or protocols. For this reason the design and realization process was driven by few key points:

- Easy and fast to use
- Contactless stimulation
- Allow long time stimulation protocols without requiring disassembly and restarting the experiment

[2]Ran on a Macbook 5,1 (Intel COre 2 Duo, 2GHz CPU) running Mac OS X.

- Allow easy sample collection during all the stimulation phases
- Possibility to use different types of tissues, constructs or cover slips with different thickness in the chamber
- Allow adequate oxygenation
- Light, small and transparent

The design process was aimed at exactly replicating the FEM model dimensions 5.2. The FEM piston was 14 mm in diameter and 10 mm height, we decide to split the piston in two parts, the head and the shaft, in order to simplify the bioreactor assembly and the cleaning phase. The head is the real functional part and it was designed with the same diameter as the FEM model (figure 5.3.b). The shaft diameter was reduced to 6 mm (figure 5.3.e) in order to minimize the weight of the system and the tolerance of this part was imposed to be very low (H7) in order to obtain a perfect alignment and parallelism of the system.

The shaft was drilled on the top and threaded for the linear motor coupling, a cavity was designed in the top part in order to allow a seeger insertion used as excursion limit. The excursion limit is useful during the assembly phase when the piston shaft is not coupled to the motor and it can slide down and impact with the cell surface during the SQPR experiment assembly.

The external part of the chamber is designed as a cylinder (figure 5.3.a) in order to reproduce the FEM dimensions, and have internal end external diameters respectively of 18 mm and 25 mm. The external height of the chamber is 65 mm but the internal cavity where the medium is inserted is only 40 mm. The top part is necessarily thick to allow a perfect linear motion of the piston inside the chamber and to ensure a high parallelism of the piston and cell support surfaces. The piston shaft

and the hole where it is inserted are both grinded and a H7 tolerance is required.

The chamber external cylinder have a base larger than the body (50 mm), that fits on a quick snap fixing system designed on the SQPR holding frame. The internal diameter of the chamber is also grinded in order to allow a perfect linearity of the wall. The high dimensional accuracy of the internal cavity is critical factor due to the fact that the distance between the piston head and the internal chamber wall is very important in the hydrodynamic pressure generation principle (the presence of the wall is the difference between the analytical and FEM model5.1.1).

The SQPR chamber has also two holes near the top of the internal cavity to allow sample collection during the experiments. The cavity holes are also important for medium oxygenation and they have a diameter of 4 mm in order to allow a perfect fit of the standard syringe and Luer-Lock connectors. In fact, during the experiment the holes are closed using syringe filters in order to prevent any contamination and allowing incubator atmosphere to diffuse in the SQPR cavity.

The SQPR bottom is made of two parts, the base and the samples brace. The base is an aluminum disc of 65 mm in diameter and 10 mm thick (figure 5.3.f), it is an holder for the brace and it is not in contact with the medium. The braces are various and they can be changed depending by the used sample (fresh tissues, gels, cover slips etc), they are made of Derlin, with a diameter of 18 mm and a height (H)[3] of 12 mm. The braces have two cavities with a diameter of 14.9 mm for the O-Ring insertion that sealed the system preventing medium leakage from the internal SQPR cavity (figure 5.3.c,d).

[3](H) is the distance between the aluminum base and the surface where the samples are placed.

The braces are used as tissue supports, but they have to prevent the piston impacting with the cell cultures during the "finding home" routine2.1.2. The impact is avoided through a 1.5 mm thick ring realized on the brace top (figure 5.3.d), where the cultures are inserted, the different braces present rings of various thickness in order to allow the insertion in the culture cavity of different samples/constructs such as fresh tissues or scaffolds.

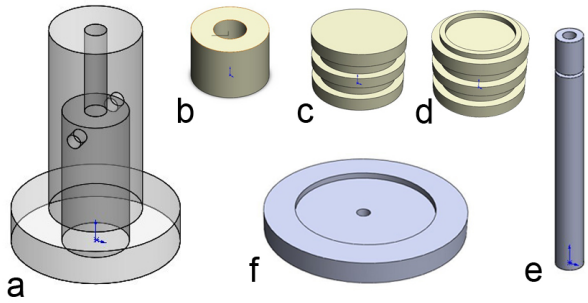

Figure 5.3: *The SQPR bioreactor parts: a) The Plexiglass chamber with the stimulation cavity, b) The piston Derlin top part, c) The basic sample bracer, d) The sample bracer with ring, e) The piston shaft and f) The aluminum base (parts are not equally scaled).*

The basic brace have no ring on the top surface, the other braces are:

- scaffold brace (ring height 2 mm)
- cover slips brace (ring height 1 mm)
- fresh tissue brace (ring height 3 mm)
- Gel construct brace (ring height 5 mm)

The aluminum base and the Derlin braces are coupled through a screw threaded on the brace bottom. The SQPR bioreactor requires a frame

system where the linear stepper motor is fixed and where the SQPR chamber is inserted after sample insertion. The SQPR frame system has to be light, easy to assembly and clean and has to allow easy sample collection. The frame system is made of three Nylon plates assembled together with screws and two columns used as a support to be placed in the anterior part of the system in order to ensure stability of the frame during the stimulation. The vertical plate of the frame is drilled and threaded, the horizontal plates have holes with cavities for the insertion of screws. The bottom horizontal plate has a small cavity to assist the SQPR chamber alignment phase and it is equipped with the fast plug holding system. The fast plug holding system is composed of two L-shaped Derlin plates screwed on the bottom of the frame and where the SQPR aluminum base has to be inserted. The tolerance between the SQPR base and the L shaped holders is very low and this allows the entire system to be solidly held together. The top vertical plate of the frame is where the linear stepper motor is fixed, a 6 mm in diameter hole at the center allow the motor shaft to be connected with the SQPR piston shaft and two screws are used to fix the motor to the top frame. The motor is protected from the humid incubator environment through a case, coupled through a flat round gasket to the top part of the frame, where the motor cable is inserted through a water proof connector (figure 5.4.b).

The two frontal columns are made of nylon and they are inserted in the system only before starting the experiments. They are required to prevent any deformation of the frame as consequence of the *finding home* procedure where the motor pushes the piston to the base of the SQPR chamber for 2 seconds (impacting with the brace ring). In fact if frame deformation occurs during the *finding home* procedure, the piston alignment is compromised and the generated pressure will be uncharacterised.

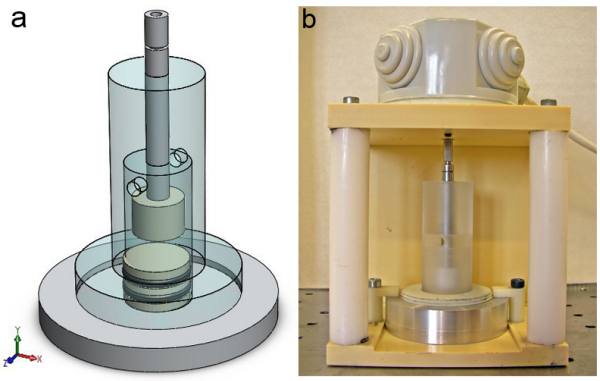

Figure 5.4: *a) The SQPR stimulation unit assembled and b) The SQPR bioreactor in its framework during setup of an experiment.*

The frontal columns reduce the working space of the SQPR system but sample collection and disassembly are still possible.

5.1.2 SQPR design and model validation

FEM models results

In this section a comparison between the analytical and FEM models is presented in order to demonstrate the validity of the finite element approach to solve the complex SQPR bioreactor fluid dynamics. The analysis was performed for a piston approaching phase that stops 300 μm (piston channel height) over the cell culture, with an approaching and retraction speed respectively of -0.0116 and 0.002 m/s. Figure 5.5 shows a comparison between the FEM and the analytical model of the SQPR bioreactor environment. The difference in calculated pressure between the two models is 7% (which corresponds to 89 Pa) (calculated at the center of the chamber) during the approaching step and it is due to the

over-pressure determined by the bioreator walls that are not considered by the analytical model.

Figure 5.5.e shows the velocity field during the approaching phase. The modulus of the velocity increases with the radial coordinate as in the analytical model and present a parabolic profile in each section. The differences in shear stress at the cell surface are shown in figure 5.5.c, 3D plots of pressure distribution and shear stress in the channel are shown in figure 5.5.b and d.

SQPR chamber preliminary tests

A set of preliminary tests oriented to verify the SQPR chamber assembly, sealing and functionality was performed. The chamber was completely disassembled and all its parts washed in ethanol in order to simulate and identify any problem related with the classical sterilization process. After rinsing all the bioreactor parts with PBS, the system was assembled, connected with the linear motor and the SQPR cavity filled with 4 ml of DMEM medium. The SQPR stepper motor was connected with the P.GIO system and a squeeze pressure experiment started. During this preliminary experiment the oxygenation holes were closed in order to prevent medium evaporation and the medium level monitored every 6 hours for 2 days. During the experiments no medium reduction was noted indicating that the chamber is correctly sealed, the piston range was also monitored and after 48h no shifts were noted indicating that the P.GIO system and the SQPR motor are able to support long term experiments. All the calibration and free movement procedures were also tested and sample insertion procedures were also simulated and found to be essentially smooth and trouble-free.

5.2 VSC Vascular Stimulation Chamber

Smoking, stress, lack of a suitable physical training, a fatty diet are all determinant factors of setting in vascular diseases, and are the primary causes of death in industrialized countries [131, 132]. Despite the large quantity of studies on this subject the precise relationship between these risk factors and the pathogenesis of these diseases is not completely understood at biochemical and mechanical level [133, 134, 135]. It is well-known that the shear stress influences the physiology of vascular tracts, but the difficulty of modulating the forces that act on them does not allow the determination of precise quantitative effects [136]. This shortage of knowledge affects the cure. Autologous vascular grafts are the only vascular substitutes with long term patency [137]. This surgical technique is limited by poor availability of donor sites. For this reason we designed and realized a bioreactor able to reproduce the physio-pathological situations of a vascular tract with an inner diameter of less than 6 mm.

This device has two possible applications:

- To engineer vascular conduits that can be used as grafts for the cure of main diseases of vascular system, due to scarce mechanical and biological properties of commercial grafts.

- To study the relationship between the different components of a blood vessel at the biomechanical and biological level.

In a previous study, the vessel chamber was modeled through analytical and a finite element analyses in order to establish a working geometry to mimic the physiological environment and to determinate the bioreactor's working window. The system was designed and realised in way to be manageable, low volume, low cost and amenable to easy medium sampling.

The system has been tested in terms of fluid dynamic characteristics in order to verify the correspondence with the models developed. Moreover its capacity to modulate the mechanical properties of the vascular tract has been performed by subjecting porcine blood vessels to several transmural pressures, simulating different physio-pathological states.

5.2.1 Material and methods

Analytical and FEM analyses

Many studies present in the literature have proposed vessel chambers for vascular characterization [138, 139] without an adequate analytical and finite element models, able to evaluate the correlation between physiological stresses and those induced by the systems induced. The first step of the analytic analysis of the bioreactor starts from a fluid-dynamic point of view. The absence of turbulent flow in the bioreactor is validated by the low Reynold's number of the system. Combining Reynolds number, friction Fanning parameter and Bernoulli's equation, the hydraulic circuit has been studied, evaluating the pressure drop along it. The mechanical analytical model has been developed comparing the vessel placed in the culture chamber with a pressurized elastic tube locked by a rigid flange 5.6

The vessel wall, of radius R, thickness h and elastic modulus E, reflects the Hooke's law, which, in a cylindrical coordinate system and in MKS units, can be expressed as:

$$\sigma_{zz} = \frac{E}{1-\upsilon^2}(\epsilon_{zz} + \upsilon\epsilon_{\theta\theta}) \tag{5.5}$$

$$\sigma_{\theta\theta} = \frac{E}{1-\upsilon^2}(\epsilon_{\theta\theta} + \upsilon\epsilon_{zz}) \tag{5.6}$$

Whereas radial stress can be neglected using the thin wall approximation. Solving these equations with boundary conditions of constant pressure inside the vessel, longitudinal stress equal to zero and negligible shear stress, the final result is:

$$W_{rr} = \frac{pR^2}{Eh}[1 - e^{-kz}(\sin kz + \cos kz)] \tag{5.7}$$

The previous formula 5.7, where p is the pressure, shows how the radial displacement W varies as function of longitudinal coordinate: after an initial transient, due to the stress shielding of the flange, the displacement is close to Laplace's law after a fixed distance from the inlet. The parameter k depends on the geometry and on the mechanical properties of the materials.

A FEM model developed with COMSOL Multiphysics[4] allowed estimation of strains, shear stresses, transmural pressure and flow inside the vessel 5.7.

Vascual stimulation chamber realization

A bioreactor chamber have to be made of a biocompatible, easy to work, low cost, sterilizable, and transparent material in order to allow the direct analysis of experiments. It should also have small dimensions. A bioreactor should be easy to use even for a non-specialised operator, and its sterility should be conserved for a long time. For this reason, the vessel chamber wasrealised by casting Poly-dimethylsilosane (PDMS)[5]. The mould was made in aluminum according to the technical requirements and the results of FEM modeling analysis. The cell chamber is composed of two modular parts, easy to assemble with a water tight seal. The

[4]COMSOL Inc, Burlington,USA.

[5]Dow Corning, USA.

PDMS is cast in the mould, cured in an oven at 60°Cfor 4 hours and then peeled off.

The vessel chamber is composed of:

- A top, in which silicone tubes are mechanically inserted and sealed to connect to the perfusion system. These tubes allow insertion of the connectors for the locking of the perfused vessel
- A bottom, which, once assembled with the top, creates small internal volume where the vessel is bathed in a culture medium

The vascular stimulation chamber has two inlet and two outlet connections, two for the intra and two for the extra vessel medium circulation, all these connections are fabricated by inserting standard Luer Lock connectors into the silicone 5.8.a. To increase the seal of vessel chamber the two parts are clamped between two Derlin plates and held with screws. 5.8.b.

The vascular stimulation chamber can be connected to the SUITE platform for maintenance of the culture environment or used as a free standing application in an incubator. In both case the transmural pressure is achieved through the P.GIO 2 dedicated unit.

Vascular pressure generator design and realization

The Vascular pressure generator design is based on a classic syringe pump used to compress a reservoir of medium connected in parallel to the intra vascular medium circuit. The pressure generator is made by a sliding unit where the syringe is placed and actuated. The sliding unit is actuated through a 12 VDC motor equipped with an encoder used for the position feedback. The sliding unit is equipped with a safety switch used to prevent the complete compression of the syringe that avoids mechanical failure and damage in case of tube breaks or disconnections.

The pressure feedback is archived through the P.GIO pressure sensor connected to the syringe through a T connector.

The pressure generator is used to compress air, the system is plugged to the intra vascular circuit mixing chamber in order to impose a controlled transmural pressure. The extra vascular circuit is kept at environmental pressure through an open tube attached to a syringe filter5.9.

5.3 LFC Laminar Flow Chamber

A laminar flow chamber was specifically designed to enable cells to be subject to a large range of shear stresses. Several cardiovascular pathologies are associated with altered patterns of flow and shear stress [140, 141]. The study of endothelial cell response to different flow conditions is therefore important for understanding and curing cardiovascular disease. Using finite element methods and imposing a number of design criteria such as maximum volume and minimum area for cell culture, as well as the range of shear stresses desired, we converged to a final design for the chamber. Figure 5.10 shows the chamber design and the constant and controlled velocity vector, in the cell culture zone. By changing the flow rate of the fluid, constant and controlled shear stresses ranging from 410^{-2} to 9010^{-3} Pacan be applied to simulate aortic as well as capillary shears, in physiological or pathological states. Equation 5.3 allows, the shear stress (τ) on the cell layer to be calculated from the applied volume flow rate (Q) with a medium viscosity (μ), cell chamber cross section (A) and a distance between the center of the chamber and the cell monolayer (z).

$$\tau = \mu \frac{Q}{A \cdot Z}$$

The laminar flow bioreactor chamber is realized through a polydimethylsiloxane (PDMS) casting process on an aluminum mould (Figure 5.11.b). The cell chamber is 198 mm long, 49 mm wide and 7 mm high (Figure 5.11.a).

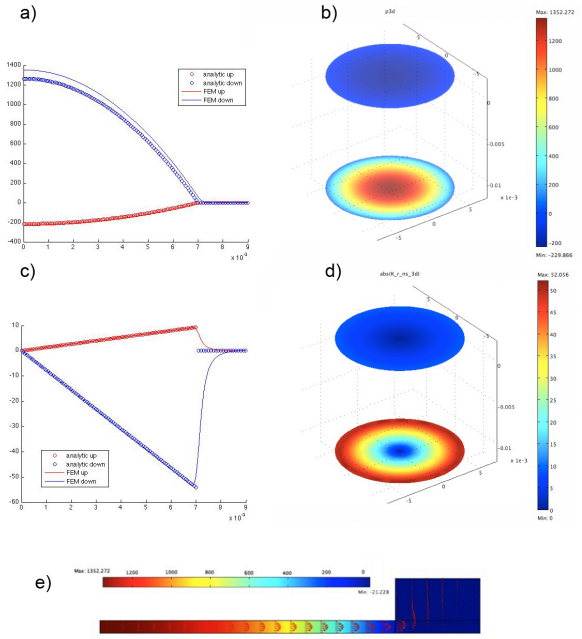

Figure 5.5: *FEM results: Comparison between finite element model of bioreactor (solid line) and analytic model of squeeze pressure* (Pa) *(a) and shear stress* (Pa) *(c) generation during the approaching (blue) and the retraction (red) phase; Surface plot of pressure (b) and shear stress (d) distribution inside the channel and (e) Velocity field in the channel during the approaching phase.*

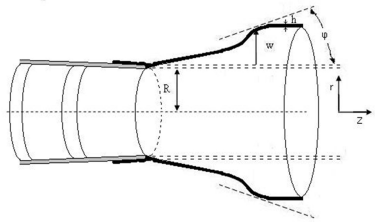

Figure 5.6: *Schematic diagram of the blood vessel placed in the culture chamber.*

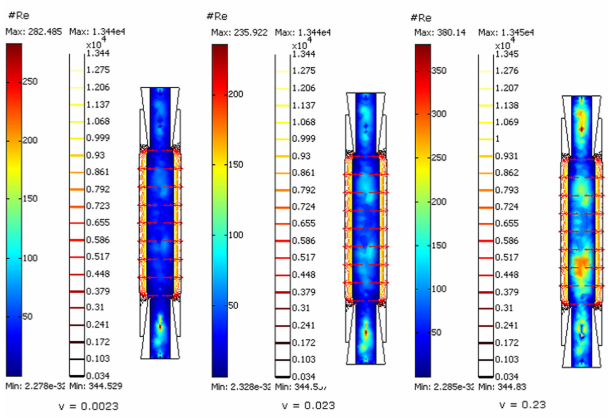

Figure 5.7: *Parametric analysis of the bioreactor system as function of fluid velocity (0.0023* m/s*; 0.023* m/s*; 0.23* m/s*): Reynolds number (surface plot), circumferential stress (contour plot) and radial strain (arrow plot) are shown. All values are in MKS units.*

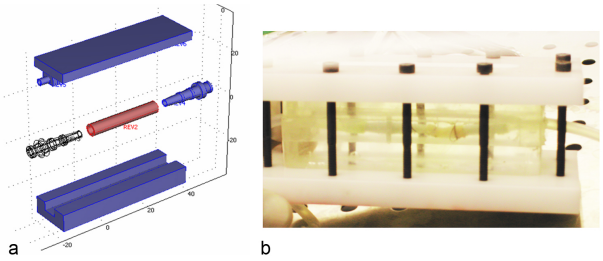

Figure 5.8: *a) CAD design of the vascular culture chamber and b) The Vascular Stimulation chamber during the assembly phase.*

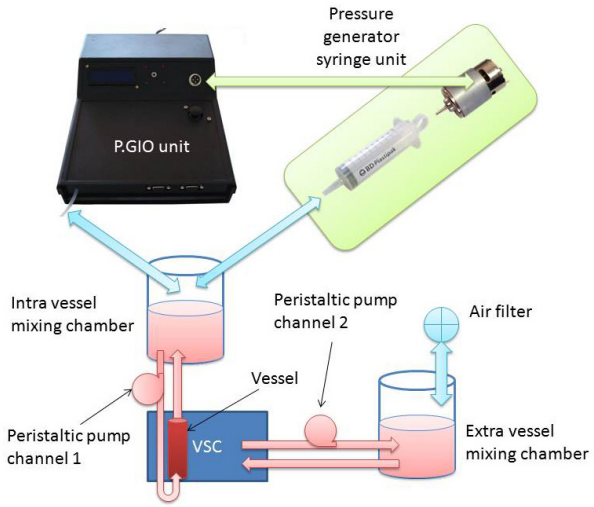

Figure 5.9: *VSC and P.GIO connections schema.*

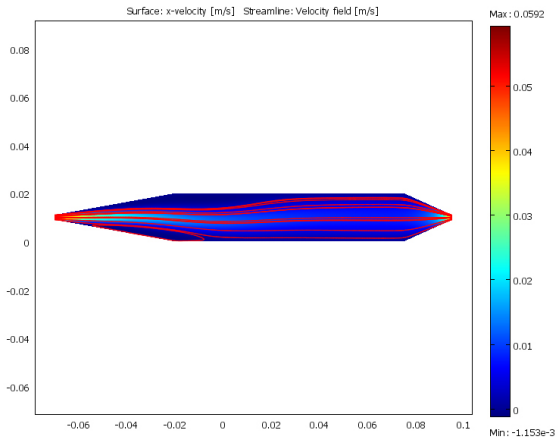

Figure 5.10: *FEM simulation of the laminar flow bioreactor chamber with a medium flow speed of 0.05* m/s*(12* mL/min*).*

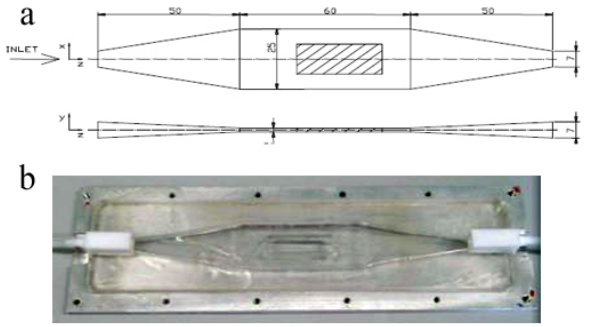

Figure 5.11: *(a) CAD design of the Laminar Flow chambers and (b) the Laminar Flow Chamber mould.*

Chapter 6

Cell and Tissue Tests on Stimulus Specific Chambers

The SUITE platform is a complete system for the maintenance of the cell culture environment, and can apply different types of stimuli on cells. The application of precise and well-controlled stimuli is important in order to better understand the correlation between physical variables and pathologies, and allows a more accurate study of tissue physiology and pathologies. In this chapter tests on the three stimulation chambers are described.

6.1 SQPR Squeeze Pressure Chamber tests

The goal of this study was to test the hypothesis that contact-less mechanical stimulation of chondrocyte cultures, can promote differentiation and enhance matrix production, compared to a static culture. For this reason, bovine adult chondrocytes (BAC) were seeded in different constructs and subjected to a controlled, contact-less overpressure, using the SQPR chambers 5.1 and the P.GIO 2.0 system 2. In order to simulate the knee's physiologic environment, the SQPR bioreactor was used to apply

a cyclic pressure of 15 kPa with a frequency of 1 Hz. This stimulation was chosen in order to mimic the intra-articular synovial fluid pressure oscillations during continuous passive motion [114]. With this type of stimulation the construct is subjected to localized overpressure and a low shear stress at the same time as described in the section on SQPR design 5.1. The viability of the cells was examined before and after the stimulation, to test the culture conditions, and the production of GAGs was analyzed in order to evaluate how the applied stimulation influences cell activity in terms of matrix production [127, 128].

6.1.1 Material and methods

Bovine articular chondrocytes where extracted using the same protocols described in the MCmB 2.0 chondrocyte cellular tests section 4.3 and used for construct seeding.

Constructs seeding and cultivation

During the validation tests, two different PGA scaffolds were used: 100% PGA felt, 1 and 2 mm thick with a diameter of 5 mm and a density of 70 mg/c^{3}m.

The two different constructs (1 and 2 mm thick) where seeded using the same procedure [142] but with different cell concentrations. The scaffolds were previously sterilized by washing them with isopropanol for 15 min and rinsing several times with sterile PBS. The PGA was placed in dishes and pre-wetted with FCS for 10-15 minutes and threaded onto needles embedded in the spinner flask lead. Cells were inoculated adding different amounts of cell suspension in order to obtain a cell density of 2.5×10^6 cells for the 1 mm thick scaffolds and 4×10^6 cells for the 2 mm thick scaffolds. The culture flask was filled with 200 ml of complete

medium, to completely cover the constructs. The cells were agitated at 50 rpm with a magnetic stir bar for 3 days in a 37°C5% CO_2 incubator [143]. After 3 days of agitation in incubator cell-polymer constructs were transferred to deeper Petri dishes (4 scaffold in each one), adding expansion media (complete media + Fibroblasts Grow Factors FGF). The dishes were left in a rotating shaker, which gently mix the media at 30 rpm. After three days of orbital agitation the media was removed and replaced with complete media (Dulbecco's Modified Eagle's Medium containing 10% v/v FCS, 10,000 units/ml penicillin, 10 mg/mL streptomycin, 10 mM HEPES, non-essential amminaacid and L-glutamine 2mM.) supplemented with 0.1% v/v 50 µg/mL Ascorbic Acid and 0.1% v/v 5 mg/mL insulin[1]. Starting from here, the cells began matrix production. Medium was completely replaced three times/week.

Experimental Protocol

The final purpose of this experiment was the validation of the SQPR bioreactor chamber as a cell culture system able to stimulate chondrocytes culture in physiological like condition. Experiments on condrocytes constructs where conducted applying a continuous pulsatile pressure for 24 or 48h. In order to simulate the joint environment all the experiments where performed using a High Viscosity media (HV media) that better approximates the characteristics of the synovial fluid (1-10 $Pa \cdot s$) [144, 145]. For this reason, 5% w/v of Dextran 500000MW was added to the complete media, already supplied with 0.1% v/v 50 µg/mL Ascorbic Acid and 0.1% v/v 5 mg/mL insulin[2].

Cell viability was evaluated using the Alamar Blue assay [3], as pre-

[1] All cellular reagents and equipments purchased from Sigma-Aldrich UK.
[2] Sigma-Aldrich UK.
[3] Alamar Blue is a cell viability reagent from Invitrogen.

viously described 4.1 in order to demonstrate the vitality of the culture in the SQPR system. The stimuli mediated effects were investigated analyzing the concentration of GAGs which is directly correlated with the extent of matrix production. For this reason, total glycosaminoglycan content was determined by analysis of papain-digested samples using the dimethyl-methylene blue (DMB) spectrophotometric method [113].

An experimental protocol was planned and applied to all of the different constructs in order to allow a future comparison between the different approaches. The bioreactor was previously sterilized leaving all components in a solution of 70% ethanol for 30 minutes. Then, one scaffold was placed in each bioreactor (two experiments were performed in parallel) and one left in the 12-well plate as a static control; 4 mL of High Viscosity media (HV) were added in each one, and both bioreactors were placed in the 37°C5% CO_2 incubator. The Alamar Blue assay was performed twice in all experiments: 24h before the stimulation, to assess the initial cell activity, and then just after the stimulation, to evaluate if the system permits normal growth and survival of the cultures. At the end of the experiment, 0.5 mL of media were collected from the bioreactor and from the control and used for GAGs assay. Immediately after the end of the experiment, the Alamar Blue assay was made to check the cell viability. Each construct experiment was carried out for a minimum of three independent trials, and a statistical analysis was performed using ANOVA.

6.1.2 Results

The cell experiments were carried out for 24 and 48h in the case of the 1 mm thick scaffolds and only for 24h in the case of the 2 mm one. All the constructs were used within the one week after seeding. The experiments were carried out in triplicate, using scaffolds 5,6 and 7 days post seeding,

after which the statistical analysis was performed. Figure 6.1 shows the normalized viability, with respect to controls, of the 1 mm thick scaffolds after 24h and 48h of stimulation in comparison with the static control. The viability of the stimulated construct is comparable with the static control indicating that the HPC bioreactor environment is compatible with cell survival and that the imposed pulsatile stimuli do not damage the cell cultures.

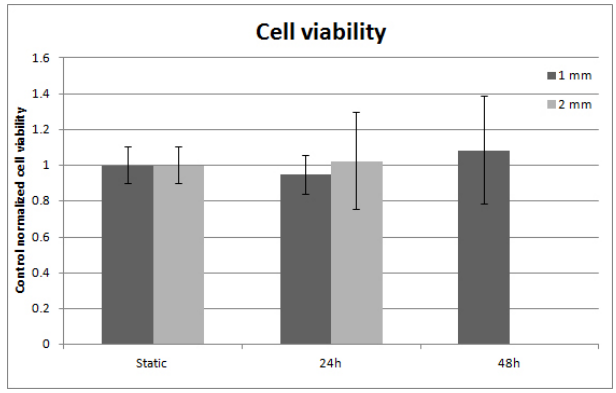

Figure 6.1: *Viability of chondrocyte constructs (1 and 2* mm *thick) after 24 and 48 hours of stimulation in SQPR bioreactor. All the constructs have a viability similar to the control, indicating that the SQPR stimulation does not damage the cell culture. All data are normalised with respect to the control.*

The collected media samples were analyzed with the DMMB assay, as previously described in section 4.3.1 and the results are shown in figure 6.2. The glycosaminoglycan concentration in the 24h and 48h 1 mm stimulated scaffolds shows (figure 6.2.a) a relevant increase respectively of 70% (4.73 mg/mL control and 8,08 mg/ml bioreactor) for the 24h construct and 250% (6.40 mg/mL control and 16.66 mg/mL bioreactor)

for the 48h one. The 2 mm thick constructs show a lower level of GAG concentration (figure 6.2.b) in the medium but the control/bioreactor difference after 24h of stimulation is higher than in the 1 mm scaffold with an increase of 95% (1.96 mg/mL and 3.80 mg/mL bioreactor) in the medium GAG concentration. This could be due the entrappment of GAGs in the thicker scaffolds, such that their diffusion in the medium is limited [146, 147]. These results demonstrate how the contact-less stimulation imposed by the SQPR system is able to enhance ECM production in chondrocyte constructs giving rise to a very high difference in the ECM production speed. As shown in figure 6.2 the stimulated cultures present a GAG production rate higher than the static control. Analysing the 1 mm scaffolds GAG production curves it is possible to note that after 24h the slope of the static control tends to decrease indicating that these cultures gradually loose the ability to produce ECM. The 1 mm curves in the bioreactor do not shown this change in the production rate after 24h of stimulation, indicating that the contact-less pressure induces the constructs to maintain increased metabolic activity in order to maintain a high rate of ECM production instead of lapsing into a quiescent phase.

6.2 VSC Vascular Stimualtion Chamber tests

In this section the VSC tests are described. Porcine carotid arteries were cultured for 24 hours varying the applied transmural pressure and the flow rate. The mechanical properties of the vessel were tested before and after the experiment in order to evaluate how this physical stimulus influences the remodeling of extracellular matrix and orientation of collagen fibers. The results obtained have demonstrated that this device was able to reproduce different physiological and pathological situations.

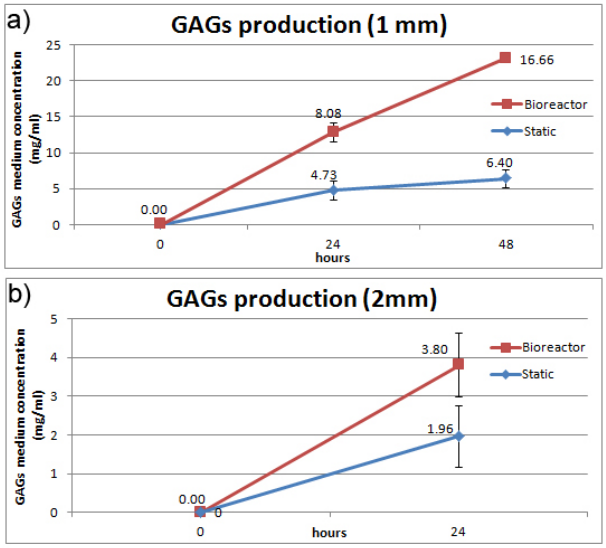

Figure 6.2: *Concentration of GAGs in medium in static controls and SQPR stimulated constructs (1 (a) and 2 (b)* mm *thick) after 24 and 48 hours of cyclic contact-less stimulation.*

6.2.1 Material and methods

Mechanical tests

The mechanical properties of vessels before and after culture in the VSC bioreactor were measured using an isotonic transducer[4], where the applied force has a resolution of $1x10^{-3}$N. The system is connected to a pc for the signal acquisition through a dedicated I/O board. Three specimens for each case were tested and fixed to transducer with nylon suture wire. During the stress-strain tests, the applied weights were changed every 3 minutes, and the elastic modulus of each sample was calculated using the

[4]Model 7006, UGO Basile Biological Research Apparatus, Comerio, Italy.

final part of the curve.

Culture of vessels in the VSC bioreactor

The specimens analysed in this study were longitudinal and circumferential strips of porcine carotid artery with dimensions of 10 mm length, 2 mm width, and thickness around 1 mm. The porcine vessel was divided in two parts; one used as control and placed in static condition, and one placed in the VSC bioreactor. All the experiments were carried out within 24 hours from the vessel extraction.

The vessel was installed in the bioreactor under a laminar flow hood in sterile conditions and locked to the connectors by clamp with a surgical knot. After sealing and blocking with the dedicated Derlin frame 5.8.b the VSC bioreactor extra vessel circuit was filled with DMEM Dulbecco Modified Essential Medium supplemented with 30% (FBS) Fetal Bovine Serum], 2% penicillin/streptomycin and 2% L-glutammina[5].

The peristaltic pump was switched on in order to fill the vessel and the entire circuit with media and the same culture medium was used to perfuse the vessel filling the intra vascular mixing chamber. After a preliminary check in order to detect any leakage or vessel clamping problem, the VSC chamber was placed in an incubator at 37°Cand 5% CO2.

The medium flow rates (the two media circuits are separated but have the same flow speed) were imposed to 0 or 10 mL/min in order to investigate any shear stress related mechanical changes in vessel physiology. Three different transmural pressures where applied (0, 60 and 120 mmHg) using the P.GIO hydrostatic pressure generator 5.2.1 in order to simulate hypotensive, physiological and hypertensive conditions respectively. The protocol was oriented to investigate any correlations between

[5]All reagents from Sigma, Italy.

applied stimuli and changes in mechanical properties of the vessels all the chosen pressure-shear combinations where tested. All the experiments were carried out for 24 hours.

6.2.2 Results

As shown in figure 6.3.b and in table 6.1 shear stress stimulation results in an increase of the longitudinal Young's modulus, while the transmural pressure has an opposite effect. The vessel stimulated with no pressure and 10 mL/min flow rate shows a 40% (16.95 kPa)increase in Young's modulus with respect to the control (11.65 kPa). The reduction in the pressure mediated circumferential Young's modulus is attenuated by the flow effect and the 10 mL/min 120 mmHg samples shown a circumferential Young's modulus that is only 30% (21.84 kPa) lower than the control one (30.69 kPa). On the other hand the 0 mL/min 120 mmHg samples have a greater reduction in circumferential Young's modulus (80% (11.91 kPa)) lower than the control (73.84 kPa). The tangential post stimulation Young's moduli (figure 6.3.a) do not shown any relevant changes except for the high pressure and flow rate experiments that demonstrate a 30% (67.66 kPa) increase of the tangenzial Young's modulus with respect to the control (50.69 kPa).

This phenomenon could be explained taking into account that the cellular component of the vascular wall is able to perceive changes of physical stimuli and adapts the ECM organization by changing the collagen fiber organization and orientation.

These experiments demonstrated the possibility of modulating the mechanical properties of blood vessel walls in an in-vitro environment by applying different stimuli. This innovative vessel stimulation chamber can be used in connection with other chambers of the SUITE platform in order to better investigate the pharmacology of anti-hypertensive drugs

Table 6.1: *Longitudinal young module and percentage increase post stimulation in the VSC bioreactor.*

$\frac{mL}{min}$		0 mmHg		60 mmHg		120 mmHg	
		kPa	%	kPa	%	kPa	%
0	Bio.			15.81	-23.80	11.91	-83.87
	Control			20.75		73.84	
10	Bio.	16.95	+45.49	26.42	+34.93	21.84	-28.83
	Control	11.65		19.58		30.69	

and study how the presence of other tissues can interact with the stimuli mediated collagen re-organization. The VSC bioreactor allows independent application of the applied pressure and the flow rate, in order to investigate how these parameters are correlated with vascular diseases. A particular application where the VSC bioreactor can be used is the study of the post stent implantation re-stenosis processes simulating physiological conditions in-vitro and investigating how these influence the behavior of the vessel wall.

6.3 LFC Laminar Flow Chamber tests

6.3.1 Materials and methods

The cells used for the laminar flow experiments were human umbilical vein endothelial cells (HUVEC) [148, 149, 141]. They were placed in the cell culture chambers, and in an incubator for 24 hours in order to ensure their adhesion on the gelatin-treated PDMS base. After incubation the cell culture chambers were plugged into the bioreactor system and 4 sets

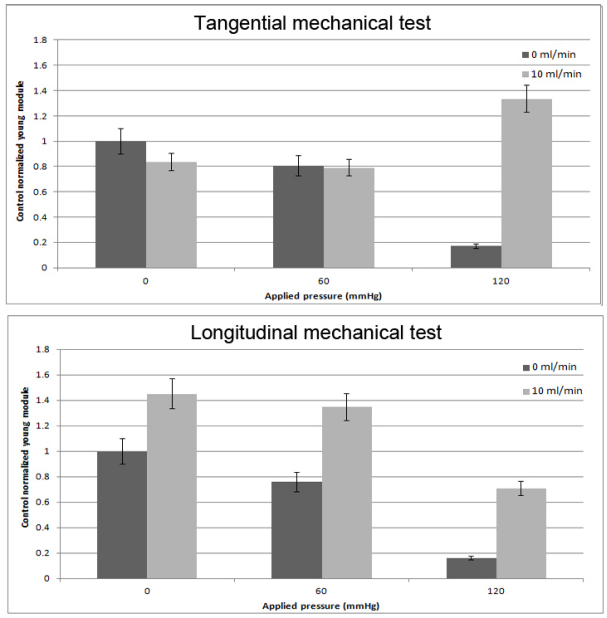

Figure 6.3: *Normalized tangential (a) and longitudinal (b) young module of vessels after 24h of stimulation in the VSC bioreactor.*

of experiments at 4 different flow rates were ran for 24 hours. At the end of each experiment the culture medium was analyzed for nitric oxide (NO) and endothelin (EN-2)[150]. Nitric oxide and endothelin are respectively a vasodilator and a powerful vasoconstrictive molecule. Cell morphology and orientation were also assessed by calculating cell eccentricity.

6.3.2 Results

The vascular endothelium is a dynamic organ that responds to various physical and humoral conditions, by producing several biologically active substances, both vasoconstrictors and vasodilators, which control these processes. Therefore to assess the ability of the laminar flow system to

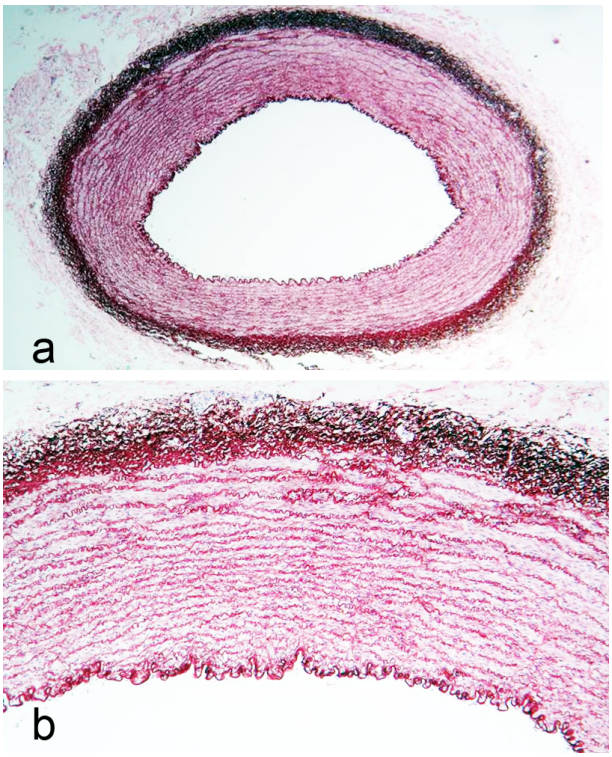

Figure 6.4: *Histological section of a porcine carotid after 24h in the VSC bioreactor.*

maintain functional properties that cells possess in physiological conditions the production of these important vasoactive factors were examined in endothelial cells culture under different shear stress stimulation conditions. The results are shown in Figure 6.5.a and b.

Even at shear stress values much lower than those typical of the in-vivo environment, significant variations in ET-1 and NO concentrations can be observed, as well as structural modifications induced by flow. As reported in Figure 6.5.b, shear stress induces downregulation of ET-1 with

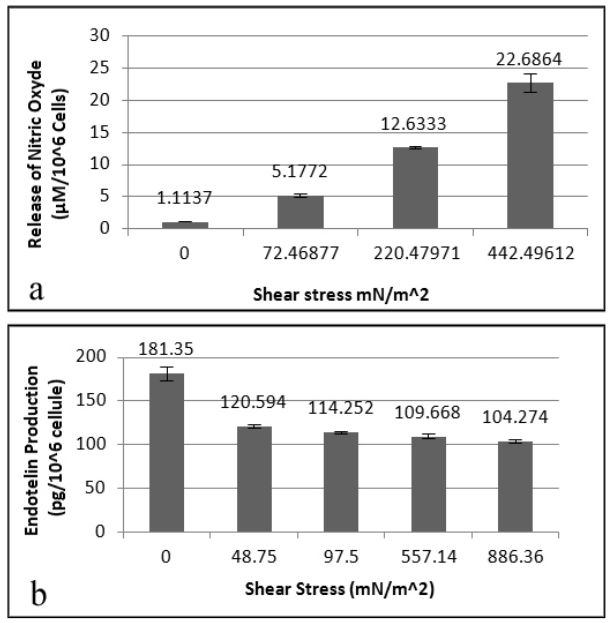

Figure 6.5: *(a) Nitric oxide production (*µmol*/10^6 cells) after 24 h in the laminar flow bioreactor chambers with different shear stress and (b) Endothelin production (*pg*/10^6 cells) after 24 h in the laminar flow chamber with different shear stress.*

respect to static conditions. This result is in accordance with some literature reports [151, 152]. In particular, the decrease of ET-1 production has been related to a reduction of synthesis of mRNA for ET-1 in HUVECs [153]. NO concentrations on the other hand increased with shear stress 6.5.a, as generally reported in the literature [154, 155]. Flow also induced structural reorganisation of endothelial cells, even at the low stresses used here. Endothelial cells, which are known to respond strongly to flow through the shear stress sensitive mechanoreceptors [156]. Changed their morpohology becoming more elongated and aligning with the direction

of flow. This well-known phenomenon which has been ascribed to the reorganization of F-actin and microtubule networks, is activated through mechanoreceptors. As can be observed in the micrographs of HUVEC exposed to different levels of shear stress in figure 6.6, the cells are elongated along flow lines, and this effect increases with the increasing shear stress.

The culture do not show any type of cell membrane damage or formation of picnotic nuclei. In these experiment cells are used as environmental sensors, where information relative to flow conditions are transduced into secretion of proteins. Is possible to observe also a change in eccentricity of endothelial cells, which respond to shear stress by orienting and elongating along the direction of flow as observed in-vivo [141, 157, 158, 140].

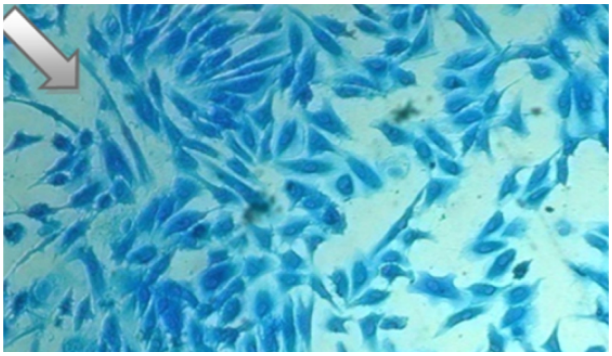

Figure 6.6: *Cell culture after 24 hours of treatment, we can observe how the cells have an elliptical shape and are oriented with the medium flow (indicated by the arrow).*

Chapter 7

Conclusions

A new experimental bioreactor control framework, called **SUITE** (Supervising Unit for In-vitro TEsting) was presented, through which high throughput experiments can be performed in an *in vivo*-like simulated environment for a long time. This thesis has described how by integrating different technologies and research fields a new concept of cell culture bioreactor was designed. Bioreactors were used as alternative in-vitro HTS systems to overcome the limits due to the environment discrepancy problem. More relevant and more predictive data from experiments can be obtained as a result of the capability of this innovative system to better simulate a physiological environment than the classic static cell culture protocols. The presented system is an innovative platform able to perform High throughput experiments in more physiological like environments. With the **SUITE** (Supervising Unit for In-vitro TEsting) platform it is possible to perform experiments using cell culture or tissues with a consequent reduction of required animals. The experiments performed with the SUITE are organized as a High Throughput experiments, and the data is collected by a main supervision system which can also impose control variables on multiple bioreactors running in parallel.

The SUITE system is composed of different parts described in this work, the environmental control unit is the core of the system and is where

all the environmental variables are collected by various sensors placed along the system, the various cell culture chambers are the stimulation zones of the system and in these the cell cultures are maintained and stimulated.

The aim of the Environmental control unit is to adjust the temperature, pH, pressure, gas flow and dissolved oxygen percentage of the culture medium. The control apparatus is consequently composed not only of the electronic and control unit, but also of the mixing chamber, the peristaltic pump, the heater unit and the control software. The entire high throughput system design process was driven by the necessity of a system able to perform experiments in parallel, with an autonomous control and with a user friendly interface that easily allows the researcher to change the controlled variables in order to mimic different pathologies.

A “light” version of the environment control system called P.GIO (Pressure Generator of In-vivO environments) was also developed. With this ”lighter” system the environmental variables (5% CO_2 atmosphere, humidity, tempertaure and sterility) are maintained using a classic CO_2 incubator. The P.GIO system is an innovative free standing unit able to control stepper or DC motors in order to generate controlled pressures or micro movements. P.GIO is a component of the SUITE platform and can be used as autonomous motor control, as environmental control box ”slave” actuator or in connection with a PC for a direct user interaction. The P.GIO system was designed in order to be easy to use, stable and autonomous. With this system is possible to design a wide range of experiments where pressure stimulations, micro movements, polymers extrusion or drug tests are imposed on cell cultures.

The Environmental control box test demonstrated that the system is able to maintain bioreactor cultures in the environmental conditions chosen by the user also in case of external perturbation or variable target

values. The platform is also able to impose variable stimulation and it can be used as a long term cell culture stimulator. In connection with the P.GIO system the SUITE platform is able to impose complex stimulations on cell cultures such as squeeze or transmural pressures allowing the system to be used for the study of various tissues or organs diseases.

A 'system on a plate' Multi Compartmental Modular Bioreactor (MCmB) was also developed with appropriate dimensions in order to allow microwell protocols to be transferred directly to the bioreactor technology. The MCmB is a modular chamber for high throughput multi compartmental bioreactor experiments. It is designed to be used in a wide range of applications and with various cell types. Given that hepatocytes present a major challenge in cell culture the MCmB was designed using hepatocytes as a reference cell type. For this reason this innovative chamber was preliminary tested with hepatocytes and then with different cell types and experimental procedures in order to validate the MCmB as a generic cell culture system.

The first test performed on the MCmB was aimed at demonstrating the capability of the chamber to maintain the vitality and function of one of the most important yet most delicate cells in the human body: hepatocytes. With the hepatocyte tests the mass transport and fluid dynamic FEM models used for the design were also validated. In fact, through these experiments we verified that the oxygen concentration in the MCmB chamber allows hepatocyte survival and showed that their vitality is shear stress dependent. The second set of tests was focused on establishing an *in-vitro liver* model in the MCmB, in which different chambers are plugged in series and parallel in order to simulate a human liver. In the third test the MCmB was used to investigate the behavior of condrocyte cultures, in monolayers and in scaffolds cultures, under different levels of shear stress. These experiments demonstrate that the

MCmB chamber is not only a modular bioreactor for the construction of in-vitro organ models for metabolic and toxicity studies, but can also be used as a cell culture stimulation unit, in which experiments can be designed with different types of stimuli applied to connected cultures, allowing investigation of tissue and organ physiopathology in an more in-vivo-like environment.

A precise stimulus application is important in order to better understand the correlation between physical variables and pathologies allowing a more accurate study of the tissue physiology and pathologies. For this reason three stimulation chambers were also designed and tested. The SPQR (SQueeze PRessure) bioreactor chamber is a system designed to impose on different type of cell cultures or tissues slices a cyclic hydrodynamic pressure that replicate the joint physiological environment. One of the most important features of the SPQR chamber is the ability to generate a squeeze pressure without any contact with the samples. This chamber was tested using different cell types and support materials indicating that the SQPR applied stimulation is able to enhance ECM production and can be used as an in vitro system for cartilage regeneration studies. A Vascular Stimulation Chamber (VSC) was also developed and tested, with this chamber it is possible to impose various flow rates and transmural pressures on animal or human ex-vivo vessels in order to investigate how these physical stimuli interact with the vessel wall re-organization process. The VSC chamber tests demonstrated that with this innovative system is possible to induce vessel wall re-organization and that a collagen fiber orientation process is induced as consequence of applied flow rate and transmural pressure. This chamber can consequently be used as ex vivo system for the study of the post stent implantation re-stenosis process.

In summary the SUITE platform has been demonstrated to be a valid

system applicable to various tissue engineering experiments as an environment control or as a cell stimulator. Due to new European Community directives, there is an urgent requirement for innovative systems that help to reduce the number of animal required for drug testing. For this reason the SUITE system is perfectly aligned with the scientific communities needs.

The system has been tested with various scientific protocols during the course of this thesis and is in use in various European labs, however the debugging of such a complex system is a long process that will continue in the next few months.

Finally we can affirm that the SUITE platform is a complete system for cell, tissue and organ maintenance and stimulation that will help the scientific community to establish more ethical and sustainable research reducing the number of required animals and allowing the study of the correlation between physical stimulation and physiological processes.

Appendix A

Appendix

In the following section a verbatim copy of the publications referred to as numbers [159, 157, 89]

ARTICLE

BIOTECHNOLOGY and BIOENGINEERING

A Low Shear Stress Modular Bioreactor for Connected Cell Culture Under High Flow Rates

D. Mazzei, M.A. Guzzardi, S. Giusti, A. Ahluwalia

Faculty of Engineering, Interdepartmental Research Center "E. Piaggio," University of Pisa, Pisa, Italy; telephone: +39-050-2217056; fax: +39-050-2217051; e-mail: mazzei@di.unipi.it

Received 23 October 2009; revision received 18 December 2009; accepted 11 January 2010

Published online ? ? ? ? in Wiley InterScience (www.interscience.wiley.com). DOI 10.1002/bit.22671

ABSTRACT: A generic "system on a plate" modular multi-compartmental bioreactor array which enables microwell protocols to be transferred directly to the bioreactor modules, without redesign of cell culture experiments or protocols is described. The modular bioreactors are simple to assemble and use and can be easily compared with standard controls since cell numbers and medium volumes are quite similar. Starting from fluid dynamic and mass transport considerations, a modular bioreactor chamber was first modeled and then fabricated using "milli-molding," a technique adapted from soft lithography. After confirming that the shear stress was extremely low in the system in the range of useful flow rates, the bioreactor chambers were tested using hepatocytes. The results show that the bioreactor chambers can increase or maintain cell viability and function when the flow rates are below 500 μL/min, corresponding to wall shear stresses of 10^{-5} Pa or less at the cell culture surface.

Biotechnol. Bioeng. 2010;9999: 1–12.

KEYWORDS: bioprocess engineering; kinetics; shear stress; modeling; oxygen; transport phenomena; bioreactor; hepatocyte; cell culture

Introduction

The microwell (MW) plate has become a standard in cell culture. The plates are available in a variety of formats (6–1,536 wells), although for most general cell culture and tissue engineering applications, 12-, 24-, 48-, and 96-well formats appear to be the most common (Chen et al., 2009). However, the complexity of the physiological environment is not replicated in Petri dishes or microplates. All cells are exquisitely sensitive to their microenvironment which is rich with cues from other cells, and from mechanical stimuli due to flow, perfusion, and movement. MWs do not offer any form of dynamic chemical or physical stimulus to cells, such as concentration gradients, flow, pressure, or mechanical stress. This is a major limitation in experiments investigating cellular responses in vitro since the complex interplay of mechanical and biochemical factors is absent (Janmey and McCulloch, 2007). Most researchers and industry now accept that classical in vitro experiments offer poor predictive value or mechanistic understanding, and there is a shift to new technologies, generally in the form of bioreactors.

A large number of bioreactor systems for cell culture have been designed and described. They range from commercial bioreactors which apply laminar flow (Fu et al., 2008), membrane systems (Morelli et al., 2007), rotating vessel systems (Martin et al., 2004) to purpose designed devices for specific tissues such as blood vessels (Miyakawa et al., 2008), heart valves (Dumont et al., 2002), and livers (Powers et al., 2002a). In most cases, the bioreactors described are custom designed for specific requirements and necessitate the use of particular seeding methods or scaffolds with narrow dimensional and design specifications. Sizewise they can be large-scale bioartificial livers with several billions of cells and several milliliters of fluid (De Bartolo et al., 2000) down to microfluidic systems with a few hundred microliters of medium (Baudoin et al., 2007). In fact, microfluidic microfabricated bioreactors which enable the culture of different cell types in a shear stress controlled environments (Tanaka et al., 2006) are highly popular but remain very much a niche research tool. In a microbioreactor, the cell culture surface is generally around 0.5–0.8 mm^2 (Baudoin et al., 2007) and this tiny surface is seeded with a few thousand cells. Such a small number of cells, organized on a tiny surface can be only a rough approximation of an organ and cannot meaningfully predict in vivo physiology or pathophysiology (Tingley, 2006). Another problem encountered in microbioreactors is the so-called "edge effect." In a micro-scaled surface, the percentage of area close to the edge of the system is higher than in a millimeter-sized surface. A large fraction of the cell population will therefore be found in a peripheral zone of the system. Cell cultures in the edge zone are usually organized differently and have higher

Correspondence to: D. Mazzei

BIT09-882.R1(22671)

cytoskeletal tensions (McBeath et al., 2004), and they may also have different viability or activity (Francis and Palsson, 1997). The edge effect is consequently a problem that can directly affect the results obtained in micro cell culture systems as demonstrated in Lundholt et al. (2003). Furthermore, most microfluidic bioreactors are fabricated using polydimethylsiloxane (PDMS) or other elastomeric polymers, which are known to adsorb small hydrophobic molecules (Toepke and Beebe, 2006). In microfluidic circuits, where the surface area to volume ratio is high, surface adsorption can lead to nutrient or ligand depletion so giving rise to experimental artifacts such as increased metabolic consumption rates. Finally, microsystems and microbioreactors are difficult to use and assemble, and the seeding and filling processes are quite complicated. This could lead to increased experimental failure and decreased reliability and limits their usefulness and scope and also puts them out of reach of many cell culture experiments which could benefit from added dynamic stimuli. In fact, for alternative tools to become acceptable as cell culture standards, the transition from wells has to be as smooth as possible. Only then will biologists and technicians adopt and adapt to new culture methods. For this reason, we have developed a ''system on a plate'' Multi-Compartmental modular Bioreactor (MCmB) with dimensions of the order of a few millimeters, which enables MW protocols to be transferred directly to the bioreactor modules.

The main design criteria for bioreactors are based on maximizing mass transport between the cells and the culture medium and on the application of mechanical, electrical, chemical, or other stimuli. Given that hepatocytes present a major challenge in cell culture (Coleman and Presnell, 2003; Guillouzo, 1998) and are probably the ''limiting'' cell in an in vitro system, the MCmB was designed using hepatocytes as a reference cell type. Hepatocytes are known to rapidly loose phenotypic expression in vitro due to the absence of an adequately equipped microenvironment, and they are a particular focus of attention in bioreactor development (Nahmias et al., 2007).

As the main orchestrators of endogenous and exogenous metabolism in mammals, hepatocytes are extremely sensitive to oxygen concentration, with high metabolic demands (Balis et al., 1999; Schumacker et al., 1993). One of the main engineering issues in bioreactors for in vitro liver models is therefore the balance between high mass transfer and low wall shear stress to cells. Several reports describe the effects of flow and shear stress on hepatocyte cultures (Mufti and Shuler, 1995; Nakatsuka et al., 2006; Powers et al., 2002b; Tanaka et al., 2006). Moreover, many investigators have shown that the viability of hepatocyte cultures under high shear is usually lower than that of static controls, indicating that the cells are under conditions of stress (Park et al., 2007). Hepatocytes are therefore very sensitive to shear, and according to Tilles et al., (2001) hepatocyte function is compromised at wall shear stresses greater than 0.03 Pa.

To realize a generic bioreactor system, a modular chamber with shape and dimensions similar to the 24-MW was designed. The new bioreactor unit is called the Multi-Compartmental modular Bioreactor (MCmB), and it consists of a cell culture chamber made of PDMS, a widely available and reasonably priced biocompatible silicone polymer with excellent self-sealing properties, transparency and flexibility. For this reason, in systems, which have a small surface to volume ratio with respect to microfluidic circuits, its use can be highly advantageous. By plugging together different chambers in different configurations (series or parallel) it is possible to mimic different metabolic pathways in order to investigate and test multi-compartmental biological models in vitro without having to design dedicated equipment or culture chambers, but just by connecting together a set of prefabricated chambers. The MCmB stems from a previous multi-compartmental bioreactor (MCB), in which the metabolic circuit has a fixed topology (Guzzardi et al., 2009; Vozzi et al., 2009). To mimic salient features of the glucose consumption pathway, the MCB system was designed with four chambers representing the pancreas, the liver, and the two target organs, respectively. The chambers were connected by channels, and the circuit dimensions were calculated using allometric laws (West et al., 1997).

The MCmB is a further evolution of the MCB system and allows any tissue or organ model to be simulated simply by connecting the modular chambers in a desired configuration. The bioreactor design process started with the analysis of the oxygen concentration and with the assessment of the minimum concentration allowed near the cell surface, using hepatocytes as a reference. Subsequently, we developed a fluid dynamic model of the MCmB chamber in order to investigate the shear stress and to estimate the optimal chamber size to obtain both adequate oxygen diffusion and low shear stress near the cell surface. This article describes the designing, modeling, and dimensioning of the bioreactor chambers, their fabrication using precision machining and ''milli-molding,'' and testing of the bioreactors using rat hepatocytes.

Materials and Methods

Mass Transport and Flow Modeling

The first model of the MCmB (MCmB 1.0) was based on the dimensions of the classic 24-MW so as to directly compare static and dynamic cell cultures in equal sized chambers. The MCmB 1.0 was designed to allow the use of 12 mm glass or plastic cover slips, commonly used for cell culture, or different types of scaffolds. It is also possible to place a slice of tissue, pregrown cell construct, or pellets directly on the cell culture zone. A finite-element modeling (FEM) model of the cell culture chambers was developed in order to study the oxygen concentration and the shear stress at the cell surface. Cosmos Floworks, a Solidworks^{TM} (Dassault

Systèmes SolidWorks Corp., Concord, MA) extension that allows fluid-dynamic FEM analysis and Comsol Multiphysics (COMSOL AB, Stockholm, Sweden) were used for this purpose. In both the fluid dynamic and mass transport models we used the following system constants: viscosity $= 10^{-3}$ Pa s, fluid density $= 1{,}000$ kg/m^3, medium flow rate in the range between 60 and 1,000 μL/min, pressure = 1 atm or 760 mmHg, temperature = 37°C, and no slip boundary conditions. Water was chosen as a reference fluid, so that the actual values of shear stress on the walls will depend linearly on the density and viscosity of the culture medium used. Initial considerations were focused on a flow rate of 180 μL/min for the sake of comparison with our previous tests in the MCB system (Guzzardi et al., 2009; Vozzi et al., 2009).

In order to study the fluid dynamics of the modular bioreactor, we developed a parametric model in which the effect of changes in height on flow parameters (flow speed, shear stress, and stream lines) could be observed. As shown in Figure 1, the first model had a base height H which varied between 3 and 9 mm, and a 13-mm diameter base, with a 12-mm diameter, 160 μm thick cover slip placed on of the bottom of the bioreactor. The distance between the roof and the 1 mm diameter inlet and outlet tubes was fixed at 3 mm, and the FEM model was solved for different heights between the tubes and the cell culture surface: 3, 4, 6, and 9 mm.

Oxygen Concentration Analysis

A steady-state model of oxygen diffusion in the MCmB chamber was developed, in order to investigate if the cells were adequately supplied with oxygen during the experiments. We used Michaelis–Menten (MM) kinetics to model oxygen consumption and Fick's laws to model oxygen diffusion in water.

In the bioreactor circuit, which is described in the following section, air rather than O_2 is used for safety purposes. The O_2 concentration ($C_{[0]}$) in the medium just below the gas–liquid interface is directly dependent on the O_2 partial pressure in air, typically 20% or 159 mmHg, through Henry's law and we can easily calculate $C_{[0]}$ using tabulated values of the Henry constant:

$$P(O_2) = K(O_2)C[O_2]$$

with $K_{O_2} = 932.4$ atm/(mol/L) and $(P_{O_2}) = 0.2$ atm (20%), $C[O_2]$ below the gas–liquid interface or $C_{[0]} = 214\ \mu M = 0.214$ mol/m^3.

In the presence of oxygen-consuming cells, the O_2 concentration will decrease as a function of distance from the interface and the metabolic requirements of the cells. The steady-state flux of O_2 in the bioreactor chamber is due to cellular oxygen consumption at the base. The oxygen consumption rate per unit volume is given by the MM equation:

$$\frac{dC}{dt} = \frac{V_m C}{K_m + C}$$

where C is the oxygen concentration in mol/m^3, V_m is the maximum volumetric consumption rate in mol/m^3/s, and K_m is the MM constant in mol/m^3.

The flux at the base of the chamber where the cells lie are

$$J_c = -D\frac{\partial C}{\partial x} = \frac{V_{max} C}{K_m + C}\frac{1}{\text{cell area}}$$

where J_c is the O_2 mass flow at the cell surface, $(\partial C/\partial x)$ is the O_2 concentration gradient at the cell surface calculated along the axis perpendicular to the cell culture layer, D is the O_2 diffusion coefficient (in water) $D = 3 \times 10^{-9}$ m^2/s at 37°C, and V_{max} is the maximum consumption rate in mol/s.

The kinetic model was calculated for a medium flow rate of 180 μL/min, for a comparison with the MCB result, and a cell monolayer of 1.33 cm^2 surface area with 500,000 cells, which represents typical cell numbers observed 48 h after seeding HepG2 cells on a three-dimensional scaffold (Vinci et al., 2009). In order to choose the height of the bioreactor, we fixed a minimum oxygen concentration of the medium at the cell surface; $C_{min} = 0.04$ mol/m^3. Below this concentration we assume that cell function is compromised. In fact, typical oxygen concentrations in the liver are of the order of 0.04–0.15 mol/m^3 (4–15%), while 0.021 mol/m^3 (2%) is known to inhibit mitosis in hepatocytes (Smith and Mooney, 2007).

Using the data in Patzer (2004), $V_{max} = 0.048$ nmol/s for 1 million cells, giving a value of 0.024 nmol/s for 500,000 cells ($V_{max(500,000)}$), and $K_m = 0.5$ mmHg.

Figure 2 illustrates that the O_2 concentration in the MCmB is always higher than the minimal threshold and falls rapidly at the edge of the chamber near the outlet. Increasing bioreactor height from 3 to 9 mm, the oxygen concentration decreases rapidly but cell survival is always guaranteed in the central region of the chamber. Above $H = 9$ mm, however, in the bottom of the chamber the oxygen concentration is constantly below the C_{min} threshold of 0.04 mol/m^3. The maximum oxygen concentration at the base is 0.17, 0.12, 0.10, and 0.007 mol/m^3 for $H = 3$, 4, 6, and 9 mm, respectively.

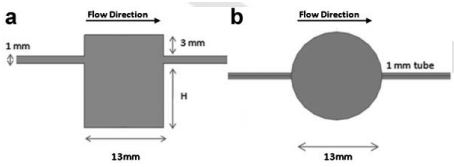

Figure 1. The FEM model geometry for the first modular bioreactor chamber. *H* is the variable height, (**a**) side view and (**b**) top view.

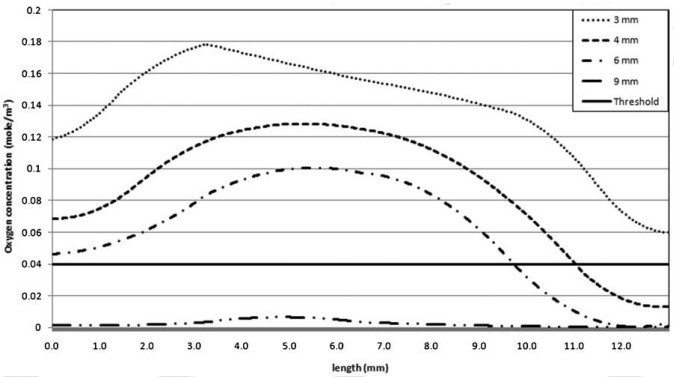

Figure 2. Theoretical oxygen concentration profile across the bioreactor chamber for different heights *H*, calculated using Michaelis–Menten kinetics and a flow rate of 180 μL/min. The minimal concentration threshold of 0.04 mol/m^3 is indicated by the solid line.

Fluid Dynamic Model

To investigate the fluid dynamics of the modular bioreactor, a parametric model similar to the mass-transfer model was developed. The height H was varied to determine its influence on the shear stress generated at the cell surface, assuming again that the cells are seeded on a 12-mm, 160 μm thick cover slip placed in the bioreactor.

Table I summarizes the results, showing how the shear stress at the cells surface decreases rapidly with increasing H. However, the laminarity of the flow is compromised by increasing the height of the bioreactors. This is a consequence of the separation of flow streamlines caused by the difference in height between the inlet tube and the base.

After evaluating the results from the fluid dynamic and mass transport modeling, we choose to realize a modular bioreactor chamber with tubes placed 6 mm over the cell surface (H). A distance of at least 1 mm between the wall of the tube and the top of the chamber is necessary to ensure mechanical stability of the tube/chamber junction. Since standard silicone tubing with an inner diameter of 1 mm has an outer diameter of 3 mm, the total height of the chamber is 10 mm. This is the best compromise between shear stress, flow, oxygen diffusion, and mechanical feasibility.

Figure 3 shows the three-dimensional FEM model of the $H = 6$ mm MCmB with an internal diameter of 13 mm, sufficient to place a slice or a scaffold of 12 mm in diameter. This bioreactor has a peak shear stress value of 6.85×10^{-6} Pa and a velocity peak of 10^{-6} m/s near the center of the base.

Chamber Fabrication

A first prototype of the bioreactor chamber (MCmB 1.0) was fabricated using "milli-molding" in order to investigate the performance of the system. Milli-molding is similar to micromolding (Xia and Whitesides, 1998), in that PDMS is used as a mold, but the master is machined using a mill or rapid prototyping rather than lithographic methods, and the features of the mold are of the order of tenths of millimeters, rather than microns.

The chamber is composed of two separate parts which are plugged together through a friction fit system. In the friction fit system two complementary geometries form a seal when brought together thus avoiding the use of o-rings or additional parts (Mazzei et al., Improved Bioreactor Chamber, GB Patent Application No. 0814034.5). PDMS (Sylgard 184, Dow Corning, Silverstar, Italy) is used to fabricate the chambers. Along with the friction fit system, the use of PDMS, which is self adhesive and deformable, ensures that the seal is watertight.

The two parts of the chamber are made by casting and curing PDMS as per the manufacturer's instructions on aluminum masters purposely machined in our workshop. Each master is made of two separate pieces which allow easy removal of the chambers after polymerization. The two parts are held together using an aluminum frame with four screws as shown in Figure 4a.

Turbulence Tests

The first prototype of the MCmB 1.0 cell culture chamber had severe problems with the build-up of air bubbles during the

Table I. Fluid dynamic FEM model results for a fixed flow rate of 180 μL/min for the first MCmB model as a function of height *H*.

Height (*H*)	3 mm	4 mm	6 mm	9 mm
Shear stress peak (Pa) at 180 μL/min	3.217×10^{-5}	1.195×10^{-5}	6.856×10^{-6}	8.747×10^{-7}
Shear stress profile (log Pa)	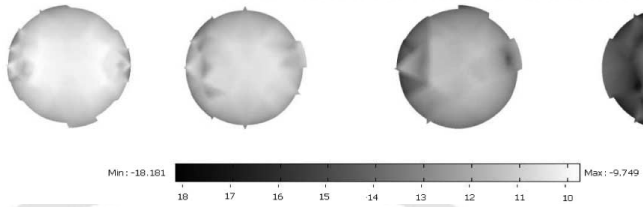			
Velocity peak (m/s) at 180 μL/min	4.429×10^{-6}	1.665×10^{-6}	9.887×10^{-7}	1.389×10^{-7}
Velocity vector	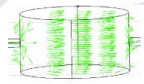 *Parallel to the cell surface*	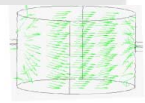 *Parallel to the cell surface*	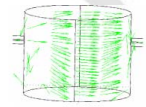 *Slightly sloped*	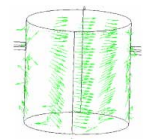 *Sloped*
Stream line	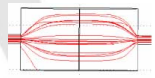 *Parallel to the cell culture*	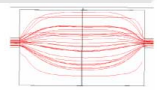 *Parallel to the cell culture*	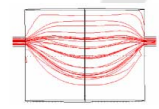 *Nearly parallel to the cell culture*	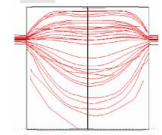 *High impact angle on the cell culture surface*

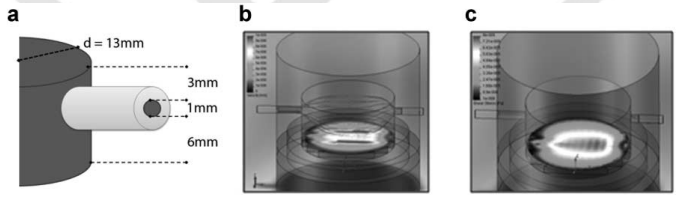

Figure 3. FEM[Q1] model of the $H = 6$ mm MCmB 1.0. **a**: Velocity and (**b**) shear stress. The analysis takes into account a 160-μm thick glass cover slip placed on the base of the chamber.

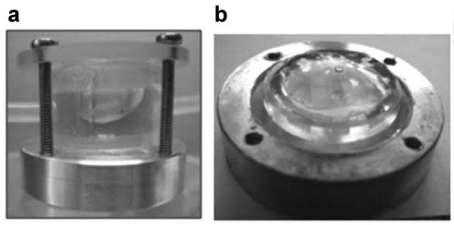

Figure 4. **a**: Bubble formed at the top of the first MCmB 1.0 chamber, and (**b**) alginate drop used for turbulence tests placed on the bottom half of the chamber.

initial phases in which the bioreactor is filled with medium. This resulted in the formation of a bubble of air at the top of the chamber (Fig. 4a), which disturbed the flow profile, causing turbulence and more importantly unpredictable values of shear stress. In order to evaluate the effects of the bubble induced turbulence, a small drop or blob of alginate was introduced in the chamber as a "turbulence sensor." An alginate blob is easily disaggregated under turbulent or high impact flow, and for this reason it is a good indicator of the presence of altered flow profiles. Moreover, cross-linked alginate at the concentrations used here has approximately the same elastic modulus as the liver (~10 kPa) (Constantinides et al., 2008; Tirella et al., unpublished work). The alginate blobs are made placing 166 μL of 2% sodium alginate (Sigma, Milan, Italy) dissolved in MEM (Sigma) on top of a glass cover slip in the chamber and cross-linking in situ with 104 μL of 0.1 M $CaCl_2$ (Fig. 4b). The volume of the blob was chosen in order to form a thin uniform coating of the glass cover slip, without interfering with the inlet tube. A peristaltic pump (Ismatec, Glattbrugg, Switzerland) was attached to the inlet, and keeping the flow rate constant at 180 μL/min, the consistency of the alginate blob after 24 h in the MCmB 1.0 at 37°C was analyzed. The alginate drop was completely disaggregated, showing that the bubble induced a turbulent environment.

Design Improvements: MCmB 2.0

In order to eliminate bubble entrapment and turbulence in the bioreactor chamber, a second prototype (MCmB 2.0) of the modular bioreactor was designed. The new bioreactor is slightly larger in diameter (15 mm) to enable 13 or 14 mm slides to be easily inserted and its top surface is sloped along and perpendicular to the axis of flow, so that bubbles are collected and conveyed to the outlet tube (Fig. 5a).

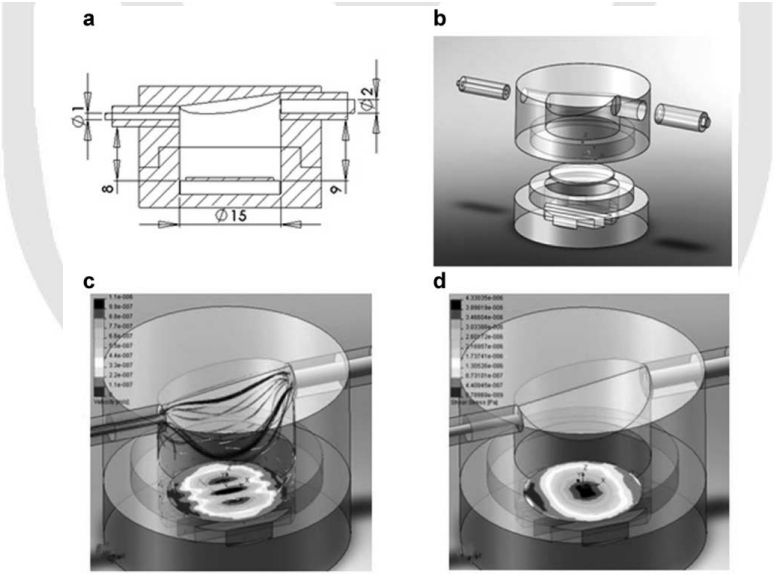

Figure 5. **a**: Dimensions of the new chamber, (**b**) three-dimensional representation of the sloped roof and ridged base, (**c**) MCmB 2.0 velocity profile, showing stream lines, and (**d**) shear stress at the base.

Furthermore, the diameter of the outlet tube was increased to 2 mm to facilitate the removal of bubbles. This also reduces the impact angle on the cell culture surface and the recirculation near the outlet wall as shown in Table II. The final height of the MCmB 2.0 is 11 mm at the inlet side and 13 mm at the outlet side, with the tubes positioned, respectively, at $H = 9$ and 10 mm from the cell surface (Fig. 5b).

Through FEM modeling a tenfold decrease in fluid velocity and shear stress on the cell surface with respect to MCmB 1.0 was observed with the introduction of the sloping roof and the increased outlet tube diameter.

The MCmB 2.0 is 3 mm higher than MCmB 1.0, we choose to increase the height of the new chamber design because this allows a further reduction in shear stress in comparison with MCmB 1.0 (6 mm in height) while maintaining the oxygen concentration over the 4% threshold.

Table II shows the velocity profile and the streamlines in the MCmB 2.0.

The base of the bioreactor chamber was also modified to ensure easy removal and support of coverslips, since the slides and thin substrates tend to stick to the flat silicone base. The three small rectangular ridges, shown in

Table II. Fluid dynamic FEM model results for the MCmB 2.0 at two different flow rates, the average height (H) of the MCmB 2.0 is 9.5 mm.

Flow rate (μL/min)	180	300
Shear stress peak (Pa)	4.295×10^{-6}	6.456×10^{-6}
Shear stress profile (log Pa)	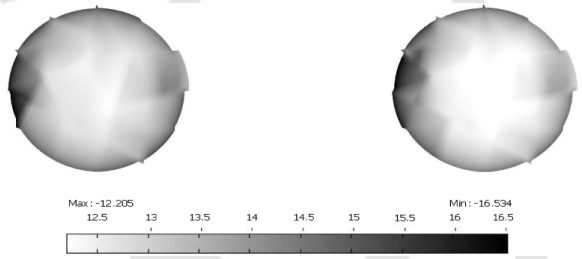	
Velocity peak (m/s)	5.939×10^{-7}	9.048×10^{-7}
Velocity vector	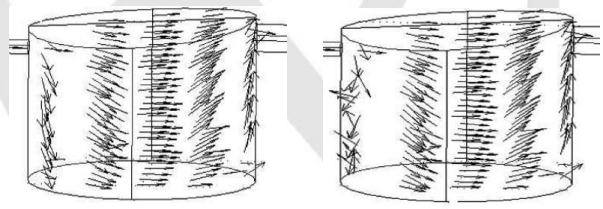	
	Parallel to the cell surface	*Parallel to the cell surface*
Stream line	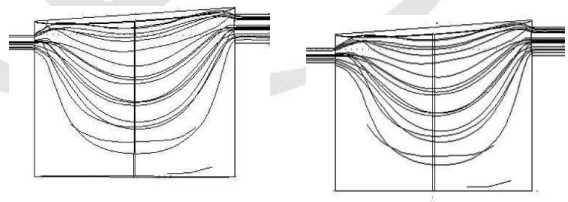	
	Parallel to the cell culture	*Parallel to the cell culture*

Figure 5b, provide support and also allow medium to flow under the support, supplying nutrients to the lower surface of tissue slices or scaffolds.

Control System

The bioreactor chambers are part of a complex gas and fluid circuit, which enables individual chambers to be connected in series or in parallel to mimic different metabolic pathways. Experimental variables such as oxygen concentration, pH, pressure, and medium flow rate through the MCmB chambers can all be controlled through a purposely designed electronic and software control system (Mazzei et al., 2008). A series of MCmB chambers plugged together in series and parallel are represented in Figure 6. Media[Q2] are moved by a peristaltic pump through to a mixing chamber, and to the MCmB chambers in a closed-loop circuit. The mixing chamber acts as a medium reservoir, a sampling port, a gas exchanger, and a flow rectifier to convert peristaltic flow into a smooth flow. The controlled injection of an appropriate combination of air and CO_2 through a dedicated algorithm enables the oxygen concentration, pH, and pressure of the medium to be tightly modulated. A microcontroller board is used to read the data collected by a sensing unit placed in the mixing chamber. The MCmB bioreactor can also be used in a classic cell culture incubator, without need for the control unit. In this case, the mixing chamber is equipped with a single gas inlet with a 0.2 μm syringe filter which allows gas exchange without risk of contamination.

Cell Culture

All cell culture reagents were all purchased from Sigma, unless otherwise specified. Primary rat hepatocytes were used to test the performance of the MCmB 2.0 bioreactor at various flow rates. Hepatocytes were isolated from adult male Wistar rats weighing between 250 and 300 g as described by Seglen (1979) and Papeleu et al. (2006). Isolated cells were assessed for vitality by trypan blue exclusion (vitality routinely greater than 90%), and then seeded on glass cover slips (2×10^5 cells per sample) pretreated with 0.1 mg/mL collagen extracted from rat tails according to standard procedures (Rajan et al., 2006), placed in 24-MW plates and left at 37°C and 5% CO_2. About 5 h after seeding, the medium was removed and replaced with FBS-free William's E complete medium. The following day, the hepatocyte seeded coverslips were placed into the MCmB 2.0 chambers and coated with 250 μL collagen gel prepared by mixing ice-cold collagen solution and acetic acid 0.2 N (to a final collagen concentration of about 1.1 mg/mL) and 10× M199. The collagen coating used in these experiments has a Young's modulus similar to the alginate blob used to evaluate the turbulence in the chamber (Wu et al., 2005). It also provides an adhesive roof to the cells and shields the cells from the effects of direct flow.

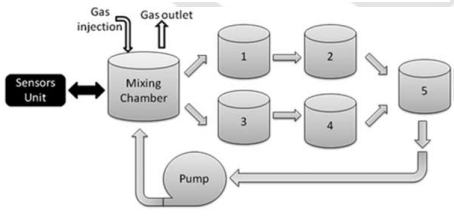

Figure 6. Scheme of the bioreactor medium and gas flow circuit.

MCmB Assembly

Prior to assembly the bioreactors with hepatocyte seeded and collagen coated slides were left in the incubator for 40 min to allow the collagen to set. The MCmB system was then assembled by connecting two chambers in series to a peristaltic pump and the mixing chamber. Finally, the system was filled with 10 mL FBS-free complete William's E, and run for up to 24 h. The first experiment was run at a flow rate of 180 μL/min. At 2, 4, 6, and 24 h a 100-μL sample of medium was withdrawn for analysis of rat albumin. A second set of experiments was carried out at various flow rates (60–100–180–250–300–500–1,000 μL/min) to determine cell viability as a function of flow rate. The bioreactors were run for 24 h after which the cover slips were removed and assessed for cell viability. Control experiments with cells from the same rat liver were run using glass slides seeded with the same number of cells, coated with collagen, and placed in 10 mL Petri dish plate multiwell (BD Biosciences, Milan, Italy).

Viability and Albumin Testing

Albumin

Albumin, which is an important marker of hepatic function, was measured using a commercial ELISA kit (Bethyl Laboratories, Montgomery, TX), according to the manufacturer's instructions. Rat albumin production is expressed as total quantities of albumin per seeded cell. Each experiment was repeated at least three times, and comparisons were only made between cells extracted from the same liver.

Viability

The viability kit used was CellTiter-Blue™ Cell Viability Assay (Promega, Madison, WI), a resazurin-based fluorescent compound metabolized by mitochondrial cytosolic

and microsomal enzymes to resorufin which can be detected with a fluorimeter (FLUOstar Omega, BMG Labtech, Offemburg, Germany) at 573 nm. Viability was assessed both in control static cultures and in the MCmB 2.0, and the results are expressed as ratio between hepatocyte viability in dynamic and static conditions after 24 h. The static control was a hepatocyte seeded and alginate-coated cover slip placed in a bioreactor base filled with medium and left open in order to allow oxygen exchange without medium flow. Each experiment was repeated at least three times, and comparisons were only made between cells extracted from the same liver.

Statistical Tests

Statistical analysis was performed using the Student's *t*-test when comparing between albumin production in static ($n = 3$) and dynamic ($n = 3$) experiments; a *P*-value of less than 0.05 was considered statistically significant. At least three dynamic experiments and three static controls were performed per flow rate for viability tests.

Results and Discussion

Oxygen Consumption and Shear Stress in the MCmB 2.0

Figure 7 shows the oxygen concentration in the two bioreactor designs; for a given flow rate, the mean value is slightly lower in the new MCmB 2.0 design. As far as oxygen consumption is concerned, the difference between the two chambers is the value of H (6 mm in MCmB 1.0 and 9 mm in MCmB 2.0) and their respective volumes. The MCmB 2.0 chamber has a slightly larger volume so the total amount of oxygen available is greater. Therefore, despite the greater distance between the tubes and the cell surface in the new chamber the minimal oxygen concentration is still guaranteed except at the outer edge of the base closest to the outlet. To minimize oxygen depletion at the edges, the bioreactor could be placed on a low-frequency oscillator or shaker. It should be noted however that the number of cells used in the model was more than twice that used in the experiments, and that the oxygen concentration is highly dependent on the flow rate and metabolic requirements of the cells.

We also characterized the Graetz number which is a dimensionless number indicating the ratio between the characteristic diffusion time and the convection time, respectively, perpendicular and parallel to the direction of flow. The Graetz number is greater than 100 even for low flow rates (60 μL/min) showing that the fraction of oxygen consumed per reactor is insignificant and so downstream chambers do not suffer from any input oxygen depletion.

Using the model we established empirical equations for the wall shear stress and peak fluid velocity at the cell surface

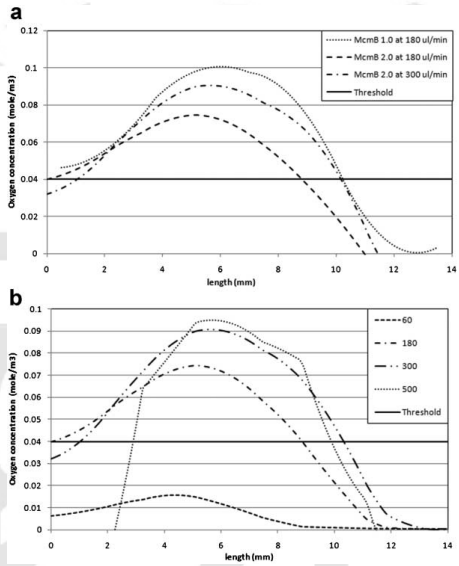

Figure 7. **a**: Oxygen concentration in the MCmB 1.0 for a flow rate of 180 μL/min and MCmB 2.0 for a flow rate of 180 and 300 μL/min, and (**b**) oxygen concentration in the MCmB 2.0 for different flow rates between 60 and 500 μL/min.

as a function of flow rate

$$\text{Shear (Pa)} = \text{Flow}(\mu\text{L/min}) \times 1.8 \times 10^{-8} + 1.1 \times 10^{-6}$$

$$\text{Flowspeed (m/s)} = \text{flow (}\mu\text{L/min)} \times 2.6 \times 10^{-9} + 1.3 \times 10^{-7}$$

Therefore, the wall shear stress at 180 and 300 μL/min is, respectively, 4.34×10^{-6} and 6.5×10^{-6} Pa and the peak flow velocity is 5.98×10^{-7} and 9.1×10^{-7} m/s.

Bubble and Turbulence Testing

As shown in Tables I and II, the MCmB 2.0 has lower values of shear stress, and the streamlines are parallel to the base of the chamber, even though its height (H) is 3 mm greater than MCmB 1.0. At a flow rate of 1,000 μL/min the gel showed signs of disaggregation after 24 h, due to the direct high impact of fluid on the base of the chamber as well as the high wall shear (not shown). The MCmB 2.0 was bubble free, as the sloped roof and the position and respective diameters of the inlet and out tubes forced bubbles to be conveyed out of the chambers. In the

turbulence tests carried out with the alginate blob, the gel showed no signs of wear even after 48 h under a flow of 500 μL/min. The alginate blob turbulence test is not only a simple method for investigating turbulent, high impact, or disturbed flow in the system but can also be used to create a cell culture environment more similar to the in vivo liver environment. As shown in Vozzi et al. (2009) and Guzzardi et al. (2009), coating the cells in an alginate or collagen gel increases hepatocyte viability and phenotypic stability during the culture.

Cell Culture Tests

Figure 8a illustrates the viability ratio between the MCmB dynamic culture at different flow rates and a static control.

The figure shows that below 180 μL/min the viability is compromised, this could be due to the lower oxygen concentration at the bottom of the bioreactor chamber for these low flow rates (shown in Fig. 7b). For flow rates in the range between 180 and 500 μL/min the viability is very close to the control and the viability peaks at 300 μL/min, this could be due to the high oxygen concentration as demonstrated in Figure 7b. A further increase in flow rates above about 500 μL/min causes a significant reduction in viability. At higher flow rates, despite the increased availability of oxygen, the cells suffer, and this is due to the high shear and impact angle of flow on the collagen coating and cells.

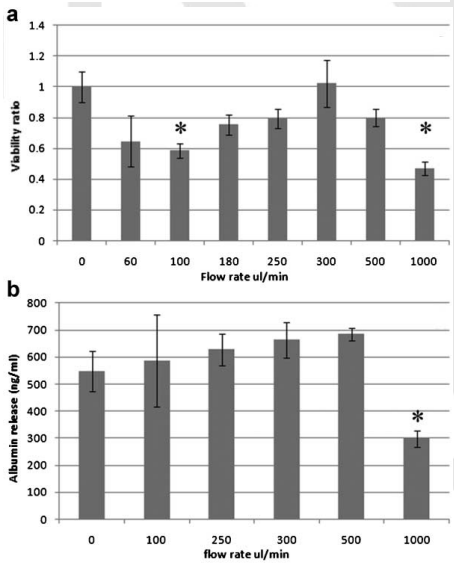

Figure 8. **a**: Hepatocyte viability, expressed as the ratio between viability in the MCmB 2.0 and controls after 24 h at different flow rates, and (**b**) rat albumin production after 24 h in the MCmB 2.0 and in the control. $^{*}P < 0.05$.

Figure 8b shows the albumin production after 24 h in the MCmB for different flow rates in the range 100–1,000 μL/min, and the static control. Albumin in the bioreactor chamber is slightly upregulated except for the 1,000 μL/min flow rate, where the cells are damaged by the shear stress as previously discussed. These results are confirmed by several reports describing dynamic hepatocyte cultures (De Bartolo et al., 2009; Powers et al., 2002b; Tilles et al., 2001) where the albumin production is maintained at control levels even in the presence of shear. We have suggested that this induction is due to two factors: the circulation of medium which provides a sustainable supply of nutrients, as well as efficient removal of metabolic products, and the mechanical stimulus due to the presence of a low velocity porous or percolative interstitial-like flow which is established through the collagen coating (Vinci et al., 2009). In fact, in the human liver, hepatocytes are never subject to direct or tangential flow; they receive nutrients through a rich capillary network and consequently only through interstitial flow driven by concentration and pressure gradients (Rutkowski and Swartz, 2006; Swartz and Fleury, 2007). Not surprisingly a large number of reports on liver bioreactors use co-cultures of hepatocytes with non-parenchymal cells, typically fibroblasts (Allen et al., 2005; Park et al., 2007; Tilles et al., 2001). These supporting cells not only provide heterotypic signals but also secrete collagen which likely forms a protective coating over the cells shielding them from direct fluid flow.

Conclusions

The objective of this study was to design, realize, and test a modular bioreactor chamber for culture of hepatocytes and other cells, which do not support high shear stress, with dimensions similar to a MW. The various steps of modeling and design of the modular bioreactor, as well as its fabrication using "milli-molding" are described. The main features of the final design are the complete absence of bubbles, due to the particular design of the top part of the chamber, and the very low wall shear stress in the cell culture region. In addition, the bioreactor chambers can be connected together in series or in parallel as desired, using different cell types, tissue slices, or scaffolds in order to recreate in vitro models of metabolism or diseases. Two chambers were connected in series and tested over 24 h using primary rat hepatocytes.

At flow rates below about 500 μL/min the maximum wall shear stress at the base of the chamber chamber is of the order of 10^{-5} Pa or less. Cell viability is maintained at these flow rates, while the expression of albumin is increased. The chambers are easy to assemble and use and can be

employed as a generic dynamic cell culture tool, in place of static multiwells.

The authors wish to thank Kirkstall Ltd for its contribution to the patenting and development of the bioreactors.

References

Allen JW, Khetani SR, Bhatia SN. 2005. In vitro zonation and toxicity in a hepatocyte bioreactor. Toxicol Sci 84(1):110–119.

Balis UJ, Behnia K, Dwarakanath B, Sangeeta N. 1999. Oxygen consumption characteristics of porcine hepatocytes. Metab Eng 1:49–62.

Baudoin R, Corlu A, Griscom L, Legallais CE. 2007. Trends in the development of microfluidic cell biochips for in vitro hepatotoxicity. Toxicol In Vitro 21:535–544.

Chen A, Chitta R, Chang D, Amanullah A. 2009. Twenty-four well plate miniature bioreactor system as a scale-down model for cell culture process development. Biotechnol Bioeng 102(1):148–160.

Coleman WB, Presnell SC. 2003. Plasticity of the hepatocyte phenotype in vitro: Complex phenotypic transitions in proliferating hepatocyte cultures suggest bipotent differentiation capacity of mature hepatocytes. Hepatology 24:1542–1546.

Constantinides G, Kalcioglu ZI, McFarland M, Smith JF, Van Vliet KJ. 2008. Probing mechanical properties of fully hydrated gels and biological tissues. J Biomech 41(15):3285–3289.

De Bartolo L, Jarosch-Von Schweder G, Haverich A, Bader A. 2000. A novel full-scale flat membrane bioreactor utilizing porcine hepatocytes: Cell viability and tissue-specific functions. Biotechnol Prog 16(1):102–108.

De Bartolo L, Salerno S, Curcio E, Piscioneri A, Rende M, Morelli S, Tasselli F, Bader A, Drioli E. 2009. Human hepatocyte functions in a crossed hollow fiber membrane bioreactor. Biomaterials 30(13):2531–2543.

Dumont K, Yperman J, Verbeken E, Segers P, Meuris B. 2002. Design of a new pulsatile bioreactor for tissue engineered aortic heart valve formation. Artif Organs 26:710–714.

Francis K, Palsson BO. 1997. Effective intercellular communication distances are determined by the relative time constants for cyto/chemokine secretion and diffusion. Proc Natl Acad Sci USA 94:12258–12262.

Fu Q, Wu C, Shen Y, Zheng S, Chen R. 2008. Effect of LIMK2 RNAi on reorganization of the actin cytoskeleton in osteoblasts induced by fluid shear stress. J Biomech 41(15):3225–3228.

Guillouzo A. 1998. Liver cell models in vitro toxicology. Environ Health Perspect 106:532–551.

Guzzardi[Q3] M, Vozzi F, Ahluwalia A. 2009. Study of the cross-talk between hepatocytes and HUVEC using a novel multi compartmental bioreactor: A comparison between connected cultures and co-cultures. Tissue Eng Part A [Epub].

Janmey PA, McCulloch CA. 2007. Cell mechanics: Integrating cell responses to mechanical stimuli. Annu Rev Biomed Eng 9:1–34.

Lundholt BK, Scudder KM, Pagliaro L. 2003. A[Q4] simple technique for reducing edge effect in cell-based assays. J Biomol Screen, 566–570.

Martin I, Wendt D, Heberer M. 2004. The role of bioreactors in tissue engineering. Trends Biotechnol 22:80–86.

Mazzei D, Vozzi F, Cisternino A, Vozzi G, Ahluwalia A. 2008. A high-throughput bioreactor system for simulating physiological environments. IEEE Trans Ind Electr 55(9):3273–3280.

McBeath R, Pirone DM, Nelson CM, Bhadriraju K, Chen CS. 2004. Cell shape, cytoskeletal tension, and RhoA regulate stem cell lineage commitment. Dev Cell 6(4):483–495.

Miyakawa A, Dallan LAO, Lacchini S, Borin TF, Krieger JE. 2008. Human saphenous vein organ culture under controlled hemodynamic conditions. Clinics 63(5):683–688.

Morelli S, Salerno S, Rende M, Lopez LC, Favia P, Procino A, Memoli B, Andreucci VE, d'Agostino R, Drioli E, De Bartolo L. 2007. Human hepatocyte functions in a galactosylated membrane bioreactor. J Membr Sci 302:27–35.

Mufti NA, Shuler M. 1995. Induction of cytochrome P-450IA1 activity in response to sublethal stresses in microcarrier-attached Hep G2. Biotechnol Prog 11(6):659–663.

Nahmias Y, Berthiaume F, Yarmush ML. 2007. Integration of technologies for hepatic tissue engineering. Adv Biochem Eng Biotechnol 103:309–329.

Nakatsuka H, Sokabe T, Yamamoto K, Sato Y, Hatakeyama K, Kamiya A, Ando J. 2006. Shear stress induces hepatocyte PAI-1 gene expression through cooperative Sp1/Ets-1 activation of transcription. Am J Physiol Gastrointest Liver Physiol 291(1):G26–G34.

Papeleu P, Vanhaecke T, Henkens T, Elaut G, Vinken M, Snykers S, Rogiers V. 2006. Isolation of rat hepatocytes. Methods Mol Biol 320:229–237.

Park[Q5] J, Berthiaume F, Toner M, Yarmush L, Tilles A. 2005. Microfabricated grooved substrates as platforms for bioartificial liver reactors. Biotech Bioeng 90:632–644.

Park J, Li Y, Berthiaume F, Toner M, Yarmush ML, Tilles AW. 2007. Radial flow hepatocyte bioreactor using stacked microfabricated grooved substrates. Biotechnol Bioeng 99(2):455–467.

Patzer JF. 2004. Oxygen consumption in a hollow fiber bioartificial liver—Revisited. Artif Organs 28(1):83–98.

Powers MJ, Domandsky K, Kaazempur-Mofrad MR, Kalezi A, Capitano A, Upadhyaya A, Kurzawski P, Wack KE, Stolz DB, Kamm R, Griffith LG. 2002a. A microfabricated array bireactor for perfused 3D liver culture. Biotechnol Bioeng 78:257–269.

Powers MJ, Janigian DM, Wack KE, Baker CS, Beer Stolz D, Griffith LG. 2002b. Functional behavior of primary rat liver cells in a three-dimensional perfused microarray bioreactor. Tissue Eng 8(3):499–513.

Rajan N, Habermehl J, Coté MF, Doillon CJ, Mantovani D. 2006. Preparation of ready-to-use, storable and reconstituted type I collagen from rat tail tendon for tissue engineering applications. Nat Protoc 1(6):2753–2758.

Rutkowski JM, Swartz MA. 2006. A driving force for change: Interstitial flow as a morphoregulator. Trends Cell Biol 17:45–50.

Schumacker PT, Chandel N, Agusti AG. 1993. Oxygen conformance of cellular respiration in hepatocytes. Am J Physiol Lung Cell Mol Physiol 265:L395–L402.

Seglen PO. 1979. Hepatocyte suspensions and cultures as tools in experimental carcinogenesis. J Toxicol Environ Health 5(2–3):551–560.

Smith MK, Mooney DJ. 2007. Hypoxia leads to necrotic hepatocyte death. J Biomed Mater Res A 80(3):520–529.

Swartz MA, Fleury ME. 2007. Interstitial flow and its effects in soft tissues. Annu Rev Biomed Eng 9:229–256.

Tanaka Y, Yamato M, Okano T, Kitamori T, Sato K. 2006. Evaluation of effects of shear stress on hepatocytes by a microchip-based system. Meas Sci Technol 17:3167–3170.

Tilles AW, Baskaran H, Roy P, Yarmush ML, Toner M. 2001. Effects of oxygenation and flow on the viability and function of rat hepatocytes cocultured in a microchannel flat-plate bioreactor. Biotechnol Bioeng 73(5):379–389.

Tingley SK. 2006. High-throughput[Q6] cell culture: A real-world evaluation. Innovat Pharm Technol, 54–58.

Toepke MW, Beebe DJ. 2006. PDMS absorption of small molecules and consequences in microfluidic applications. Lab Chip 6:1484–1486.

Vinci B, Cavallone D, Mazzei D, Vozzi G, Domenici C, Brunetto M, Ahluwalia A. 2009. In-vitro[Q7] liver model using microfabricated scaffolds in a modular bioreactor. Biotechnol J. 10.1002/biot.200900074.

Vozzi F, Heinrich JM, Bader A, Ahluwalia AD. 2009. Connected culture of murine hepatocytes and HUVEC in a multi-compartmental bioreactor. Tissue Eng Part A 15(6):1291–1299.

West BG, Brown JH, Enquist BJ. 1997. General model for the origin of allometric scaling laws in biology. Science 276:122–126.

Wu CC, Ding SJ, Wang YH, Tang MJ, Chang HC. 2005. Mechanical properties of collagen gels derived from rats of different ages. J Biomater Sci Polym Ed 16(10):1261–1275.

Xia Y, Whitesides GM. 1998. Soft lithography. Annu Rev Mater Sci 28:153–184.

A High-Throughput Bioreactor System for Simulating Physiological Environments

Daniele Mazzei, *Member, IEEE*, Federico Vozzi, Antonio Cisternino, Giovanni Vozzi, *Member, IEEE*, and Arti Ahluwalia, *Member, IEEE*

***Abstract*—The optimization of *in vitro* cell culture for tissue engineering, pharmacological, or metabolic studies requires a large number of experiments to be performed under varying conditions. In this paper, we describe a high-throughput bioreactor system that allows the conduction of parallel experiments in a simulated *in vivo*-like environment. Our bioreactors consist of tissue-, organ-, or system-specific culture chambers and a mixing device controlled by an embedded system that regulates the insertion of gas in the culture medium in order to control pH and pressure. Each culture chamber and mixing device possesses an autonomous control system that is able to ensure an optimal environment for cells. A computer communicates with the embedded system to acquire data and set up experimental variables. With this apparatus, we can perform a high-throughput experiment controlling several bioreactors working in parallel. In this paper, we discuss the architecture and design of the system, and the results of some experiments which simulate physiological and pathological conditions are presented.**

***Index Terms*—Bioreactor, cell culture, high throughput, mimic physiological environments.**

I. Introduction

CELL CULTURE is an essential tool in biological science, clinical science, and biomedical studies. This approach is a fundamental step in preclinical drug testing, and for this reason, it is of great interest to the pharmaceutical industry to employ cheaper and more ethical systems which can supply accurate and predictive information on the effects of chemicals on the human body.

Because drug testing involves a large number of tests on identical cell cultures, a single well culture is inadequate and costly both in time and money. The "high-throughput screening" (HTS) is a methodology for scientific experimentation widely used in drug discovery, based on a brute-force approach to collect a large amount of experimental data in less time and using less animals.

HTS is achieved nowadays using multiwell equipment to contain the cell cultures subject to treatment [1]. An automatic machine collects data, usually with an optical system, during the treatment. Collected data can vary widely in nature, for instance, concentrations of physiological metabolites or proteins.

The parallel nature of HTS makes it possible to collect a large amount of data from a small number of experiments and in a very short time. The multiwell system, however, suffers from a significant problem that may affect the relevance of tests: the environment discrepancy problem [2]. The environment discrepancy problem lies in the fact that the tissue grown in wells is only a brutal approximation of biological reality. There are several relevant factors that are missing in this environment; for instance, the cells in the well are not subject to the convective flow of nutrients present in the physiological environment. Another meaningful example is the lack of the typical pressure peaks and the presence of constant solute concentrations, unlike in biological systems where gradients of concentration are the basis of most important processes. In [3], it is discussed how the multiwell approach does not scale fully as expected by an HTS system because the collected data are not directly usable in drug testing. This seems to be a paradox because the multiwell has been the core element of the HTS methodology.

In this paper, we propose to use bioreactors to obtain an HTS system that overcomes the limits due to the environment discrepancy problem and obtain valid data from experiments which simulate a physiological environment.

A bioreactor is a system able to maintain a cell culture in a controlled environment aimed at the simulation of a living organism. Two principal elements in the system combine to provide a biomimetic habitat: the environmental control system and the structural, chemical, and microfluid dynamic framework of the bioreactor.

Although several different types of bioreactors [4], [5] have been reported, particularly for tissue engineering and pharmaceutical applications, none has been specifically designed for HTS. Pulsatile flow systems [6], rotating wall low shear reactors [7], [8], and compression bioreactors [9], for example, are all very large and bulky devices which do not lend themselves well to HTS or miniaturization. On the other hand, microfluidic systems, such as those described by Kane *et al.* [10], and the animal on-a-chip device in [11] are more amenable to parallel processing.

Here, we present a new bioreactor, called multicompartment bioreactor (MCB), through which we are able to perform

Manuscript received February 29, 2008; revised June 12, 2008. First published July 9, 2008; last published August 29, 2008 (projected).

D. Mazzei is with the Interdepartmental Research Center "E. Piaggio," Faculty of Engineering, University of Pisa, 56126 Pisa, Italy (e-mail: mazzei@di.unipi.it).

F. Vozzi is with the Interdepartmental Research Center "E. Piaggio," Faculty of Engineering, University of Pisa, 56126 Pisa, Italy, and also with the Institute of Clinical Physiology, National Council of Research, 56124 Pisa, Italy (e-mail: vozzi@farm.unipi.it).

A. Cisternino is with the Department of Computer Science, University of Pisa, 56125 Pisa, Italy (e-mail: cisterni@di.unipi.it).

G. Vozzi is with the Department of Chemical Engineering and the Interdepartmental Research Center "E. Piaggio," Faculty of Engineering, University of Pisa, 56126 Pisa, Italy.

A. Ahluwalia is with the Department of Information Engineering and the Interdepartmental Research Center "E. Piaggio," Faculty of Engineering, University of Pisa, 56126 Pisa, Italy, and also with the Institute of Clinical Physiology, National Council of Research, 56124 Pisa, Italy (e-mail: arti.ahluwalia@ing.unipi.it).

Color versions of one or more of the figures in this paper are available online at http://ieeexplore.ieee.org.

Digital Object Identifier 10.1109/TIE.2008.928122

high-throughput experiments in an *in vivo*-like simulated environment for a long time (more than a week). Two different compartmental cell culture chambers which simulate a blood vessel and the metabolic system, respectively, are described. Each chamber uses the same basic environmental control system and can be used for HTS experiments.

The first is a laminar flow chamber, in which known shear stresses and hydrostatic pressures can be applied in order to mimic physiological or pathological conditions in the cardiovascular system. The second unit is a multicompartmental device in which different cell types are cultured in series and in parallel to simulate a metabolic system [12]. Together with the environmental control system, the chambers provide a biomimetic habitat for cells and enable different *in vivo* scenarios to be more closely approximated.

The data extracted from this kind of culture is more predictive of the *in vivo* response with respect to the multiwell approach particularly for drug related studies because the bioreactor minimizes the environment discrepancy problem.

II. Materials and Methods

The MCB bioreactor is a complex system. In this section, we discuss the three main elements of the system: the bioreactor hardware, the embedded system and the control software, and the algorithm used to regulate pH. Two HTS experimental protocols using two different culture chambers are also described.

A. Bioreactor Hardware

The bioreactor system consists of the following parts:
1) cell culture chamber;
2) mixing chamber;
3) electronic circuit and electrovalve box;
4) peristaltic pump;
5) PC;
6) heating system.

1) Cell Culture Chamber: This part of the system is the core of the bioreactor: It contains the cell monolayer or scaffold where cells are seeded. The chamber is made entirely of *polydimethylsiloxane* (PDMS), a biocompatible silicone polymer (Sylgard 184, Dow Corning).

We have developed several types of cell culture chambers [13], [14], and each unit can be plugged into the system and used for different kinds of experiments. A laminar flow chamber was specifically designed to enable cells to be subject to a large range of shear stresses. Several cardiovascular pathologies are associated with altered patterns of flow and shear stress. The study of endothelial cell response to different flow conditions is therefore important for understanding and curing cardiovascular diseases.

Using finite-element methods and imposing a number of design criteria such as maximum volume and minimum area for cell culture, as well as the range of shear stresses desired, we converged to a final design for the chamber. Fig. 1 shows the chamber design and the constant and controlled velocity vector in the cell culture zone.

By changing the flow rate of the fluid, constant and controlled shear stresses ranging from 40×10^{-3} to 900×10^{-3} Pa can be applied to simulate aortic as well as capillary shears in physiological or pathological states.

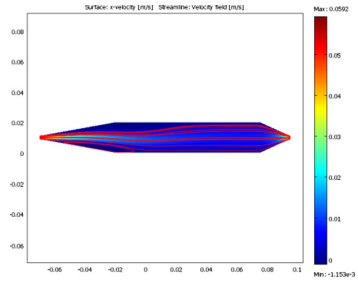

Fig. 1. Finite-element method simulation of the laminar flow bioreactor chamber with a medium flow speed of 0.05 m/s (12 mL/min).

Equation (1) allows the shear stress (τ) on the cell layer to be calculated from the applied volume flow rate (Q) with a medium viscosity (μ), cell chamber cross section (A), and a distance between the center of the chamber and the cell monolayer (z)

$$\tau = \mu \frac{Q}{A \cdot z}. \tag{1}$$

A completely different chamber configuration was adopted to simulate the metabolic system. Here, we used allometric principles to design a series of interconnected chambers in order to represent the principal components of the human metabolic system, focusing on the metabolism of glucose, which is the most important energy source for all organisms. Central to glucose metabolism are the liver and the pancreas, followed by insulin- and glucose-dependent target tissues. To design the system, the relationship between different parameters such as metabolism, time, volume distribution, and organ dimensions was considered in order to scale the physiological interactions present in the human body [15].

Thus, volume, flow rates, and cell numbers were downscaled using relationships based on allometry [16]. The simplest connected culture chamber device refers to a system with four cell types considered relevant to glucose metabolism (hepatocytes, pancreatic islets, visceral adipose tissue, and endothelial cells).

The general equation for allometric scaling is

$$Y = Y_o M^b \tag{2}$$

where Y is the parameter in question (flow rate, metabolism, etc.), Y_o is the proportionality factor, M is body mass, and b is the allometric scaling exponent. The mass of the standard human body is 68.5 kg, and our system is approximately 20 g.

In the case of volume and of the cell ratios, the exponent $b = 1$. Consequently, we first considered the ratios of cells in the system and scaled these down linearly in accordance with the allometric equation. The flow rate was scaled using $b = 3/4$ with respect to the portal flow rate. This flow rate also corresponds to small blood vessel and capillary flow velocities and to the range of shear stress typically found in blood vessels [17]. Because our main focus of interest is the study of glucose metabolism, the reference physiological data were referred to data on blood glucose levels in normal humans [18]. Through these data, the distance between the liver compartment and the other three compartments were estimated (liver–pancreas from

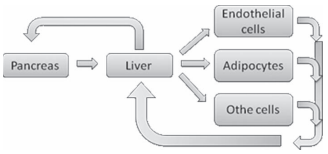

Fig. 2. MCB chamber topological scheme.

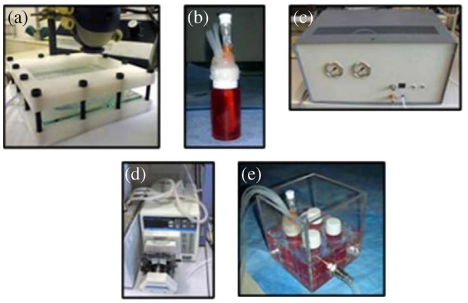

Fig. 3. (a) Cell culture chamber. (b) Mixing chamber. (c) Electronic and electrovalve box. (d) Peristaltic pump. (e) Heating box with four mixing chambers ready for the experiment.

5 to 7 cm and liver–adipocyte from 9 to 17 cm, with times of about 2 and 15 min, respectively) [19]–[21]. A schematic of the connected culture MCB chamber is shown in Fig. 2.

Each MCB unit is realized using an appropriate mould, in which silicone tubing is inserted during the fabrication process such that it is integrated into the chamber. PDMS is cast and cured in the mould by heating at 65 °C and then carefully removed, washed, and sterilized with H_2O_2 gas plasma. Following the sterilization phase, cells are seeded onto the chambers as necessary, and the bioreactor is assembled. The PDMS base is then covered with a gas plasma sterile glass plate, and the two are clamped together by a Teflon frame which can be tightened with screws [Fig. 3(a)] [22].

Medium flow in the chambers is generated by a peristaltic pump (P720, Instech, Plymouth, PA, USA) connected to the tubing and controlled by the electronic control unit for the regulation of flow rate. The electronic unit also controls a heating system below the culture chamber, which maintains the cell culture at constant temperature.

2) Mixing Chamber: The mixing chamber [Fig. 3(b)] is connected in series with each cell culture chamber and serves for pH and oxygen regulation as well as to remove air bubbles; essentially, the medium is perfused with gas according to the measured pH. The medium is inserted in this chamber through a needle with the flow imposed by the peristaltic pump. pH regulation is performed by inserting two different gases in the mixing chamber: CO_2 and air (not O_2 because of flammability risks). The culture medium contains bicarbonate buffer, and its pH can be closely regulated through diffusion of gases; in particular, the diffusion of O_2 (Air) tends to raise the pH, whereas CO_2 tends to lower it [23].

3) Electronic Circuit and Electrovalve Unit: This part of the system is the heart of the bioreactor control unit; there are the electronic circuits for the sensors, for communication with the PC, and for the actuation of the electrovalves. The electrovalves are used to select the gas that is injected in the mixing chambers and are connected to a pressure regulator used to control the pressure inside the cell culture chamber.

4) Computer: The computer is plugged to the electronic circuit and electrovalve unit through a network cable; there is an embedded system board responsible for controlling the system. We use a *Wildfire 5282* [24], a microcontroller unit based on a Motorola Coldfire microcontroller. The *Wildfire* board is used to control the pressure regulator and the electrovalves and for reading the sensor data; the data are stored on a secure digital card and are sent to the computer using the user datagram protocol (UDP) over the Ethernet connection.

The system is equipped with a liquid crystal display to allow an immediate control of the experiment parameters without a PC.

5) Heating System: The bioreactor heating system consists of a Plexiglas box where the mixing chambers[1] are inserted [see Fig. 3(d)]. Water heated by a thermostatic bath is inserted in the heating box, or it is also possible to equip the box with a resistor heater placed under the culture unit.

Culture chambers are also heated independently using a dedicated resistive heater [25]. Both the resistive heaters are controlled by the electronic unit through a pulsewidth-modulation (PWM) power regulator. The PWM signal is generated by one of the digital I/O wildfire channels and is amplified by a dedicated FET-based electronic circuit.

Two thermistors are used to monitor the temperature of the mixing and culture chambers, respectively, and feedback control ensures that the temperature is constant [26], [27].

B. Control System

The microcontrolled board runs the μTNetOS operating system (OS), a general purpose OS for microcontrolled systems [28] developed for the purpose.

μTNetOS is a generated OS: The system generator takes as input the description of an eXtensible Markup Language (XML)-based protocol and generates an instance of the OS with the entire communication system tailored for the particular protocol. It uses cooperative multitasking to run concurrent activities.

We have developed an application targeting the instance of μTNetOS tailored for bioreactors. The goal of the application is to make the bioreactor autonomous by monitoring the environmental variables and taking appropriate actions according to a policy defined through a networked computer and stored within the controller.

Because Ethernet is a communication bus, the graphical application used to control an experiment can receive UDP packets from several units running in parallel. This is very important in the context of HTS methodology [29]. The network also allows connections through the Internet, allowing remote monitoring of experiments, an important feature because experiments run for several days [30].

A high-throughput bioreactor experiment employs many bioreactors with different cell culture chambers. A pathology

[1] At least four of them are allowed.

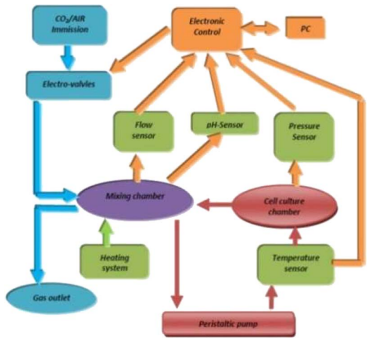

Fig. 4. Schematic flowchart of the bioreactor system. In orange are the electronic control unit and electronic connections; in green are the sensors, and in red are the culture chamber and the medium circuit. The gas connection and apparatus are represented in blue.

can be simulated in one of the Bioreactors, and the others used a control reference; we can setup the environmental variables of the bioreactors in order to simulate one or more pathologies and observe the influence of this different environment on tissue function during an experiment.

μTNetOS messaging complies with an XML-based standard defined by a robotics programming framework called Robotics4.NET [31], [32]. The framework proposes a software architecture inspired by the architecture of the human nervous system. In this context, the software running on the autonomous embedded system of the bioreactor is perceived as a roblet, a sort of peripheral organ abstraction provided by the framework.

A program based on Robotics4.Net is composed of three ingredients.

1) The brain: It is the core of the control system.
2) The bodymap: It is a sort of black board used to send and receive messages.
3) The roblets: They are the appendix of the system, like the parts of our nervous system. They read data from the environment and convert the brain signal into an action.

In our case, each of the bioreactor systems is perceived as a roblet that communicates with the program on the computer hosting the bodymap.

Because the connections among the roblets and the bodymap are based on a data gram-oriented protocol, the brain can be powered off and restarted afterward without affecting the activity of roblets.

In a bioreactor system, it is necessary to control many parameters: the amount of nutrients flowing in the cell culture chamber, the hydrostatic pressure inside the system, the shear stress of the flow on the cell culture, the flow of gas, the temperature flux generated by the heating system, and the pH of the medium (Fig. 4). These parameters are established using a graphical interface and sent to the roblets running on the bioreactors.

To control the nutrient flow and the shear stress, it is necessary to regulate the speed of the peristaltic pump used to perfuse the nutrients inside the bioreactor, this control is operated by a serial connection between the pump and the controller board and is monitored in a feedback mode through an appropriate control pin of the pump. The hydrostatic pressure inside the

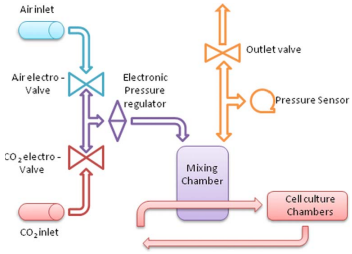

Fig. 5. Schematic connection of the pressure regulation system.

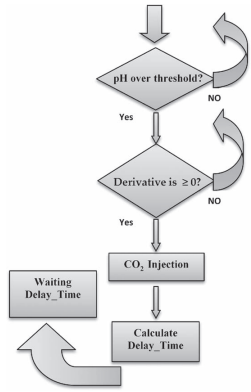

Fig. 6. Flow diagram of the control algorithm for pH regulation.

circuit and the flow of gas through the mixing chamber are regulated by fine control of the pressure regulator and of the outlet; the outlet can be set manually in order to obtain the desired pressure in the mixing chamber. The system reads the pressure inside the mixing chamber with a pressure sensor plugged in parallel with the outlet; in this way, we can control the system in a classic feedback mode (Fig. 5).

The heat flux and the temperature of the cell culture chamber is controlled by a feedback system, which reads the temperature of the cell culture chamber through a negative temperature coefficient sensor placed near the cell monolayer and imposes a voltage across a dedicated resistive heater placed under the cell culture chamber.

As mentioned in [33], the pH is more complex to control than the other parameters because of delays between gas infusion and ionic dissociation; for this reason, we studied a dedicated control strategy based on a variable delay time, which is reported in the following section.

C. pH Control Algorithm

To control the pH in the medium, we developed a control adaptive algorithm based on a step strategy. This control algorithm is a high priority service running on μTNetOS.

A formal model of the algorithm has been also defined using the abstract state machines (ASM) formalism [34].

The pH response to the diffusion of CO_2 and air is very difficult to predict, because it depends strongly on the environmental variables of the particular experiment such as temperature, volume of medium, type of medium, hydrostatic pressure, number of cells, and their metabolic state. For this reason, we do not use the mathematical model of the CO_2 and air diffusion in water medium but instead use a function defined by an algorithm.

Our system continuously inserts air in the mixing chamber through an appropriate needle; when the pH goes over the safety threshold (0.05 units of pH over a user-defined threshold), the control inserts a known CO_2 impulse, in the mixing chamber, and waits a *delay time*. In this way, we can insert a known amount of CO_2 inside the mixing chamber and wait to evaluate the effect of this operation. If the pH returns under the safety threshold, we can stop the pH control phase; otherwise, after the *delay time* has passed, the control inserts a new impulse of CO_2 and waits for the *delay time*. The *delay time* is adjusted at every step in a manner dependent on the value of pH and the derivative of pH with time.

The pH control strategy includes one safety logic test used to evaluate whether the pH is decreasing or not; in the case of a negative derivative, if the pH value is over the safety threshold, the control does not insert CO_2 because we can assume that the last CO_2 injection was sufficient for the pH control and the pH can return under the threshold in a short time; this test prevents an excessive fall in pH, because the CO_2 injection causes a large drop in pH but with a substantial delay (Fig. 6)

$$\begin{aligned}\mathrm{TDelay}(n) = \mathrm{TDelay}(n-1) \\ \times \left[A(\mathrm{pH} - \mathrm{pH}*) + B\left(\mathrm{pH}(n) - \mathrm{pH}(n-1)\right)\right]. \quad (3)\end{aligned}$$

Equation (3) describes how the time delay is calculated by the roblets running on the Wildfire 5282 board. The delay time to use at the current step is proportional to the delay time of the last step but with an additional value that is directly proportional to the difference of the current and expected pH values and a part that is proportional to the first derivative of the pH signal coming from the pH meter.

The multiplicative constants A and B are between zero and one; in this way, we added only a part of the $(n-1)$ *delay time* for every control step.

These constants can be predicted by the formal model based on ASM [35] for a water environment but are very sensitive to the physical condition of the experiment (volume and type of medium, pressure, and temperature). Consequently, we have to calibrate the system through the user interface before starting a new session, in order to match the pH control parameter with the experimental setup.

D. GUI Software

Our *graphical user interface* (GUI) is developed in C#.Net and is based on a multitab structure; we use the GUI to read data from the bioreactors and to set up the experimental variables of each one. The user interface also features a tool for sensor calibration, in order to perform the sensor calibration with the same software that we used for bioreactor control.

The user has control over the experiments, including a manual overdrive, although the autonomous control software running on the embedded systems avoids commands that could damage the system or the experiment.

When the user interface is open, it seeks out connected bioreactors; when one is found, the GUI switches in the view mode. In this section, we can see data of the bioreactor selected by the menu, and experimental settings can be changed through the configuration tab.

E. Cell Culture Experiments

The MCB bioreactor system was tested in a "*virtual laboratory*," in which we simulated a typical parallel experiment with four "animals." For each experiment, we installed four bioreactors, and we performed laminar flow and connected culture HTS trails, respectively, with cells in the bioreactor under a constant flow of nutrients and gas.

These experiments demonstrate how our bioreactors can be used to conduct experiments in a high-throughput manner with four parallel chambers and how we can control and store data with a single computer placed in any location.

1) Laminar Flow Chamber: The cells used for the laminar flow experiments were human umbilical vein endothelial cells (HUVEC) [36]. They were placed in the cell culture chambers and in an incubator for 24 h in order to ensure their adhesion on the gelatin-treated PDMS base. After incubation, the cell culture chambers were plugged into the bioreactor system, and we ran four sets of experiments at four different flow rates (including zero) for 24 h. At the end of each experiment, we analyzed the culture medium for nitric oxide (NO), a vasodilator, and endothelin (EN-2) [37], a powerful vasoconstrictive molecule which counteracts the effects of vasodilation. Cell morphology and orientation were also assessed by calculating cell eccentricity.

2) Connected Culture Chamber: To demonstrate the application of HTS in the MCB connected culture chamber, hepatocytes and endothelial cells (HUVEC) were used in a ratio similar to that in the liver. Hepatocytes were extracted directly from freshly explanted murine (black mice, strain C57BL/6) liver and cultured according to standard procedures [38]. The endothelial cells were prepared according to the method described by Jaffe *et al.* [36].

Glass slides of 12-mm diameters with 80 000 hepatocytes and 8000 HUVEC were inserted into the connected culture bioreactors and then connected to the mixing device and pump and filled with 30-mL William's culture medium. Controls using only hepatocytes in the absence of HUVEC were also conducted. For these experiments, a flow rate of 175 μl/min was applied to four systems running in parallel. Experiments were carried out for 24 h, during which 2 mL of the medium was withdrawn for analysis at 2 h 40 min, 4 h 20 min, 6 h, and 24 h and was replaced with 2 mL of fresh medium. During each withdrawal, albumin, an important biomarker for hepatocyte synthetic function, was quantified using a commercial enzyme-linked immunosorbent assay kit and the data compared with standard static multiwell cultures.

III. Results

The experiments showed how the high-throughput bioreactors system can run for up to 24 h in order to simulate the classic parallel "animal" experiments; in this way, we can greatly

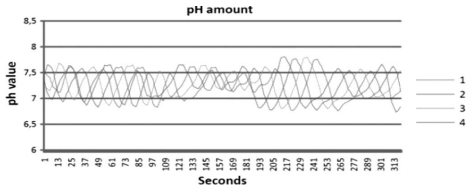

Fig. 7. The pH in the four bioreactor systems during the laminar flow experiment; the numbers in the legend are the four bioreactors ID labels. The acquisition was carried out over 24 h but a 300-s window is shown here.

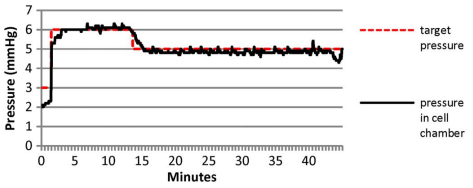

Fig. 8. Pressure graph shows how the control system is able to maintain the desired value of pressure inside the bioreactors.

reduce the number of "animals" that are necessary for the experiments. Another important aspect of the new bioreactor system is that, in this mode, it is possible to perform experiments in an *in vivo*-like biomimetic habitat instead of in a multiwell, which is a brutal approximation of the physiological environment.

The data extracted from the bioreactors during the experiments show how the new system is able to correctly control the environmental variables.

Fig. 7 shows how the new bioreactor system is able to maintain a pH value in the medium around the physiological value of 7.4. It has a maximum error deviation of -1.2 and $+0.3$; the asymmetry of the pH error deviation is a consequence of the pH control strategy. In fact, when CO_2 is inserted inside the chamber, we have a rapid drop of pH; otherwise, when air is inserted, the pH increases slowly; for this reason, it is very difficult to prevent the excessive undershoot of pH because an opening time of the CO_2 electrovalve of only 0.5 s is necessary to control the pH but at the same time gives rise to a slow but large drop in pH. The pressure graph (Fig. 8) shows a pressure step experiment; in this experiment, we choose to increase the pressure in the cell culture chamber with a step in order to simulate hypertensive stress.

A. HTS Laminar Flow

The vascular endothelium is a dynamic organ that responds to various physical and humoral conditions by producing several biologically active substances, both vasoconstrictors and vasodilators, which control these processes. Therefore, to assess the ability of the laminar flow system in maintaining functional properties that cells possess in physiological conditions, we examined the production of these important vasoactive factors (NO and EN-2) by endothelial cells in different shear stress conditions. The results are shown in Figs. 9 and 10.

Endothelin production decreases even at very low shear stresses, indicating that the cells respond to static conditions by overexpressing vasoconstrictive functions in an effort to compensate for the lack of mechanical stimulus normally produced by flow. This is also reflected in NO production, which increases steadily with shear stress. Fig. 11 shows the change in eccentricity of endothelial cells, which respond to shear stress by orienting and elongating along the direction of flow as observed *in vivo*.

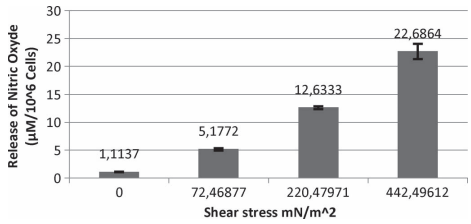

Fig. 9. NO production (micromole per 10^6 cells) after 24 h in the laminar flow bioreactor chambers with different shear stresses.

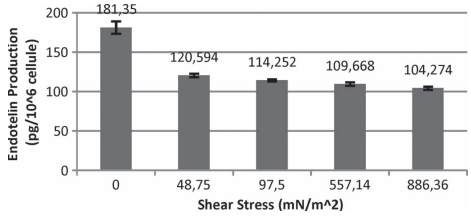

Fig. 10. Endothelin production (picogram per 10^6 cells) after 24 h in the laminar flow chamber with different shear stresses.

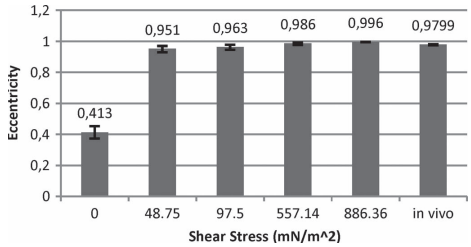

Fig. 11. Change in the cell eccentricity E during a 24-h experiment in a laminar flow chamber with different shear stresses compared with the capillary physiological eccentricity ($E = a/(2b)$) with a as the major radius and b as the minor).

In Fig. 12, a cell culture after 24 h of laminar flow treatment with the MCB laminar bioreactors is shown. We can observe the vitality of the cells, that do not show any type of cell membrane damage or formation of picnotic nuclei.

The cells can be used as sensors of the environment, to evaluate the consequence of flow treatment. In the micrograph, the endothelial cells are oriented with the medium flow and have elliptical shapes similar to their *in vivo* morphology.

B. HTS Connected Cultures

The connected culture system was conceived using biomimetic principles to reproduce salient features of the

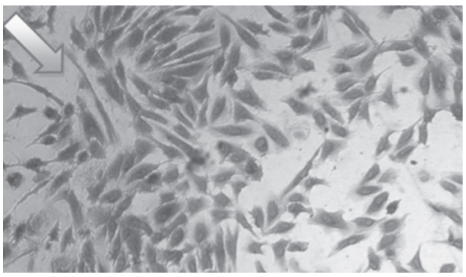

Fig. 12. Cell culture after 24 h of treatment; we can observe how the cells have an elliptical shape and are oriented with the medium flow (indicated by the arrow).

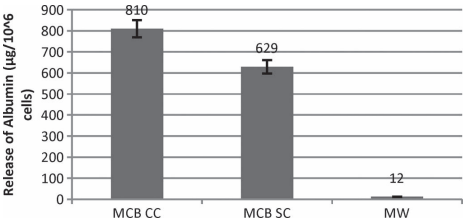

Fig. 13. Albumin production after 24 h of experiment in an HTS MCB connected culture; the MCB CC system is a dynamic (175 μl/min) connected culture of hepatocytes and HUVEC, MCB SC is a dynamic culture in MCB with only hepatocytes, and MW is a static hepatocyte multiwell culture.

metabolic system with particular regard to the metabolism of glucose, fat, and protein. The chamber was designed using allometric laws conserving proportions and ratios between different organs. It allows cell–cell crosstalk to be studied in a rigorous and controlled manner, by addressing and interrogating one cell type at a time, and could lead to a better understanding of the physiological and biochemical complexity. Obviously, a focal point of the system is the hepatocyte chamber, because the liver is the principal metabolic organ in the body. This initial study was therefore on a hepatocyte–endothelial connected culture model considering only proportions between the two cell populations in the liver. Overall, large differences in albumin production were observed between static multiwell and dynamic cultures, and smaller but nonetheless significant differences were observed between dynamic monocultures and connected cultures: evidence of crosstalk between two cell types. Strictly speaking, the static monoculture conditions cannot be directly compared with the connected culture as the medium volumes are quite different. The availability of oxygen and nutrients is increased, the fluid is well mixed, and nutrient depletion in the medium is negligible in the bioreactor system. This is shown in Fig. 13, which shows that albumin production is upregulated by about 1.5 times when compared with connected cultures with dynamic monocultures and over 50 times when comparing dynamic and static multiwell monocultures.

IV. Conclusion

In this paper, we have presented an alternative HTS approach for cell culture. Using a purposely designed and constructed autonomous software and electronic control and acquisition system combined with specific cell culture chambers, it is possible to simulate a biomimetic habitat for cells. The control system and software enable the temperature, pH, pressure, and flow to be tightly regulated or modulated to simulate physiological or pathological environments. Special chamber designs can be used for approximating the geometry, fluid dynamics, and chemical environment of different organs or systems.

The experiments demonstrate how the high-throughput MCB bioreactor system is able to perform experiments in parallel, combining the advantages of *in vivo*-like simulated environments with an HTS control strategy. So as not to limit the applications of the systems, the OS μTNetOS was generated and not written *ad hoc*; in this way, we can easily change the hardware platform without reengineering the OS. A further innovative aspect is the modular architecture of the hardware which is mirrored by the human nervous system-inspired software architecture.

Our efforts are now being directed to predictive drug toxicology, nanotoxicology, and the works of hypertension-related cardiovascular diseases.

References

[1] J. J. Burbaum and N. H. Sigal, "New technologies for high-throughput screening," *Curr. Opin. Chem. Biol.*, vol. 1, no. 1, pp. 72–78, Jun. 1997.

[2] P. J. Hung and P. J. Lee, "Continuous perfusion microfluidic cell culture array for high-throughput cell-based assays," *Biotechnol. Bioeng.*, vol. 89, no. 1, pp. 1–8, Dec. 3, 2004.

[3] S. K. Tingley, "High-throughput cell culture: A real-world evaluation," *Innov. Pharm. Technol.*, pp. 54–58, Feb. 2006.

[4] Y. Martina and P. Vermette, "Bioreactors for tissue mass culture: Design, characterization, and recent advances," *Biomaterials*, vol. 26, no. 35, pp. 7481–7503, Dec. 2005. Review.

[5] M. J. Jaasma, N. A. Plunkett, and F. J. O'Brien, "Design and validation of a dynamic flow perfusion bioreactor for use with compliant tissue engineering scaffolds," *J. Biotechnol.*, vol. 133, no. 4, pp. 490–496, Feb. 29, 2008.

[6] K. Dumont, J. Yperman, and P. R. Verdonck, "Design of a new pulsatile bioreactor for tissue engineered aortic heart valve formation," *Artif. Organs*, vol. 26, no. 8, pp. 710–714, Aug. 2002.

[7] F. Anton, K. Suck, and S. Diederichs, "Design and characterization of a rotating bed system bioreactor for tissue engineering applications," *Biotechnol. Prog.*, vol. 24, no. 1, pp. 140–147, Jan./Feb. 2008.

[8] M. Ingram, G. B. Techy, and R. Saroufeem, "Three dimensional growth patterns of various human tumor cell lines in simulated microgravity of a NASA bioreactor," *In Vitro Cell. Dev. Biol., Anim.*, vol. 33, no. 6, pp. 459–466, Jun. 1997.

[9] E. M. Darling and K. A. Athanasiou, "Articular cartilage bioreactors and bioprocesses," *Tissue Eng.*, vol. 9, no. 1, pp. 9–26, 2003.

[10] B. J. Kane, M. J. Zinner, M. L. Yarmush, and M. Toner, "Liver-specific functional studies in a microfluidic array of primary Mammalian hepatocytes," *Anal. Chem.*, vol. 78, no. 13, pp. 4291–4298, Jun. 2006.

[11] A. Sin, G. T. Baxter, and M. L. Shuler, "Animal on a chip: A microscale cell culture analog device for evaluating toxicological and pharmacological profiles," in *Proc. SPIE—Microfluidics* and *BioMEMS*, Sep. 2001, vol. 4560, pp. 98–101.

[12] F. Vozzi, J. M. Heinrich, A. Bader, and A. D. Ahluwalia, "Connected culture of Murine Hepatocytes and HUVEC in a multi-compartmental bioreactor," *Tissue Eng.*, submitted for publication.

[13] A. Ahluwalia, G. Vozzi *et al.*, "Bioreattori bi-e tridimensionali high-throughput sensorizzati e/o dotati da sistemi di filtrazione e di trasduzione ed attuazione," Patent N PI2006A000121, Nov. 8, 2006.

[14] A. Ahluwalia, G. Vozzi, and F. Vozzi, "Bioreattore per lo studio degli effetti sulle attività cellulari di stimoli imposti," Patent N PI2004A000046, Jun. 2004.

[15] G. B. West and J. H. Brown, Eds., *Scaling in Biology*. New York: Oxford Univ. Press, 2000.

[16] G. B. West, J. H. Brown, and B. J. Enquist, "A general model for the origin of allometric scaling laws in biology," *Science*, vol. 276, no. 5309, pp. 122–126, Apr. 1997.

[17] Y. C. Fung *et al.*, *Biomechanics of the Circulation*. New York: Springer-Verlag, 1997.
[18] R. L. Fournier, *Basic Transport Phenomena in Biomedical Engineering Book*. New York: Taylor & Francis, 1999.
[19] B. Capaldo, A. Gastaldelli *et al.*, "Splanchnic and leg substrate exchange after ingestion of a natural mixed meal in humans," *Diabetes*, vol. 48, no. 5, pp. 958–966, May 1999.
[20] C. Meyer *et al.*, "Role of human liver, kidney, and skeletal muscle in postprandial glucose homeostasis," *Amer. J. Endocrinol. Metab.*, vol. 282, no. 2, pp. E419–E427, Feb. 2002.
[21] A. D. Cherrington, M. C. Moore *et al.*, "All insulin action on the liver *in vivo*," *Biochem. Soc. Trans.*, vol. 35, pt. 5, pp. 1171–1174, Nov. 2007.
[22] J. M. Wilkinson and A. D. Ahluwalia, "A novel multichamber bioreactor system for early stage toxicology screening," in *Proc. Nanotechnol.—Towards Reducing Animal Testing*, London, U.K., May 28–29, 2008, pp. 50–52.
[23] M. C. F. Magalhãesa and R. N. Correia, "Inorganic plasma with physiological CO_2/HCO_3- buffer," *Biomaterials*, vol. 24, no. 9, pp. 1541–1548, Apr. 2003.
[24] "SteroidMicros web page," *Wildfire 5282 Data Sheet*. [Online]. Available: http://www.steroidmicros.com/
[25] "Omega Catalogs," *Kapton Insulated Flexible Heaters Data Sheet, Omega Web Catalog*. [Online]. Available: http://www.omega.com
[26] J. B. Christen and A. G. Andreou, "Design, fabrication, and testing of a hybrid CMOS/PDMS microsystem for cell culture and incubation," *IEEE Trans. Biomed. Circuits Syst.*, vol. 1, no. 1, pp. 3–18, Mar. 2007.
[27] J. B. Christen and A. G. Andreou, "Hybrid silicon/silicone (polydimethylsiloxane) microsystem for cell culture," in *Proc. 28th IEEE Annu. Int. Conf. EMBS*, Aug. 30–Sep. 3, 2006, pp. 2490–2493.
[28] H. Hassan *et al.*, "Remote laboratory architecture for the validation of industrial control applications," *IEEE Trans. Ind. Electron.*, vol. 54, no. 6, pp. 3094–3102, Dec. 2007.
[29] A. Faro, O. Mirabella, and C. Nigro, "Performance evaluation of the standard proway network for process control," *IEEE Trans. Ind. Electron.*, vol. IE-33, no. 1, pp. 9–20, Feb. 1986.
[30] D. T. Nguyen, S.-R. Oh *et al.*, "A framework for Internet-based interaction of humans, robots, and responsive environments using agent technology,"*IEEE Trans. Ind. Electron.*, vol. 52, no. 6, pp. 1521–1529, Dec. 2005.
[31] A. Cisternino, D. Colombo, G. Ennas, and D. Picciaia, "Robotics4.NET: Software body for controlling robots," *Proc. Inst. Elect. Eng.—Software*, vol. 152, no. 5, pp. 215–222, Oct. 2005.
[32] A. Cisternino, F. Cicchi, and D. Mazzei, *μTNetOS: Operating System Generation for Micro-Controllers*, 2007. submitted for publication.
[33] M. A. Henson and D. E. Seborg, "Adaptive nonlinear control of a pH neutralization process," *IEEE Trans. Control Syst. Technol.*, vol. 2, no. 3, pp. 169–182, Aug. 1994.
[34] E. Boerger and R. Staerk, *Abstract State Machines—A Method for High-Level System Design and Analysis*. New York: Springer-Verlag, 2003.
[35] V. Gervasi and D. Mazzei, "Using abstract state machines in modeling biological systems," in *Proc. GNB*, Pisa, Italy, 2008, pp. 79–80.
[36] E. A. Jaffe, R. L. Nachman, C. G. Becker, and C. R. Minick, "Culture of human endothelial cells derived from umbilical vein. Identification by morphologic and immunologic criteria," *J. Clin. Invest.*, vol. 52, no. 11, pp. 2745–2756, Nov. 1973.
[37] J. D. Cohen, "Overview of physiology, vascular biology, and mechanisms of hypertension," *J. Manag. Care Pharm.*, vol. 13, pp. S6–S8, Jun. 2007. (5 Suppl), Review.
[38] P. O. Seglen, "Preparation of isolated rat liver cells," *Methods Cell Biol.*, vol. 13, pp. 29–83, 1976.

Daniele Mazzei (M'04) received the M.S. degree in biomedical engineering from the University of Pisa, Pisa, Italy, in 2006, where is currently working toward the Ph.D. degree in biomedical engineering.

He is with the Interdepartmental Research Center "E. Piaggio," Faculty of Engineering, University of Pisa, where he is part of the Multicompartment Bioreactor Team headed by Prof. A. Ahluwalia in Pisa and in collaboration with the Computer Science Department, University of Pisa, on developing embedded systems to control and monitor biological processes. His research interests are focused on developing bioreactor systems for tissue engineering and high-throughput screenings. Also, he is currently studying the relationship between shear stress and cell culture.

Mr. Mazzei has been an IEEE Industrial Electronics Society member since 2007. He was the recipient of a student scholarship to present this paper in Vigo, Spain, during the International Symposium on Industrial Electronics 2007. In July 2005, he attended the 8th European Space Agency Student Parabolic Flight Campaign held in Bordeaux, France, and the results of this work were published in "Verification of Fitts' law in microgravity and hypergravity environments" by G. Ciofani, V. Lombardo, D. Mazzei, A. Migliore, M. C. Carrozza, P. Dario, and S. Micera.

Federico Vozzi received the M.Sc. degree in pharmaceutical chemistry in 2003 and the Ph.D. degree in drug science in 2007, both from the Faculty of Pharmacy, University of Pisa, Pisa, Italy.

He is a Postdoctoral Researcher with the Interdepartmental Research Centre "E. Piaggio," Faculty of Engineering, University of Pisa. He is also with the Institute of Clinical Physiology, National Council of Research, Pisa. His research interests are focused on bioengineering, with particular attention to the development and testing of new bioreactor systems for dynamic cell cultures, tissue regeneration, and drug testing.

Antonio Cisternino received the M.S. and Ph.D. degrees from the University of Pisa, Pisa, Italy, in 1999 and 2003, respectively.

He was an Intern in the fall of 2001, working on generics and runtime code generation for the .NET Common Language Runtime. From 2003 to 2006, he was a Fellow Researcher with the Department of Computer Science, University of Pisa, where he has been an Assistant Professor since 2006. He has collaborated with the Microsoft Robotics Studio team and visited Redmond, WA, in May 2006. He has coauthored the Expert F# book and published in several international journals and conferences. His research interests are domain-specific languages and self-evolving software infrastructures.

Dr. Cisternino is the recipient of three research grants from Microsoft Research and has actively collaborated with Microsoft Corporation since 2001.

Giovanni Vozzi (M'07) received the B.S. degree in electronic engineering from the University of Pisa, Pisa, Italy, in 1998, and the Ph.D. degree in bioengineering from the Politecnico di Milano, Milan, Italy, in 2002.

He is currently a Research Assistant with the Department of Chemical Engineering, Faculty of Engineering, University of Pisa, where he is also with the Interdepartmental Research Center "E. Piaggio." His research interests concern the development of microfabrication systems and, in particular, the realization of polymeric structures for application in tissue engineering. He is also involved in projects related to the development of cellular models able to predict the cell function and mimic the cellular experiments. He is also interested in bioreactor design at meso- and microscale for the study of cellular behavior and crosstalking.

Dr. Vozzi has been a member of the IEEE Industrial Electronics Society since 2007.

Arti Ahluwalia (M'02) received the B.Sc. degree in physics (U.K.), the M.Sc. degree in instrumentation and analytical science (U.K.), and the Ph.D. degree in bioengineering (Italy).

She is an Associate Professor of Bioengineering with the Department of Information Engineering, Faculty of Engineering, University of Pisa, Pisa, Italy, the Vice Director of the Interdepartmental Research Center "E. Piaggio," and the Head of the Bio Group. She is also with the Institute of Clinical Physiology, National Council of Research, Pisa. The main focus of her research is centered on the interaction between biological systems and man-made devices or structures, spanning biomolecular films, surface engineering, and biosensing to microfabrication, biomaterials, and biotechnologies for tissue engineering.

Biotechnol. J. 2009, 4 DOI 10.1002/biot.200900074 www.biotechnology-journal.com

Research Article

In vitro liver model using microfabricated scaffolds in a modular bioreactor

Bruna Vinci[1], *Daniela Cavallone*[2], *Giovanni Vozzi*[1], *Daniele Mazzei*[1], *Claudio Domenici*[3], *Maurizia Brunetto*[2] *and Arti Ahluwalia*[1]

[1] Interdepartmental Research Centre E. Piaggio, University of Pisa, Pisa, Italy
[2] U.O. Epatologia, Azienda Ospedaliera Universitaria Pisana, Pisa, Italy
[3] CNR Institute of Clinical Physiology, Pisa, Italy

Hepatocyte function on 3-D microfabricated polymer scaffolds realised with the pressure-activated microsyringe was tested under static and dynamic conditions. The dynamic cell culture was obtained using the multicompartment modular bioreactor system. Hepatocyte cell density, glucose consumption, and albumin secretion rate were measured daily over a week. Cells seeded on scaffolds showed an increase in cell density compared with monolayer controls. Moreover, in dynamic culture, cell metabolic function increased three times in comparison with static monolayer cultures. These results suggest that cell density and cell-cell interactions are mediated by the architecture of the substrate, while the endogenous biochemical functions are regulated by a sustainable supply of nutrients and interstitial-like flow. Thus, a combination of 3-D scaffolds and dynamic flow conditions are both important for the development of a hepatic tissue model for applications in drug testing and regenerative medicine.

Received 26 March 2009
Revised 24 July 2009
Accepted 29 July 2009

Keywords: Bioreactor · Liver model · Microfabrication · Scaffold

1 Introduction

A great deal of effort is being made to preserve liver-specific function *in vitro*. There are several driving forces for this, perhaps the two most important are drug testing and bioartificial liver devices. For the moment, the prevailing opinion in the literature is that it is impossible to maintain an adequately differentiated hepatic phenotype after isolation from the liver for more than a week [1]. Several parameters are known to play a role in maintaining liver function; among these are the presence of an adequate nutrient supply, an extracellular environment rich with ligands for adhesion and signalling, and a spatial architecture resembling that of the native liver, as well as a multicomponent medium. These parameters form what we call here the tripartite of cues: a trio of biochemical, biophysical and biomechanical signalling systems that interact synergically to support both form and function in all living tissues [2].

A wide variety of methods have been and are being developed to maintain and study the function of hepatocytes *in vitro*. Many of these are based on devising complex cocktails of culture medium, which often include inducing agents to drive hepatocytes towards expression of P450 cytochromes [3]. Others use engineering-based methods such as scaffolds and bioreactors. Several authors have used 3-D structures such as collagen [4], or loofa

Correspondence: Professor Arti Ahluwalia, Interdepartmental Research Centre E. Piaggio, University of Pisa, via Diotisalvi 2, 56126 Pisa, Italy
E-mail: arti.ahluwalia@ing.unipi.it
Fax: +39-0502217051

Abbreviations: ANCOVA, analysis of covariance; **CAD/CAM**, computer aided design/computer aided manufacturing; **MCmB**, multicompartment modular bioreactor; **PAM**, pressure-activated microsyringe; **PLGA**, poly-DL-lactide-co-glycolide; **PLLA**, poly-L-lactide

sponges in static and perfused cell culture conditions [5] and hydrogel encapsulated hepatocytes [6]. In the past few years the use of bioreactors has become very popular because a dynamic cell culture system allows efficient metabolite exchange, and may also provide an indirect physical stimulus through percolative or interstitial-like flow [7]. The bioreactors can be divided into two main groups: those for large-scale culture, such as flat membrane systems, and microfabricated systems, which involve 2- or 3-D cultures and microfluidics. The simplest systems are continuous flow reactors, such as that proposed by Catapano and De Bartolo [8], which are useful for large-scale culture, particularly for artificial liver applications. A microfabricated array reactor with deep wells for hepatocyte spheroids was described by Powers *et al.* [9, 10]. In this system, the wells were perfused by the medium and the cells were reported to remain viable for 2 weeks, with high levels of urea and albumin secretion. Hongo *et al.* [11] and Kataoka *et al.* [12] describe the culture of porous scaffolds in a radial flow bioreactor, so combining two of the cues in a single experiment. It is also recognised that co-culture of hepatocytes and non-parenchymal cells augments liver phenotypic function. Bhatia and colleagues [13, 14] pioneered the use of 2-D micropatterns in mono- and co-culture, and they have reported on various combinations of heterotypic cultures as well as a comparative study that highlights the differences in gene expression in different co-culture combinations. Several reports by the group of Yarmush and Toner on microfabricated grooved substrates for hepatocyte co-cultures have been published, showing the advantage of grooves with respect to flat surfaces [15, 16]. Finally, sandwich cultures, in which hepatocytes are either supplied with an adhesive protein-based roof and floor to recreate a pseudo 3-D extracellular matrix environment, have also been widely reported to enhance hepatic function [17]. Despite the extensive literature on the subject, it is not clear how strongly each of these parameters influence hepatic phenotype; quite likely the biochemical, biophysical and mechanical stimuli provide multiple cues that act in unison to mimic the *in vivo* hepatic environment. The aim of this work was to gain a better understanding of the role of a 3-D architecture and convective mass transfer on hepatocytes *in vitro*. We therefore designed an *in vitro* model of the liver using a bottom-up engineering approach, *i.e.* a step-wise increase of the number of cues in the system. For this study we considered only cues that can be controlled externally using mechanical and structural design parameters. Biochemical control of hepatocyte function is far more complex because the cells themselves modulate the chemistry of their environment. Firstly, the influence of a 3-D open-pore microfabricated scaffold on HepG2 cell proliferation and metabolic function was assessed using two different biomaterials. The most suitable material was then selected for experiments using a low-shear, high-flow bioreactor (Mazzei *et al.*, A low shear stress modular bioreactor for connected cell culture under high flow rates; *Biotech. Bioeng.*, submitted), and both cell proliferation and metabolism were analysed and compared with controls.

2 Materials and methods

2.1 Microfabrication with pressure-activated microsyringe

The pressure-assisted microsyringe (PAM) deposition method has been described in several references [18]. Basically it consists of a pressure-activated syringe, which is controlled by a computer-aided design/computer-aided manufacturing (CAD/CAM) fabrication system. The syringe is a stainless steel barrel with a glass capillary needle with a diameter of 5–20 μm. It is filled with a viscous polymer solution and mounted on a three-axis micropositioner. Pressurised air is used to extrude the polymer solution through the micro-needle and deposit it on a solid substrate such as a glass cover slip. The CAD/CAM system allows an infinite range of structures with a lateral resolution of 5 μm to be designed and fabricated. 3-D polymeric scaffolds are assembled by depositing a water-soluble polymeric spacer (Hydrofilm, Lucart, Italy) of about 10–20 μm between the layers. This avoids the collapse of subsequent layers and creates large pores in which cells are able to penetrate and adhere. After the microfabrication step, scaffolds are immersed in water. During this process the polymer spacer is dissolved away and the scaffolds float off the substrates and can be handled with tweezers.

PAM has the highest resolution of all 3-D CAD/CAM microfabrication methods used in tissue engineering, and the fidelity of the scaffolds is about 10% [19]. Apart from the machine-dependent deposition parameters such as needle-bore size and motor speed and precision, the fidelity depends mainly on the viscosity and surface tension of the polymer.

2.2 Polymer and scaffold treatment

The polymers used in this study were: poly-DL-lactide-co-glycolide (PLGA) 75:25 and poly-L-lactide (PLLA) (Lactel, NPPharm-F, Bazainville, France).

PLGA and PLLA are biodegradable polymers widely used in tissue engineering applications. Our group has tested these polymers in the form of spin-coated films and PAM scaffolds and their suitability for cell adhesion and tissue engineering has been evaluated [20]. Solutions of 20% PLGA and 10% PLLA in chloroform have excellent deposition characteristics in terms of their viscosity and surface tension, and these concentrations were used for all experiments. Hexagonal unit cell structures were microfabricated with 50-μm line width and 500-μm unit side length (Fig. 1A illustrates the definition of these terms), and were composed of three layers with 70 hexagons each (Fig. 1A). Each layer was laterally offset by 250 μm so that the hexagons were not piled flush but formed small open pores in the scaffold. The dimensions were chosen because they mimic the characteristic size of hepatic lobules [21]. Figure 1B shows an example of a PLGA 3-D scaffold. Polymer films were realised by spin coating (Delta 10TT, SÜSS MicroTec) at 7500 rpm for 15 s on 13-mm diameter glass cover slips. These films were used as a monolayer static control to investigate how cell function is influenced by a 3-D topology and to compare and normalise the experimental data with respect to the polymer's intrinsic characteristics rather than laboratory tissue culture plastic.

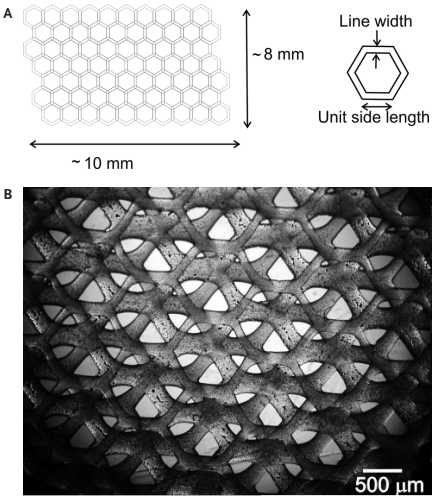

Figure 1. (A) CAD design of one layer of the hexagonal scaffold showing approximate total dimensions which define the nominal area. On the right, the terms unit side length and line width are defined for one unit hexagon. (B) Optical micrograph of a 3-D PLGA scaffold.

Before cell seeding, to remove all traces of solvent, the scaffolds and films were placed in a desiccator under vacuum for at least 1 week, and then washed extensively with deionised water and dried in an oven at 50°C. Following this, the structures were placed in 24-well plates (Sarstedt, Verona, Italy) and sterilised using a standard hospital H_2O_2 Gas-Plasma protocol available at our clinical facilities. To promote cell attachment, 5 μg/cm^2 purified collagen, PureCol™ (INAMED, Leimuiden, The Netherlands), was pipetted over the structures and after 1-h incubation at 37°C, they were washed with PBS three times and equilibrated with fresh medium overnight in the incubator.

2.3 Bioreactor design and assembly

The multicompartment modular bioreactor (MCmB) bioreactor was developed to enable cell and tissue culture in a variety of configurations ([22] and Mazzei *et al.*, submitted). Its main characteristics are high flow rates and low wall shear stresses. In its simplest form, as used in this work, it is made of polydimethyldisiloxane (PDMS; Dow Corning, Italy), and has the same dimensions as a 24-microwell plate (15 mm diameter and 2 mL volume). A patented sloping roof ensures the absence of bubbles in the chamber. A finite element modeling (FEM) model of the cell culture chamber was developed to study the shear stress at the cell surface. Cosmos Floworks, a Solidworks™ (Dassault Systèmes SolidWorks Corp. Concord, MA, USA) extension, which allows fluid-dynamic FEM analysis as well as 3-D CAD was used for this purpose. In the fluid dynamic model we used the following system constants: viscosity, 10^{-3} Pa·s; fluid density, 1000 kg/m^3; medium flow rate, 250 μL/min; pressure, 1 atmosphere (760 mmHg); temperature, 37°C; and no slip boundary conditions. Figure 2A shows a 3-D representation of the chamber, and in Fig. 2B the velocity streamlines modelled using SolidWorks™ are drawn.

Three MCmB bioreactors were connected in parallel to a pump (Instec P720, Instec, Boulder, Colorado, USA) and a mixing chamber, which serves to facilitate assembly of the flow circuit, allows gaseous mixing and acts as a bubble trap. A flow rate of 250 μL/min was used in all experiments, and the average shear stress in the cell culture zone was calculated by fluid dynamic simulation. The maximum wall shear stress at the flow rate used was about 10^{-5} Pa.

In our experience, even small flow rates may damage hepatocytes. Therefore, all the cultures were protected with a thin coating of alginate as described in the section on cell culture. In the

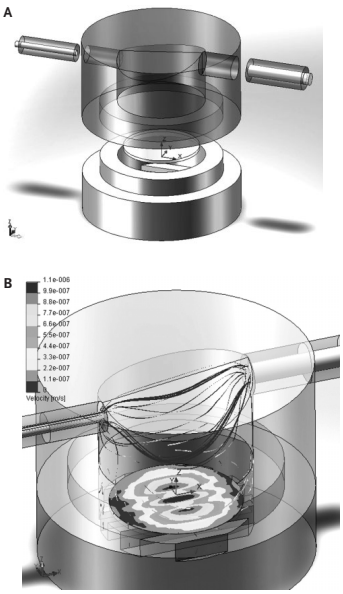

Figure 2. (A) A 3-D representation of the MCmB cell culture chamber, (B) velocity streamlines at a flow rate of 250 μL/min.

bioreactor experiments the medium was not changed since sufficient nutrients were present in the 10-mL closed loop circuit (2 mL in each bioreactor, 7 mL in the mixing chamber and about 1 mL in the tubing).

2.4 Cell culture

Since primary hepatocytes rapidly lose liver morphology and differentiated functions *in vitro*, in this study we used the HepG2 cell line as an alternative model cell. HepG2 cells maintain the main synthetic and endogenous functions of primary hepatocytes, as well some exogenous metabolic functions [23]. Furthermore, the HepG2 cell line is simple to culture and, by virtue of its immortality, it is possible to make standard comparisons that remain valid over time and for all experiments.

HepG2 human hepatoblastoma cells were a kind gift from Dr. S. Quarta, University of Padova. The cells were grown in Eagle's minimal essential medium (EMEM, 1 g/L glucose) supplemented with 5% foetal bovine serum, 1% non-essential amino acids, 1% EMEM vitamins, 2 mM L-glutamine, 100 U/mL penicillin and 100 μg/mL streptomycin in a humidified incubator at 37°C, 5% CO_2 (Heraeus SpA, Milan, Italy). The cells were all used at the same passage (no. 22 after receipt) and passaged using 0.05% trypsin with 0.02% EDTA in PBS (all reagents from Eurolone, Milan, Italy). Cells were seeded (100 000 cells/cm^2) on the films or scaffolds using 2 mL of complete medium per well. After 24 h, the structures were moved to a new microwell plate to eliminate interference from non-adherent cells.

Both scaffolds and films were coated with an alginate film consisting of 250 μL 1% sodium alginate dissolved in serum-free medium, cross-linked with 50 μL 1% $CaCl_2$ (both from Sigma-Aldrich, Milan, Italy). Excess alginate was removed with a pipette. The resulting film had a thickness of a few tens of microns as measured by an optical profilometer (Opto NCDT, model ILD1400-10, UK), having a nominal resolution of 1 μm. The profilometer uses a small laser spot (0.7 mm × 0.5 mm) which is reflected off a surface. Displacements were calibrated using an uncoated glass slide as a reference. The coating was not uniform and flat as observed by an optical microscope, and this was also reflected in the scatter of the profilometer readings across the slide (40–100 μm). At the low alginate concentrations used, the diffusion coefficient of oxygen and of small solutes is similar to that in water [24–26].

Finally, 2 mL fresh medium was added to each well to begin the experiment. Cells were maintained on the structures for a week and cell counting and medium collection was performed daily. The experiment was performed in triplicate using 21 structures, three samples were sacrificed for counting per day, and the culture medium was changed every third day.

2.5 Bioreactor culture

For the dynamic experiments, cells were seeded as described for the static cultures. At 24 h after seeding, the scaffolds were transferred to a glass slide, placed in the MCmB (one scaffold per bioreactor) and coated with an alginate film. The alginate coating was used to protect the cells from direct mechanical stress, while allowing adequate nutrient diffusion. The coating also stops the scaffolds from floating off the slides. Medium was perfused and re-circulated through the chambers at a flow rate of 250 μL/min. A total of 21 scaffolds were used for the bioreactor experiments. In particular, three bioreactors with three scaffolds were used per time point, and at the end of each time point the bioreactors were disassembled for cell counting and a final sample of medium collected. In addition, up to

200 μL media (50 μL per assay) was withdrawn from the mixing chambers for analysis at fixed intervals. All cell culture experiments were carried out in the same incubator.

2.6 Cell analysis and assays

2.6.1 Cell viability and density

At the end of each time period, the cells adhered on the structures were trypsinised off the scaffolds and membranes and counted using a Burker chamber. Cell viability was evaluated using trypan blue exclusion, and this was always greater than 95%. To ensure that all cells had been accounted for, the scaffolds were also stained with trypan blue and typically only a few cells were observed on the scaffolds after trypsinisation. Cell morphology was assessed using an optical microscope (AX70, Olympus Italia, Milan).

Because the 3-D scaffolds are composed of three layers of hexagons, the "true" area available for cell adhesion is difficult to estimate. According to the CAD model shown in Fig. 1A, the total surface area of one layer of the scaffold is about 0.06 cm^2; however, a 3-D scaffold may also have adhesive surfaces in more than one plane. Therefore, we use the term "nominal area" to refer to the overall area of the scaffold or film. Cell densities are expressed as the total number of cells counted divided by the nominal 2-D surface area of the samples. The PAM scaffolds have a nominal surface area of 0.8 cm^2 and a large percentage of this is free space of the pores, while the spin-coated films have an area of 1.33 cm^2.

2.6.2 Biochemical assays

Albumin production, which characterises the specific functional activity of liver cells, was measured by an enzyme-linked immunosorbent assay (ELISA) (Bethyl Laboratories, Montgomery, TX, USA). A standard curve was made using purified human albumin under the conditions recommended by the manufacturer. Species specificity of the anti-human albumin antibodies was verified using foetal bovine serum (FBS). Glucose consumption and urea production were quantified using commercial enzymatic kits according to the manufacturers' instructions (Megazyme International Poncarale, Italy, and Urea Kit, Sigma-Aldrich, respectively). To compare data from different experiments with different cell numbers and media volumes the glucose, albumin and urea data were expressed as quantities consumed or produced per cell per day, and therefore as rates, not cumulative quantities.

2.7 Statistical analysis

Statistical analysis was performed using analysis of covariance (ANCOVA) for comparison of trends (Matlab Statistics Toolbox, The MathWorks Inc.); a p value of less than 0.05 was considered statistically significant. Each data point is represented as the mean and SD of three samples and at each time point three scaffolds were analysed destructively (by trypsinisation) for cell counting.

3 Results

3.1 Comparison between 2-D films and 3-D scaffolds in static culture

As shown in Fig. 3, the cell density was higher on the scaffolds than on films particularly from day 4 onwards (ANCOVA, $p<0.01$). The cells seeded on 3-D structures proliferated throughout the duration of the experiment and the rate of increase was modulated by the media changes (day 3 and 6), whereas the cells seeded on 2-D films proliferated until the day 4 and the rate of increase did not appear to be influenced by the media changes (day 3 and 6). This could be due to removal of loosely adherent cells when the medium was aspirated.

Figure 4 shows the glucose consumption rate. Glucose was consumed at a constant rate (5.2 ± 0.3 ng/cell per day, $p=0.004$, ANCOVA) by cells seeded on 3-D scaffolds and the consumption was not influenced by the continuous cell proliferation in three dimensions. The cells on the 2-D films consumed a higher quantity of glucose than 3-D scaffolds in the first 2 days. After this period, the glucose consumption per cell was constant and similar to that of the 3-D scaffolds. The initial high glucose consumption by cells seeded on polymeric films does not seem to depend on the rate of prolif-

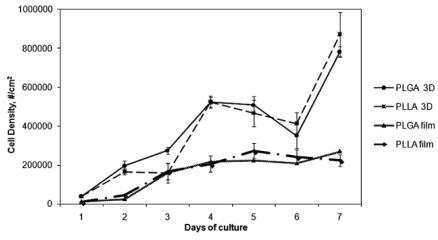

Figure 3. Cell density (defined as cell number/nominal surface area in cm^2) for 2-D PLGA and PLLA films, 3-D PLGA and PLLA scaffolds ($n=3$ per data point).

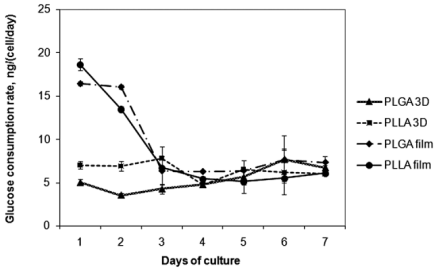

Figure 4. Glucose consumption rate in static conditions in 2-D films and 3-D scaffolds of PLGA and PLLA (n=3 per data point).

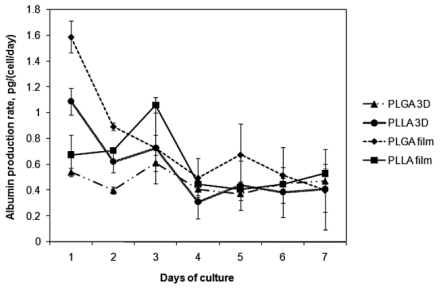

Figure 5. Albumin production rate in static conditions for 2-D films and 3-D scaffolds of PLGA and PLLA (n=3 per data point).

eration but could represent increased energetic requirements due to cell-matrix interactions. In fact, 2-D films present a large surface area to the cells for adhesion, whereas the 3-D scaffold is more porous and there are fewer adhesive sites per unit area. Once the adhesion process is over, all cells converge to a constant glucose consumption rate.

Albumin is one of the functional marker proteins of the liver. Human albumin was produced in similar quantities by 3-D scaffolds and 2-D films during the experiment (Fig. 5), and the production rates are similar to those reported in [23, 27]. An analysis of the production rates using ANCOVA indicated that the albumin production rate was higher in the first 2 days than on subsequent days (days 1–2: 0.82 ± 0.32 pg/cell per day, days 4–7: 0.49 ± 0.05 pg/cell per day, p<0.05). Although the cell proliferation rate was higher on the 3-D scaffolds than on the 2-D films, we found no differences in cell behaviour with respect to the two polymers. PLGA and PLLA are known to have different surface and mechanical properties, and this result implies that in our experiments only the microtopology influences cell proliferation and not the differences in physico-chemical properties between the polymers.

3.2 3-D scaffolds in dynamic conditions in the MCmB

Having established that 3-D scaffolds can increase the cell density consistently for up to 7 days, the next step was to select the polymer to be used. Since there were no significant cell metabolic and proliferative differences between the two polymers, PLGA was selected for successive experiments because of its deposition characteristics. The choice was based on the fact that 20% PLGA is slightly more viscous than 10% PLLA, and the scaffolds obtained using the PAM system are of higher fidelity than the corresponding PLLA scaffolds [28].

For each time point three bioreactors were set up in parallel with one 3-D scaffold per chamber. In the bioreactors, the cell density increased smoothly over time, as the peaks due to media changes were absent, and density values were similar to those in static conditions (Fig. 6).

Glucose consumption was slightly higher in the MCmB with a constant consumption rate of 7.6 ± 0.1 ng/cell per day (p=0.0001 ANCOVA) with respect to the 3-D scaffold in static conditions (5.2 ± 0.2 ng/cell per day, p=0.001, ANCOVA) (Fig. 7). Therefore, the cell energy requirements are greater in the bioreactor, and glucose is used as a substrate. This may be due to an up-regulation of liver-specific synthetic function in the bioreactor, as shown in Fig. 8; a large increase in albumin production rate per cell was observed in dynamic culture. In the first 2 days, the albumin production rate was ten times higher in the MCmB than in static

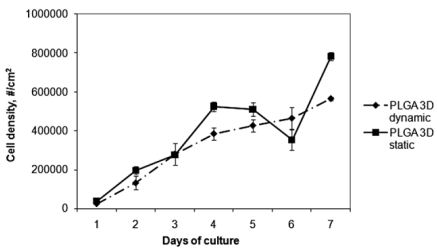

Figure 6. Cell density (defined as cell number/nominal surface area in cm^2) for PLGA scaffolds in the bioreactor and in static conditions (n=3 per data point).

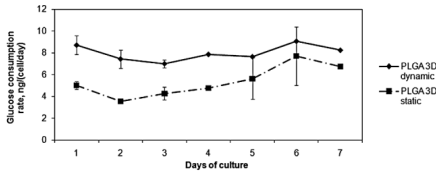

Figure 7. Glucose production rate in static and dynamic conditions for PLGA 3-D scaffolds (n=3 per data point).

conditions and then decreased progressively, maintaining a value four to five times greater than in static culture. In fact, the average albumin production rate in the bioreactor over the 7 days was 3.12 ± 0.43 pg/cell per day, compared with 0.65 ± 0.16 pg/cell per day (p=0.02, ANCOVA) in the scaffolds in static conditions.

To ensure that the increased albumin production rate was not due to the increased volume of medium in the bioreactor, a final experiment was performed using 3-D scaffolds cultured in 50-mm petri dishes in which the total medium volume was 10 mL. The albumin production rate was 0.50 ± 0.14 pg/cell per day over the 2-day period of analysis, indicating that the volume of medium does not influence the secretion rate of this protein in static conditions.

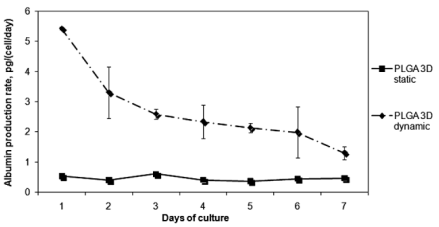

Figure 8. Albumin production rate in static and dynamic conditions for PLGA 3-D scaffolds (n=3 per data point).

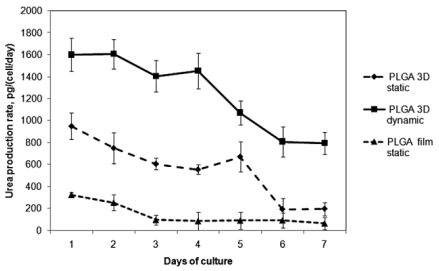

Figure 9. Urea production rate in static conditions for PLGA 2-D films and 3-D scaffolds and in dynamic conditions for PLGA 3-D scaffolds (n=3 per data point).

Figure 9 shows the that urea production rate, indicative of an intact nitrogen metabolism pathway, is significantly enhanced in the dynamic 3-D culture with respect to both the 2-D and 3-D static conditions. In static conditions, the 2-D films and 3-D scaffolds converged to the same production rate towards the end of the culture period (136 ± 101 pg/cell per day), while the average urea production rate in the bioreactor was significantly higher throughout the experiment (559 ± 71 pg/cell per day for the 3-D scaffolds in static conditions compared to 1248 ± 71 pg/cell per day for the 3-D scaffolds in dynamic conditions; p<0.00001, ANCOVA).

We also monitored the macroscopic morphology of the cells on the 3-D scaffolds and 2-D films (Fig. 10). Although we found little difference between cell morphology and spreading on scaffolds in the dynamic and static cultures, the cells grown for 5 days on 2- and 3-D surfaces were quite different. On the films, cells were spread evenly and typically had larger dimensions than on the 3-D substrates, and even after 5 days free spaces between cells were apparent. This indicates greater cell-substrate interaction than cell-cell contact on the films. Cultures grown on 3-D scaffolds spread and migrated into the structure so that even the voids were colonised. The cells were closely packed, and smaller, forming aggregates. This is indicative of greater interactions between adjacent cells. Therefore, even though the quantity of solid substrate is minimal, the cells seeded on the 3-D scaffolds assemble in the pores to maximise cell-cell interaction and cell density.

4 Discussion

Hepatocytes, like all cells, are dramatically affected by the physical and chemical nature of their microenvironment. This is one of the reasons why *in vitro* cell culture experiments are so difficult to compare from laboratory to laboratory. The hepatic cell habitat comprises three main features, or cues, which are known to influence cell behaviour; the biochemistry, the architecture and the supply of nutrients to meet the metabolic demands of the cells. In this work we investigated two of the main cues known to influence hepatocyte function, a 3-D topology and convective flow.

Several investigators have shown that cell culture in three dimensions represents a more physiologically relevant environment. However, the extent to which this influences hepatocyte function

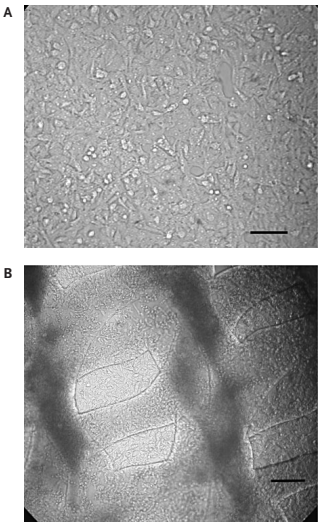

Figure 10. Micrographs of HepG2 cells on (A) PLGA film, and (B) 3-D PLGA scaffold after 5 days in culture. The bar indicates 50 μm.

with respect to the provision of oxygen and other nutrients is unclear. Moreover, the relationship between the topological features of a scaffold and hepatic function has not been studied in depth. As far as HepG2 cells are concerned, our results show that the main contribution of the scaffold is to increase cell density and to promote the formation of aggregates, which allows greater cell-cell contact with respect to cell-substrate interactions. Thus, we observed a large increase in the number of cells per unit area, but the expression of albumin per cell was the same as on a monolayer, as was the glucose consumption rate per cell, while the urea production rates also converged to similar values after 5 days in culture. Similar results have also been reported by Glicklis *et al.* [29] and Bokhari *et al.* [30].

On the other hand, convective transport is often mandatory in 3-D scaffolds, especially if they are thicker than a few hundred microns. Indeed, bioreactors for hepatocyte culture are generally designed for allowing adequate mass transfer to high density 3-D cultures in porous sponges or encapsulated spheroids. One of the main engineering issues in bioreactors for *in vitro* liver models is the balance between high mass transfer and low wall shear stress to cells. There appears to be some debate on the effects of shear stress on hepatocytes. Some papers cite extremely high values of shear (0.5 Pa [31]) and some also report on enhancement of cytochrome expression in conditions of fairly high shear stress [32]. Other investigators cite somewhat lower values of maximum shear stress that these cells can support (0.03 Pa [33]), even in the presence of non-parenchymal cells, which afford support and protection. The application of direct fluid flow parallel to the cell surface is certainly not physiological, since hepatocytes are not in direct contact with flowing blood in capillaries. In this context, Wang and Tarbell's model [34] is often cited to justify direct shear stress on cells of the order of 0.1 Pa [9]. These values should be applied with caution as some models predict even lower values of wall shear from porous flow [35]. Here, we effectively shield the cells from the effect of direct flow, although the highly permeable alginate coating allows low velocity porous or percolative flow perpendicular to the convective flow provided by the pumps. This flow is similar to interstitial flow [7], and allows the passage of essential nutrients and catabolites thanks to concentration gradients established between the scaffold and the moving fluid. In the bioreactor then, the cell density on 3-D scaffolds remains unchanged with respect to static cultures, but the metabolic and synthetic function in the form of albumin and urea production rates per cell are greatly enhanced, as reported in Figs. 6–9. Similar results have also been reported for 2-D cultures in dynamic and static conditions [27, 36], suggesting that these observations can also be generalised to 2-D systems.

The objective of this work was to recreate a biomimetic environment for hepatocytes and to determine, first singly and then together, the influence of a 3-D porous architecture and enhanced mass transport on liver cultures. HepG2 cells were initially studied on 2-D polymeric membranes and 3-D scaffolds. The results of this first stage demonstrated that the 3-D scaffolds promote cell proliferation, such that final cell densities are significantly higher than on 2-D surfaces. Other metabolic parameters were unchanged, indicating that the baseline metabolic cell function was unaltered. While the endogenous synthetic and metabolic functions (glucose consumption rate, albumin and urea production rates) of hepatocytes do not appear to be significantly related to cell morphology and 3-D organisation, this does not necessarily mean that all functions are unaltered in three dimensions. In fact, Bokhari *et al.* [30] observe an increase in exogenous metabolic function in HepG2 cells on 3-D scaffolds with respect to 2-D cultures, while the endogenous functions are unaltered. In the second phase of experiments, the scaffolds were placed a bioreactor and culture medium was pumped

through the system in a closed-loop. Neither cell proliferation nor glucose consumption rate per cell increased significantly with respect to the scaffolds in static conditions, but protein synthesis rates increased dramatically about four- to tenfold, and urea production rates by two- to fivefold. These experiments established then that 3-D HepG2 cultures in a dynamic environment are metabolically more efficient than static monolayer hepatocyte cultures and that the critical factor that drives endogenous metabolism in our experiments is the interstitial-like flow.

Our results demonstrate that, to more closely approximate functional hepatic tissue, it is important to give to cells two important stimuli, the topographical and the physical stimulus. The microtopology and porosity of the 3-D scaffolds increases cell density due to the formation of cell/cell aggregates, thus maximising cell-cell interactions. The second stimulus is produced by the flow of culture medium in the bioreactor which contributes to an increased metabolic turnover. Although the hepatocytes are protected from direct open channel flow by a thin coating of gel, the flow allows a sustainable supply of nutrients to the cells, as well as a physical stimulus in the form of indirect interstitial-like flow.

The authors have declared no conflict of interest.

5 References

[1] Guillouzo, A., Liver cell models in *in vitro* toxicology. *Environ. Health Perspect.* 1998, *106*, 551–532.

[2] Ahluwalia, A., Minieri, M., Dinardo, P., Engineering the stem cell niche: Technologies and tools for applying biochemical, physical and structural stimuli and their effects on stem cells, in: Artmann, G. M., Jürgen, H., Minger, S. (Eds), *Stem Cell Engineering*, Vol. 1: *Principles*, Springer, Berlin 2009, in press.

[3] Pichard-Garcia, L., Gerbal-Chaloin, S., Ferrini, J., Fabre, J. *et al.*, Use of long-term cultures of human hepatocytes to study cytochrome P450 gene expression. *Methods Enzymol.* 2002. *357*, 311–321.

[4] Harada, K., Mitaka, T., Miyamoto, S., Sugimoto, S. *et al.,* Rapid formation of hepatic organoid in collagen sponge by rat small hepatocytes and hepatic nonparenchymal cells. *J. Hepatol.* 2003, *39*, 716–723.

[5] Chen, J., Yu, S., Hsu, B. R., Fu, S. H., Loofa sponge as a scaffold for the culture of human hepatocyte cell line. *Biotechnol. Prog*. 2003, *19*, 522–527.

[6] Underhill, G. H., Chen, A. A., Albrecht, D. R., Bhatia, S. N., Assessment of hepatocellular function within PEG hydrogels. *Biomaterials* 2007, *28*, 256–270.

[7] Rutkowski, J. M., Swartz, M. A., A driving force for change: interstitial flow as a morphoregulator, 2006. *Trends Cell Biol.* 2006, *17*, 45–50.

[8] Catapano, G., De Bartolo, L., The importance of the kinetic characterization of liver cell metabolic reactions to the design of hybrid liver support devices. *Int. J. Artif. Organs* 1996, *19*, 670–676.

[9] Powers, M. J., Domandsky, K., Kaazempur-Mofrad, M. R., Kalezi, A. *et al.,* A microfabricated array bioreactor for perfused 3D liver culture. *Biotechnol. Bioeng*. 2002, *78*, 257–269.

[10] Powers, M. J., Janigian, D., Baker, C., Wack, K. *et al.,* Functional behavior of primary rat liver cells in a 3D perfused microarray bioreactor. *Tissue Eng,* 2002, *8*, 499–513.

[11] Hongo, T., Kajikawa, M., Ishida, S., Ozawa, S. *et al.,* Three-dimensional high-density culture of HepG2 Cells in a 5-mL radial-flow bioreactor for construction of artificial liver. *J. Biosci. Bioeng.* 2005, *99*, 237–244.

[12] Kataoka, K., Nagao, Y., Nukui, T., Akiyama, I. *et al.,* An organic-inorganic hybrid scaffold for the culture of HepG2 in a bioreactor. *Biomaterials* 2005, *26*, 2509–2516.

[13] Bhatia, S., Yarmush, M., Toner, M., Controlling cell interactions by micropatterning in co-cultures: Hepatocytes and 3T3 fibroblasts. *J. Biomed. Mater. Res.* 1997, *34*, 189–199.

[14] Khetani, S. R., Szulgit, G., Del Rio, J. A., Barlow, C., Bhatia, S., Exploring interactions between rat hepatocytes and nonparenchymal cells using gene expression profiling. *Hepatology* 2004, *40*, 545–554.

[15] Park, J., Berthiaume, F., Toner, M., Yarmush, M. L. *et al.,* Microfabricated grooved substrates as platforms for bioartificial liver reactors. *Biotechnol. Bioeng*. 2005, *90*, 632–644.

[16] Park, J., Li, Y., Berthiaume, F., Toner, M. *et al.,* Radial flow hepatocyte bioreactor using stacked microfabricated grooved substrates. *Biotechnol. Bioeng.* 2008, *99*, 455–467.

[17] Berthiaume, F., Moghe, P. V., Toner, M., Yarmush, M. L., Effect of extracellular matrix topology on cell structure, function, and physiological responsiveness: Hepatocytes cultured in a sandwich configuration. *FASEB J.* 1996, *10*, 1471–1484.

[18] Vozzi, G., Previti, A., De Rossi, D., Ahluwalia, A., Microsyringe-based deposition of two-dimensional and three-dimensional polymer scaffolds with a well-defined geometry for application to tissue engineering. *Tissue Eng.* 2002, *8*, 1089–1098.

[19] Vozzi, G., Ahluwalia A., Rapid prototyping for tissue engineering applications, in: Chu, P. K., Liu,, X. (Eds.), *Biomaterials Fabrication and Processing Handbook,* CRC Press, Boca Raton 2008, pp. 95–114.

[20] Mariani, M., Rosatini, F., Vozzi, G., Previti, A. *et al.,* Characterisation of tissue engineering scaffolds microfabricated with PAM. *Tissue Eng.* 2006, *12*, 547–558.

[21] Bhunchet, E., Wake, K., The portal lobule in rat liver fibrosis: A re-evaluation of the liver unit. *Hepatology* 1998, *27*, 481–487.

[22] Mazzei, D., Vozzi, F., Cisternino, A., Vozzi, G. *et al.,* A high-throughput bioreactor system for simulating physiological environments. *IEEE Trans. Ind. Electron.* 2008, *55*, 3273–3280.

[23] Bouma, M. E., Rogier, E., Verthier, N., Labarre, C. *et al.,* Further cellular investigation of the human hepatoblastoma-derived cell line HepG2: Morphology and immunocytochemical studies of hepatic-secreted proteins. *In vitro Cell. Dev. Biol.* 1989, *25*, 267–275.

[24] Oyaas, J., Storrø, I., Svendsen, H., Levine, D. W., The effective diffusion coefficient and the distribution constant for small molecules in calcium-alginate gel beads. *Biotechnol. Bioeng*. 1995, *47*, 492–500.

[25] Grassi, M., Colombo, I., Lapasin, R., Experimental determination of the theophylline diffusion coefficient in swollen sodium-alginate membranes. *J. Control Release*. 2001, *76*, 93–105.

[26] Venancio, A., Teixeira, J. A., Characterization of sugar diffusion coefficients in alginate membranes. *Biotechnol. Tech.* 1997, *11*, 183–186.

[27] Guzzardi, M. A., Vozzi, F., Ahluwalia, A., Study of the crosstalk between hepatocytes and endothelial cells using a novel multi-compartmental bioreactor: a comparison between connected cultures and co-cultures, *Tissue Eng. A* 2009, in press, http://dx.doi.org/10.1089/ten.te.2009.0695.

[28] Vozzi, G., Ahluwalia, A., Microfabrication for tissue engineering: rethinking the cells-on-a-scaffold approach. *J. Mater. Chem.* 2007, *17*, 1248–1254.

[29] Glicklis, R., Shapiro, L., Agbaria, R. Merchuk, J. C. *et al.,* Hepatocyte behavior within three-dimensional porous alginate scaffolds. *Biotechnol. Bioeng*. 2000, *6*, 344–353.

[30] Bokhari, M., Carnachan, R. J., Cameron, N. R., Przyborski, S. A., Culture of HepG2 liver cells on three dimensional polystyrene scaffolds enhances cell structure and function during toxicological challenge. *J. Anat*. 2007, *211*, 567–576.

[31] Tanaka, Y., Yamato, M., Okano, T., Kitamori, T. *et al.,* Evaluation of effects of shear stress on hepatocytes by a microchip-based system. *Meas. Sci. Technol*. 2006, *17*, 3167–3170.

[32] Mufti, N. A., Shuler, M. L., Induction of cytochrome P-450IA1 activity in response to sublethal stresses in microcarrier-attached Hep G2 cells. *Biotechnol. Prog*. 1995, *11*, 659–663.

[33] Tilles, A. W., Baskaran, H., Roy, P, Yarmush, M. L. *et al.,* Effects of oxygenation and flow on the viability and function of rat hepatocytes cocultured in a microchannel flat-plate bioreactor. *Biotechnol. Bioeng.* 2001, *73*, 379–389.

[34] Wang, D. M., Tarbell, J. M., Modeling interstitial flow in an artery wall allows estimation of wall shear stress on smooth muscle cells. *J. Biomech. Eng.* 1995, *117*, 358–363.

[35] Boschetti, F., Raimondi, M., Migliavacca, F., Dubini G., Prediction of the micro-fluid dynamic environment imposed to three-dimensional engineered cell systems in bioreactors. *J. Biomech.* 2006, *39*, 418–425.

[36] Vozzi, F., Heinrich, J. M., Bader, A., Ahluwalia, A. D., Connected culture of murine hepatocytes and HUVEC in a multicompartmental bioreactor. *Tissue Eng. A* 2009, *15*, 1291–1299.

Bibliography

[1] Burbaum JJ and Sigal NH. New technologies for high-throughput screening. *Curr Opin Chem Biology*, 1(1):72–78, June 1997.

[2] Philip J. Lee Paul J. Hung. *Continuous Perfusion Microfluidic Cell Culture Array for High Throughput Cell-Based Assays.* Wiley InterScience, December 2004.

[3] S.K Tingley. High-throughput cell culture: A real-world evaluation. In *Innovations in pharmaceutical technology*, 2006.

[4] S. B. McMahon and J. G. Monroe. Role of primary response genes in generating cellular responses to growth factors. *FASEB J*, 6(9):2707–2715, Jun 1992.

[5] R. Graber, C. Sumida, and E. A. Nunez. Fatty acids and cell signal transduction. *J Lipid Mediat Cell Signal*, 9(2):91–116, Mar 1994.

[6] Friedemann Kiefer, Wolfgang F Vogel, and Ruediger Arnold. Signal transduction and co-stimulatory pathways. *Transpl Immunol*, 9(2-4):69–82, May 2002.

[7] Sven Schmalzriedt, Marc Jenne, Klaus Mauch, and Matthias Reuss. Integration of physiology and fluid dynamics. *Adv Biochem Eng Biotechnol*, 80:19–68, 2003.

[8] Michael H Hsieh and Hiep T Nguyen. Molecular mechanism of apoptosis induced by mechanical forces. *Int Rev Cytol*, 245:45–90, 2005.

[9] Barry M Prior, H. T. Yang, and Ronald L Terjung. What makes vessels grow with exercise training? *J Appl Physiol*, 97(3):1119–1128, Sep 2004.

[10] Kenneth A Myers, Jerome B Rattner, Nigel G Shrive, and David A Hart. Hydrostatic pressure sensation in cells: integration into the tensegrity model. *Biochem Cell Biol*, 85(5):543–551, Oct 2007.

[11] Various. Animal testing statistics in europe.

[12] Various. Home office statistics on procedures on living animals.

[13] Y. Chen. A perfusion system for high productivity of monoclonal antibody by hybridoma cells in a celligen bioreactor. *Chin J Biotechnol*, 8(3):179–186, 1992.

[14] S. Mercille, M. Johnson, S. Lanthier, A. A. Kamen, and B. Massie. Understanding factors that limit the productivity of suspension-based perfusion cultures operated at high medium renewal rates. *Biotechnol Bioeng*, 67(4):435–450, Feb 2000.

[15] M. Reuss. Stirred tank bioreactors. *Bioprocess Technol*, 21:207–255, 1995.

[16] Dianliang Wang, Wanshun Liu, Baoqin Han, and Ruian Xu. The bioreactor: a powerful tool for large-scale culture of animal cells. *Curr Pharm Biotechnol*, 6(5):397–403, Oct 2005.

[17] J. P. Tharakan, S. L. Gallagher, and P. C. Chau. Hollow-fiber bioreactors for mammalian cell culture. *Adv Biotechnol Processes*, 7:153–184, 1988.

[18] Jung-Keug Park and Doo-Hoon Lee. Bioartificial liver systems: current status and future perspective. *J Biosci Bioeng*, 99(4):311–319, Apr 2005.

[19] Ritu Saxena, George Pan, and Jay M McDonald. Osteoblast and osteoclast differentiation in modeled microgravity. *Ann N Y Acad Sci*, 1116:494–498, Nov 2007.

[20] Mark J Powers, Dena M Janigian, Kathryn E Wack, Carolyn S Baker, Donna Beer Stolz, and Linda G Griffith. Functional behavior of primary rat liver cells in a three-dimensional perfused microarray bioreactor. *Tissue Eng*, 8(3):499–513, Jul 2002.

[21] Harry L T Lee, Paolo Boccazzi, Rajeev J Ram, and Anthony J Sinskey. Microbioreactor arrays with integrated mixers and fluid injectors for high-throughput experimentation with ph and dissolved oxygen control. *Lab Chip*, 6(9):1229–1235, Sep 2006.

[22] Bill Evjen, Kent Sharkey, Thiru Thangarathinam, and Michael Kay and. *Professional XML*. Willey Publishing, 2007.

[23] Ahluwalia A. and Vozzi G. PI2006A000121. Bioreattori bi-e tridimensionali highthroughput sensorizzati e/o dotati da sistemi di filtrazione e di trasduzione ed attuazione. Italian. November 2006.

[24] Crown Industrial Estate. Ntc thermistors: type ng glass encapsulated chit thermistor.

[25] Honeywell. Airflow sensors awm3000 series microbridge mass airflow/amplified.

[26] Phidgets inc. Phidjets product manual 1115 - gas pressure sensor.

[27] Hamilton. Hamilton biotrode ph probe.

[28] Phidgets inc. 1125 - humidity/temperature sensor.

[29] Phidgets inc. 1018 - phidgetinterfacekit 8/8/8 data sheet.

[30] Phidgets inc. 1121 - voltage divider data sheet.

[31] Phidgets inc. 1058 - phidgetphsensor data sheet.

[32] Inc Building Automation Products. Understanding 4-20 ma current loops.

[33] SMC. Itv0000 series data sheet.

[34] Phidgets inc. 3051 - dual relay board data sheet.

[35] Pololu. Micro dual serial motor controller data sheet.

[36] Phidgets inc. 1014 - phidgetinterfacekit 0/0/4 data sheet.

[37] RS Components. Cartidge heater.

[38] Christen J. B. and Andreou A. G. Hybrid silicon/silicone (polydimethylsiloxane) microsystem for cell culture. In *28th Annual International Conference of the IEEE Engineering in Medicine and Biology Society*, 2006.

[39] Houcine Hassan et all. Remote laboratory architecture for the validation of industrial control applications. In IEEE transactions on industrial electronics, editor, *IEEE transactions on industrial electronics*, volume 54-6, 2007.

[40] J.B. Christen and A.G. Andreou. Design, fabrication, and testing of a hybrid cmos/pdms microsystem for cell culture and incubation, biomedical circuits and systems. In *IEEE Transactions on*, 2007.

[41] Omega Catalogs. Kapton insulated flexible heaters data sheet.

[42] Michele Silvestri. Sviluppo di un sistema di termostatazione per celle a flusso. Master's thesis, Facolt di ingegneria, Univerist di Pisa, 2007.

[43] Cisternino A., D. Colombo, G. Ennas, and D. Picciaia. Robotics4.net: software body for controlling robots. *IEE Proceedings -Software*, 152(5):215–222, October 7, 2005.

[44] Dong To Nguyen, Sang-Rok Oh, and Bum-Jae You. A framework for internet-based interaction of humans, robots, and responsive environments using agent technology. *IEEE Trans. Ind. Electron.*, 52(6):1521–1529, December 2005.

[45] Robert Pickering. *Foundations of F#*. APress, 2007.

[46] Don Syme, Adam Granicz, and Antonio Cisternino. *Expert F#*. APress, 2007.

[47] Henson M. A. and Seborg D. E. Adaptive nonlinear control of a ph neutralization process. *IEEE Trans. Control Syst. Technol.*, 2(3):169–182, September 1994.

[48] R. HEINRICH and S. M. RAPOPORT. Metabolic regulation and mathematical models. *Proq. Biophys. Molec. Biol.*, 32:1 82, 1977.

[49] E.Boerger and R. Staerk. *Abstract State Machines - A Method for High-Level System Design and Analysis*. Springer Verlag, 2003.

[50] V. Gervasi and D. Mazzei. Using abstract state machines in modeling biological systems. In *GNB 2008 Proceedings*, 2008.

[51] Valentina Resta, Elena Novelli, Giovanni Vozzi, Cristiano Scarpa, Matteo Caleo, Arti Ahluwalia, Anna Solini, Eleonora Santini, Vincenzo Parisi, Francesco Di Virgilio, and Lucia Galli-Resta. Acute

retinal ganglion cell injury caused by intraocular pressure spikes is mediated by endogenous extracellular atp. *Eur J Neurosci*, 25(9):2741–2754, May 2007.

[52] XIAMEN OCULAR. Gdm1602k lcd parallel display.

[53] Arduino. Arduino reference and guide.

[54] Atmel inc. Atmega 168 data sheet.

[55] Analog Devices. 7812 datasheet.

[56] Analog Devices. 7912 datasheets.

[57] Fairchild Semiconductor. 7805 datasheet.

[58] National Semiconductors. Lm338 datasheet.

[59] Allegro MicroSystems. A3967 microstepping driver with translator.

[60] C. De Maria, A. Tirella, A. Ahluwalia, and G. Vozzi. Pneumatic module of pam2 microfabrication system: realization of bio-inspired complex scaffolds. In 3B, editor, *3B'09*, July 2009.

[61] Crouzet. Linear actuator stepper motor.

[62] Aaron Chen, Rajesh Chitta, David Chang, and Ashraf Amanullah. Twenty-four well plate miniature bioreactor system as a scale-down model for cell culture process development. *Biotechnol Bioeng*, 102(1):148–160, Jan 2009.

[63] Paul A Janmey and Christopher A McCulloch. Cell mechanics: integrating cell responses to mechanical stimuli. *Annu Rev Biomed Eng*, 9:1–34, 2007.

[64] Qiang Fu, Changjing Wu, Yun Shen, Shucan Zheng, and Rui Chen. Effect of limk2 rnai on reorganization of the actin cytoskeleton in osteoblasts induced by fluid shear stress. *J Biomech*, 41(15):3225–3228, Nov 2008.

[65] S. Morelli and S. Salerno. Human hepatocyte functions in a galactosylated membrane bioreactor. *J Membrane Science*, 302:27–35, 2007.

[66] Ivan Martin, David Wendt, and Michael Heberer. The role of bioreactors in tissue engineering. *Trends Biotechnol*, 22(2):80–86, Feb 2004.

[67] A. Miyakawa, L.A.O. Dallan, S. Lacchini, T.F. Borin, and J.E. Krieger J. E. Human saphenous vein organculture under controlled hemodynamic conditions. 63(5):686.688, 2008.

[68] Kris Dumont, Jessa Yperman, Erik Verbeken, Patrick Segers, Bart Meuris, Stijn Vandenberghe, Willem Flameng, and Pascal R Verdonck. Design of a new pulsatile bioreactor for tissue engineered aortic heart valve formation. *Artif Organs*, 26(8):710–714, Aug 2002.

[69] Mark J Powers, Karel Domansky, Mohammad R Kaazempur-Mofrad, Artemis Kalezi, Adam Capitano, Arpita Upadhyaya, Petra Kurzawski, Kathryn E Wack, Donna Beer Stolz, Roger Kamm, and Linda G Griffith. A microfabricated array bioreactor for perfused 3d liver culture. *Biotechnol Bioeng*, 78(3):257–269, May 2002.

[70] L. De Bartolo, G. Jarosch-Von Schweder, A. Haverich, and A. Bader. A novel full-scale flat membrane bioreactor utilizing porcine hepatocytes: cell viability and tissue-specific functions. *Biotechnol Prog*, 16(1):102–108, 2000.

[71] Rgis Baudoin, Anne Corlu, Laurent Griscom, Ccile Legallais, and Eric Leclerc. Trends in the development of microfluidic cell biochips for in vitro hepatotoxicity. *Toxicol In Vitro*, 21(4):535–544, Jun 2007.

[72] Y. Tanaka, M. Yamato, T. Okano, T. Kitamori, and K. Sato. Evaluation of effects of shear stress on hepatocytes by a microchip-based system. *Meas. Sci. Technol*, 17:3167–3170, 2006.

[73] Rowena McBeath, Dana M Pirone, Celeste M Nelson, Kiran Bhadriraju, and Christopher S Chen. Cell shape, cytoskeletal tension, and rhoa regulate stem cell lineage commitment. *Dev Cell*, 6(4):483–495, Apr 2004.

[74] K. Francis and B. O. Palsson. Effective intercellular communication distances are determined by the relative time constants for cyto/chemokine secretion and diffusion. *Proc Natl Acad Sci U S A*, 94(23):12258–12262, Nov 1997.

[75] Betina Kerstin Lundholt, Kurt M Scudder, and Len Pagliaro. A simple technique for reducing edge effect in cell-based assays. *J Biomol Screen*, 8(5):566–570, Oct 2003.

[76] Michael W Toepke and David J Beebe. Pdms absorption of small molecules and consequences in microfluidic applications. *Lab Chip*, 6(12):1484–1486, Dec 2006.

[77] A. Guillouzo. Liver cell models in in vitro toxicology. *Environ Health Perspect*, 106 Suppl 2:511–532, Apr 1998.

[78] W. B. Coleman and S. C. Presnell. Plasticity of the hepatocyte phenotype in vitro: complex phenotypic transitions in proliferat-

ing hepatocyte cultures suggest bipotent differentiation capacity of mature hepatocytes. *Hepatology*, 24(6):1542–1546, Dec 1996.

[79] Yaakov Nahmias, Francois Berthiaume, and Martin L Yarmush. Integration of technologies for hepatic tissue engineering. *Adv Biochem Eng Biotechnol*, 103:309–329, 2007.

[80] P. T. Schumacker, N. Chandel, and A. G. Agusti. Oxygen conformance of cellular respiration in hepatocytes. *Am J Physiol*, 265(4 Pt 1):L395–L402, Oct 1993.

[81] U. J. Balis, K. Behnia, B. Dwarakanath, S. N. Bhatia, S. J. Sullivan, M. L. Yarmush, and M. Toner. Oxygen consumption characteristics of porcine hepatocytes. *Metab Eng*, 1(1):49–62, Jan 1999.

[82] N. A. Mufti and M. L. Shuler. Induction of cytochrome p-450ia1 activity in response to sublethal stresses in microcarrier-attached hep g2 cells. *Biotechnol Prog*, 11(6):659–663, 1995.

[83] Hideki Nakatsuka, Takaaki Sokabe, Kimiko Yamamoto, Yoshinobu Sato, Katsuyoshi Hatakeyama, Akira Kamiya, and Joji Ando. Shear stress induces hepatocyte pai-1 gene expression through cooperative sp1/ets-1 activation of transcription. *Am J Physiol Gastrointest Liver Physiol*, 291(1):G26–G34, Jul 2006.

[84] J. Park, Y. Li, M. Berthiaume, M. Toner, M.L. Yarmush, and A.W. Tilles. Radial flow hepatocyte bioreactor using stacked microfabricated grooved substrates. *Biotechnol Bioeng*, 99(2):455–467, 2007.

[85] A. W. Tilles, H. Baskaran, P. Roy, M. L. Yarmush, and M. Toner. Effects of oxygenation and flow on the viability and function of rat hepatocytes cocultured in a microchannel flat-plate bioreactor. *Biotechnol Bioeng*, 73(5):379–389, Jun 2001.

[86] F. Vozzi, J.M Heinrich, A. Bader, and A.D. Ahluwalia. Connected culture of murine hepatocytes and huvec in a multi-compartmental bioreactor. *Tissue Engineering*, Under Submission, 2009.

[87] Maria Angela Guzzardi, Federico Vozzi, and Arti Devi Ahaluwalia. Study of the cross-talk between hepatocytes and endothelial cells using a novel multi-compartmental bioreactor: a comparison between connected cultures and co-cultures. *Tissue Eng Part A*, Jun 2009.

[88] G. B. West, J. H. Brown, and B. J. Enquist. A general model for the origin of allometric scaling laws in biology. *Science*, 276(5309):122–126, Apr 1997.

[89] Bruna Vinci, Daniela Cavallone, Giovanni Vozzi, Daniele Mazzei, Claudio Domenici, Maurizia Brunetto, and Arti Ahluwalia. In vitro liver model using microfabricated scaffolds in a modular bioreactor. *Biotechnol J*, Oct 2009.

[90] Molly K Smith and David J Mooney. Hypoxia leads to necrotic hepatocyte death. *J Biomed Mater Res A*, 80(3):520–529, Mar 2007.

[91] John F Patzer. Oxygen consumption in a hollow fiber bioartificial liver–revisited. *Artif Organs*, 28(1):83–98, Jan 2004.

[92] Y. Xia and G.M Whitesides. Soft lithography. *Annu Rev Mater Sci*, 28:153–184, 1998.

[93] et all D. Mazzei. 0814034.5. Improved bioreactor chamber. Grain Bretain. 2009.

[94] Georgios Constantinides, Z. Ilke Kalcioglu, Meredith McFarland, James F Smith, and Krystyn J Van Vliet. Probing mechanical

properties of fully hydrated gels and biological tissues. *J Biomech*, 41(15):3285–3289, Nov 2008.

[95] A. Tirella. Alginate and collagen scaffolds mechanical propetries. 2009.

[96] P. O. Seglen. Hepatocyte suspensions and cultures as tools in experimental carcinogenesis. *J Toxicol Environ Health*, 5(2-3):551–560, 1979.

[97] Peggy Papeleu, Tamara Vanhaecke, Tom Henkens, Greetje Elaut, Mathieu Vinken, Sarah Snykers, and Vera Rogiers. Isolation of rat hepatocytes. *Methods Mol Biol*, 320:229–237, 2006.

[98] Navneeta Rajan, Jason Habermehl, Marie-France Cot, Charles J Doillon, and Diego Mantovani. Preparation of ready-to-use, storable and reconstituted type i collagen from rat tail tendon for tissue engineering applications. *Nat Protoc*, 1(6):2753–2758, 2006.

[99] Ching-Chou Wu, Shinn-Jyh Ding, Yao-Hsien Wang, Ming-Jer Tang, and Hsien-Chang Chang. Mechanical properties of collagen gels derived from rats of different ages. *J Biomater Sci Polym Ed*, 16(10):1261–1275, 2005.

[100] Joseph M Rutkowski and Melody A Swartz. A driving force for change: interstitial flow as a morphoregulator. *Trends Cell Biol*, 17(1):44–50, Jan 2007.

[101] Melody A Swartz and Mark E Fleury. Interstitial flow and its effects in soft tissues. *Annu Rev Biomed Eng*, 9:229–256, 2007.

[102] Jared W Allen, Salman R Khetani, and Sangeeta N Bhatia. In vitro zonation and toxicity in a hepatocyte bioreactor. *Toxicol Sci*, 84(1):110–119, Mar 2005.

[103] Giovanni Vozzi, Alfonsina Rechichi, Francesca Dini, Claudia Salvadori, Federico Vozzi, Silvia Burchielli, Fabio Carlucci, Mario Arispici, Gianluca Ciardelli, Paolo Giusti, and Arti Ahluwalia. Pam-microfabricated polyurethane scaffolds: in vivo and in vitro preliminary studies. *Macromol Biosci*, 8(1):60–68, Jan 2008.

[104] Bruna Vinci, Giovanni Vozzi, Angelo Avogaro, and Arti Ahluwalia. In-vitro engineering of the liver using multiple axis stimuli. *Biomedicine & Pharmacotherapy*, 62:492–493, 2008.

[105] G. Vozzi and A. Ahluwalia. Microfabrication for tissue engineering: rethinking the cells-on-a scaffold approach. *J. Mater. Chem.*, 17:1248–1254, 2007.

[106] M. E. Bouma, E. Rogier, N. Verthier, C. Labarre, and G. Feldmann. Further cellular investigation of the human hepatoblastoma-derived cell line hepg2: morphology and immunocytochemical studies of hepatic-secreted proteins. *In Vitro Cell Dev Biol*, 25(3 Pt 1):267–275, Mar 1989.

[107] J. Oyaas, I. Storr, H. Svendsen, and D. W. Levine. The effective diffusion coefficient and the distribution constant for small molecules in calcium-alginate gel beads. *Biotechnol Bioeng*, 47(4):492–500, Aug 1995.

[108] A. Venncio and J. A. Teixeira. Characterization of sugar diffusion coefficients in alginate membranes. *Biotechnology Techniques*, 11:183–186, 1997.

[109] H. Holtzer, J. Abbott, J. Lash, and S. Holtzer. The loss of phenotypic traits by differentiated cells in vitro, i. dedifferentiation of cartilage cells. *Proc Natl Acad Sci U S A*, 46(12):1533–1542, Dec 1960.

[110] Aileen Crawford and Sally C Dickinson. Chondrocyte isolation, expansion, and culture on polymer scaffolds. *Methods Mol Biol*, 238:147–158, 2004.

[111] D. Mazzei, A. Kwarciak, A. Crawford, and A. Ahluwalia. Mcmb bioreactor tests with condrocytes and fibroblasts under different flow rates and passages.

[112] S. Al-Nasiry, N. Geusens, M. Hanssens, C. Luyten, and R. Pijnenborg. The use of alamar blue assay for quantitative analysis of viability, migration and invasion of choriocarcinoma cells. *Hum Reprod*, 22(5):1304–1309, May 2007.

[113] R. W. Farndale, D. J. Buttle, and A. J. Barrett. Improved quantitation and discrimination of sulphated glycosaminoglycans by use of dimethylmethylene blue. *Biochim Biophys Acta*, 883(2):173–177, Sep 1986.

[114] V. C. Mow, A. Ratcliffe, and A. R. Poole. Cartilage and diarthrodial joints as paradigms for hierarchical materials and structures. *Biomaterials*, 13:67–97, 1992.

[115] I. C. Clarke. Surface characteristics of human articular cartilage–a scanning electron microscope study. *J. Anat.*, 108:23–30, Jan 1971.

[116] D. R. Eyre. Collagen: molecular diversity in the body's protein scaffold. *Science*, 207:1315–1322, Mar 1980.

[117] H. Muir, P. Bullough, and A. Maroudas. The distribution of collagen in human articular cartilage with some of its physiological implications. *J Bone Joint Surg Br*, 52:554–563, Aug 1970.

[118] H. Lipshitz, R. Etheredge, and M. J. Glimcher. Changes in the hexosamine content and swelling ratio of articular cartilage as functions

of depth from the surface. *J Bone Joint Surg Am*, 58:1149–1153, Dec 1976.

[119] Ronny Maik Schulz and Augustinus Bader. Cartilage tissue engineering and bioreactor systems for the cultivation and stimulation of chondrocytes. *Eur Biophys J*, 36(4-5):539–68, Apr 2007.

[120] N. M. Bachrach, W. B. Valhmu, E. Stazzone, A. Ratcliffe, W. M. Lai, and V. C. Mow. Changes in proteoglycan synthesis of chondrocytes in articular cartilage are associated with the time-dependent changes in their mechanical environment. *J Biomech*, 28:1561–1569, Dec 1995.

[121] F. Guilak, B. C. Meyer, A. Ratcliffe, and V. C. Mow. The effects of matrix compression on proteoglycan metabolism in articular cartilage explants. *Osteoarthr. Cartil.*, 2:91–101, Jun 1994.

[122] R. L. Sah, J. Y. Doong, A. J. Grodzinsky, A. H. Plaas, and J. D. Sandy. Effects of compression on the loss of newly synthesized proteoglycans and proteins from cartilage explants. *Arch. Biochem. Biophys.*, 286:20–29, Apr 1991.

[123] R. L. Sah, Y. J. Kim, J. Y. Doong, A. J. Grodzinsky, A. H. Plaas, and J. D. Sandy. Biosynthetic response of cartilage explants to dynamic compression. *J. Orthop. Res.*, 7:619–636, 1989.

[124] W. B. Valhmu, E. J. Stazzone, N. M. Bachrach, F. Saed-Nejad, S. G. Fischer, V. C. Mow, and A. Ratcliffe. Load-controlled compression of articular cartilage induces a transient stimulation of aggrecan gene expression. *Arch. Biochem. Biophys.*, 353:29–36, May 1998.

[125] J A Buckwalter. Articular cartilage injuries. *Clin Orthop Relat Res*, (402):21–37, Sep 2002.

[126] C R Chu, R D Coutts, M Yoshioka, F L Harwood, A Z Monosov, and D Amiel. Articular cartilage repair using allogeneic perichondrocyte-seeded biodegradable porous polylactic acid (pla): a tissue-engineering study. *J Biomed Mater Res*, 29(9):1147–54, Sep 1995.

[127] N S Dunkelman, M P Zimber, R G Lebaron, R Pavelec, M Kwan, and A F Purchio. Cartilage production by rabbit articular chondrocytes on polyglycolic acid scaffolds in a closed bioreactor system. *Biotechnol Bioeng*, 46(4):299–305, May 1995.

[128] M Sittinger, J Bujia, W W Minuth, C Hammer, and G R Burmester. Engineering of cartilage tissue using bioresorbable polymer carriers in perfusion culture. *Biomaterials*, 15(6):451–6, May 1994.

[129] S Wakitani, T Goto, R G Young, J M Mansour, V M Goldberg, and A I Caplan. Repair of large full-thickness articular cartilage defects with allograft articular chondrocytes embedded in a collagen gel. *Tissue Eng*, 4(4):429–44, 1998.

[130] Desmond F. Moore. *Principles and applications of tribology*. Pergamon Press, 1975.

[131] C. De Maria, G. Vozzi, C. Domenici, and A. Ahluwalia. A novel vascular bioreactor for remodelling and testing mechanical properties of blood vessels. In *Proc. IEEE International Symposium on Industrial Electronics ISIE 2007*, pages 2805–2809, June 4–7, 2007.

[132] Ralph L Sacco, Robert Adams, Greg Albers, Mark J Alberts, Oscar Benavente, Karen Furie, Larry B Goldstein, Philip Gorelick, Jonathan Halperin, Robert Harbaugh, S. Claiborne Johnston, Irene Katzan, Margaret Kelly-Hayes, Edgar J Kenton, Michael Marks, Lee H Schwamm, Thomas Tomsick, American Heart Association, American Stroke Association Council on Stroke, Council on Cardiovascular Radiology, Intervention, and American Academy of Neurology. Guidelines for prevention of stroke in patients with ischemic stroke or transient ischemic attack: a statement for healthcare professionals from the american heart association/american stroke association council on stroke: co-sponsored by the council on cardiovascular radiology and intervention: the american academy of neurology affirms the value of this guideline. *Stroke*, 37(2):577–617, Feb 2006.

[133] Theodora Szasz, Keshari Thakali, Gregory D Fink, and Stephanie W Watts. A comparison of arteries and veins in oxidative stress: producers, destroyers, function, and disease. *Exp Biol Med (Maywood)*, 232(1):27–37, Jan 2007.

[134] Dong-Chuan Guo, Christina L Papke, Rumin He, and Dianna M Milewicz. Pathogenesis of thoracic and abdominal aortic aneurysms. *Ann N Y Acad Sci*, 1085:339–352, Nov 2006.

[135] J. C. Choy, D. J. Granville, D. W. Hunt, and B. M. McManus. Endothelial cell apoptosis: biochemical characteristics and potential implications for atherosclerosis. *J Mol Cell Cardiol*, 33(9):1673–1690, Sep 2001.

[136] D. G. Harrison, J. Widder, I. Grumbach, W. Chen, M. Weber, and C. Searles. Endothelial mechanotransduction, nitric oxide and vascular inflammation. *J Intern Med*, 259(4):351–363, Apr 2006.

[137] Michel R Hoenig, Gordon R Campbell, Barbara E Rolfe, and Julie H Campbell. Tissue-engineered blood vessels: alternative to autologous grafts? *Arterioscler Thromb Vasc Biol*, 25(6):1128–1134, Jun 2005.

[138] Rebecca J Gusic, Richard Myung, Matus Petko, J. William Gaynor, and Keith J Gooch. Shear stress and pressure modulate saphenous vein remodeling ex vivo. *J Biomech*, 38(9):1760–1769, Sep 2005.

[139] V. Clerin, R. J. Gusic, J. O'Brien, P. M. Kirshbom, R. J. Myung, J. W. Gaynor, and K. J. Gooch. Mechanical environment, donor age, and presence of endothelium interact to modulate porcine artery viability ex vivo. *Ann Biomed Eng*, 30(9):1117–1127, 2002.

[140] A. Ahluwalia and G. Vozzi. Progress in bioengineering - technologies for regenerative medicine. *Biomedicine & Pharmacotherapy*, 60:468479, 2006.

[141] Federico Vozzi. *New bioreactor system for pharmacological tests.* PhD thesis, Scienze del farmaco e sostanze bioattive - University of Pisa, 2007.

[142] G. Vunjak-Novakovic, B. Obradovic, I. Martin, P. M. Bursac, R. Langer, and L. E. Freed. Dynamic cell seeding of polymer scaffolds for cartilage tissue engineering. *Biotechnol Prog*, 14(2):193–202, 1998.

[143] G. Vunjak-Novakovic, I. Martin, B. Obradovic, S. Treppo, A. J. Grodzinsky, R. Langer, and L. E. Freed. Bioreactor cultivation conditions modulate the composition and mechanical properties of tissue-engineered cartilage. *J Orthop Res*, 17(1):130–138, Jan 1999.

[144] N. Y. Afoke, P. D. Byers, and W. C. Hutton. Contact pressures in the human hip joint. *J Bone Joint Surg Br*, 69(4):536–541, Aug 1987.

[145] J. K. Suh, Z. Li, and S. L. Woo. Dynamic behavior of a biphasic cartilage model under cyclic compressive loading. *J Biomech*, 28(4):357–364, Apr 1995.

[146] B. Obradovic, R. L. Carrier, G. Vunjak-Novakovic, and L. E. Freed. Gas exchange is essential for bioreactor cultivation of tissue engineered cartilage. *Biotechnol Bioeng*, 63(2):197–205, Apr 1999.

[147] Debi P Mukherjee, Dollie F Smith, Shelia H Rogers, Janson E Emmanual, Kyle D Jadin, and Byron K Hayes. Effect of 3d-microstructure of bioabsorbable pga:tmc scaffolds on the growth of chondrogenic cells. *J Biomed Mater Res B Appl Biomater*, 88(1):92–102, Jan 2009.

[148] Ralph L Nachman and Eric A Jaffe. Endothelial cell culture: beginnings of modern vascular biology. *J Clin Invest*, 114(8):1037–1040, Oct 2004.

[149] E. A. Jaffe, R. L. Nachman, C. G. Becker, and C. R. Minick. Culture of human endothelial cells derived from umbilical veins. identification by morphologic and immunologic criteria. *J Clin Invest*, 52(11):2745–2756, Nov 1973.

[150] Jerome D Cohen. Overview of physiology, vascular biology, and mechanisms of hypertension. *J Manag Care Pharm*, 13(5 Suppl):S6–S8, Jun 2007.

[151] A. M. Malek, A. L. Greene, and S. Izumo. Regulation of endothelin 1 gene by fluid shear stress is transcriptionally mediated and inde-

pendent of protein kinase c and camp. *Proc Natl Acad Sci U S A*, 90(13):5999–6003, Jul 1993.

[152] M. J. Kuchan and J. A. Frangos. Shear stress regulates endothelin-1 release via protein kinase c and cgmp in cultured endothelial cells. *Am J Physiol*, 264(1 Pt 2):H150–H156, Jan 1993.

[153] J. B. Sharefkin, S. L. Diamond, S. G. Eskin, L. V. McIntire, and C. W. Dieffenbach. Fluid flow decreases preproendothelin mrna levels and suppresses endothelin-1 peptide release in cultured human endothelial cells. *J Vasc Surg*, 14(1):1–9, Jul 1991.

[154] V. Ranjan, Z. Xiao, and S. L. Diamond. Constitutive nos expression in cultured endothelial cells is elevated by fluid shear stress. *Am J Physiol*, 269(2 Pt 2):H550–H555, Aug 1995.

[155] H. Morawietz, R. Talanow, M. Szibor, U. Rueckschloss, A. Schubert, B. Bartling, D. Darmer, and J. Holtz. Regulation of the endothelin system by shear stress in human endothelial cells. *J Physiol*, 525 Pt 3:761–770, Jun 2000.

[156] Yi-Shuan J Li, Jason H Haga, and Shu Chien. Molecular basis of the effects of shear stress on vascular endothelial cells. *J Biomech*, 38(10):1949–1971, Oct 2005.

[157] D. Mazzei, F. Vozzi, A. Cisternino, G. Vozzi, and A. Ahluwalia. A high-throughput bioreactor system for simulating physiological environments. *Industrial Electronics, IEEE Transactions on*, 55-9:3273–3280, Sept 2008.

[158] F. Vozzi, F. Bianchi, A., and C. Domenici. Independent application of pressure and shear stress on endothelial cells in controlled bioreactors.

[159] D. Mazzei, M. A. Guzzardi, S. Giusti, and A. Ahluwalia. A low shear stress modular bioreactor for connected cell culture under high flow rates. *Biotechnol Bioeng*, Jan 2010.